

AN ABSTRACT OF THE THESIS OF

Douglas G. Pyle for the degree of Master of Science
in Geology presented on January 8, 1988
Title: Geochemical Evolution of the Roseburg Formation Basaltic Rocks,
Southern Oregon Coast Range

Abstract Approved: _____

Redacted for Privacy

Dr. E.J. Dasch

The Paleocene-lower Eocene volcanic rocks of the southern Oregon Coast Range Roseburg Formation are the oldest remnant eruptive sequence of an oceanic island-seamount province which is presently exposed along a north-south lineament that stretches from Vancouver, B.C. into southwestern Oregon. This seamount terrane is thought to have formed on the Farallon plate and, been subsequently accreted into its present position along the Oregon and Washington coast during subduction of this oceanic plate beneath the North American Plate during the early Tertiary

The Roseburg volcanic sequence is composed of a basal submarine tholeiitic section which grades upward into a subaerially erupted sequence of highly undersaturated alkalic basalts. Field studies show that the morphological evolution of eruptive styles within the volcanic pile (i.e. sequences of pillowed and massive flows, pyroclastic beccias and hyaloclastite deposits, subareal flows, and erosional surfaces) closely follow successive stages of growth observed at present day oceanic islands such as Hawaii. The regional distribution of basalt types reveal a progressive increase in differentiation from exposures of tholeiitic basalts in the south to exposures of alkalic basalts in the north, and demonstrate a coherence in the geochemical evolution between basalts which crop out on the east and west side of an intervening Eocene basin.

The Roseburg basaltic sequence displays the greatest amount of chemical diversity yet reported for the early Tertiary volcanic centers which comprise the Oregon-Washington Coast Range province. The tholeiitic basalts have trace element compositions which are typical of E-type MORB and tholeiites from hotspot generated oceanic islands. The alkalic suite is highly enriched in incompatible element constituents typically found in the late stage eruptive cycles of oceanic island volcanism. The generation of these two basaltic suites are related to a common mantle source composition which has undergone variable degrees of partial at different depths. Differentiation of the tholeiitic basalts results from uniform degrees of partial melting, whereas compositional variations in the alkalic basalts can be explained only by variable degrees of partial melting at deeper depths in the mantle. Fractional crystallization does not seem to be an important control on the differentiation of these two basaltic suites.

In contrast, compositional variations of basalts from other volcanic centers in the Oregon-Washington Coast Range province indicate a more dominate control of differentiation by fractional crystallization. The trace element variations in the province is related to varying influences of mid-ocean ridge spreading and hotspot volcanism. The trace element data reported here does not support models for the generation of these seamount volcanoes by marginal basin spreading possibly caused by the highly oblique subduction of the Farallon plate during this time. The regional geochemical variations exhibited by basalts from different volcanic centers in the Oregon-Washington Coast Range province is shown to be geographically controlled rather than time dependent. Generally, the available data shows a decrease in the highly incompatible trace element constituents from the southern end of the Coast Range (Roseburg basalts) to the northern volcanic centers (Metchosin and Crescent Fm. basalts). This geochemical trend is thought to be caused by a declining influence of hotspot-type volcanism on the magma compositions of basalts erupted in the northern regions of the Coast Range and/or the increasing influence of spreading ridge magmatic activity in that area.

**GEOCHEMICAL EVOLUTION
OF THE
ROSEBURG FORMATION BASALTIC ROCKS,
SOUTHERN OREGON COAST RANGE**

by

DOUGLAS G. PYLE

A THESIS

submitted to

Oregon State University

in partial fulfillment of
the requirements for
the degree of

Master of Science

Completed June 10, 1988

Commencement June 1989

APPROVED:

Redacted for Privacy

Professor of Geology in charge of Major

Redacted for Privacy

Chairman, Department of Geology

Redacted for Privacy

Dean of Graduate School

Date thesis is presented January 8, 1988

Typed by Douglas G. Pyle for Douglas G. Pyle

TABLE OF CONTENTS

	Page
CHAPTER 1: INTRODUCTION	1
I. Purpose	1
II. Objectives	3
CHAPTER 2: PREVIOUS WORK	8
I. The southern Oregon Coast Range	8
Basaltic Rocks	8
Stratigraphy	9
Structure	12
II. Oregon-Washington Coast Range, regional overview	13
Geologic Setting	13
Nature of the Crust	14
Geochemistry and Petrology	16
Age of Volcanism	17
Paleomagnetism and Plate Tectonic Configuration	19
Summary	24
CHAPTER 3: FIELD AND LABORATORY INVESTIGATIONS	28
I. Field Relationships	28
II. Methods	34
Sampling Procedure	34
Sample Preparation	36
Analytical Methods	37
CHAPTER 4: MAJOR ELEMENT GEOCHEMISTRY	40
I. Basalt Classification	40
II. Major Element Variation	51
SiO ₂ vs total alkalies	51
AFM diagram	51
MgO scatter plots	54
Primary and Parental Magmas	62
CHAPTER 5: TRACE ELEMENT GEOCHEMISTRY	64
I. Introduction	64
II. Trace element variation	74
Incompatible elements	74

Table of contents (cont.)	Page
Rare-earth element variation	83
Spider Diagrams	98
CHAPTER 6: DISCUSSION	113
I. Summary of Results	113
II. Plate Tectonic models for petrogenesis	115
Model 1: Marginal basin/Continental rifting	116
Model 2: Oceanic ridge/Hotspot	118
III Conclusions	124
BIBLIOGRAPHY	126
Appendix A Sample collection localities	140
Appendix B Normalization values	142

LIST OF FIGURES

Figures		Page
1.1	Geologic provinces of Oregon and Washington	2
1.2	Geologic map of the study area (southern Oregon Coast Range)	4
2.1	Oregon-Washington stratigraphic correlation chart	11
2.2	Oregon Coast Range crustal profiles	15
2.3	Oregon-Washington early Tertiary age progressive volcanism	18
2.4	Tectonic rotation models of Simpson and Cox (1977)	20
2.5	Model 1: subduction-marginal basin origin of Coast Range	25
2.6	Model 2: mid-ocean ridge/hotspot origin of Coast Range	27
3.1	Geologic evolution summary of Hawaiian volcanoes	32
4.1	Ne-Ol-Di-Hy-Qtz normative mineral system	50
4.2	SiO ₂ vs Na ₂ O+K ₂ O scatter plot	
	a) Oregon-Washington Coast Range	52
	b) Roseburg basalts	52
4.3	Roseburg basalt AFM diagram	53
4.4	Major element scatter plots	
	a) SiO ₂ and Al ₂ O ₃ vs MgO	55
	b) FeO(t) and CaO vs MgO	56
	c) TiO ₂ and MnO vs MgO	57
	d) Na ₂ O and K ₂ O vs MgO	58
	e) P ₂ O ₅ vs MgO and CaO/Al ₂ O ₃ vs Mg*	59
5.1	La vs Th	75
	a) Oregon Coast Range	
	b) Washington Coast Range	
5.2	Ce vs La	76
	a) Oregon Coast Range	
	b) Washington Coast Range	
5.3	La vs Ta	77
	a) Oregon Coast Range	
	b) Washington Coast Range	
5.4	Th vs Ta	78
	a) Oregon Coast Range	
	b) Washington Coast Range	
5.5	Hf vs Ta	82
	a) Oregon Coast Range	
	b) Washington Coast Range	
5.6	Chondrite normalized REE diagrams	86
	a) Roseburg exposure	
	b) Sugarloaf Mountain	
5.7	Chondrite normalized REE diagrams	87
	a) Red Hill anticline	
	b) Sutherlin Mobil Well #1	
5.8	Chondrite normalized REE diagrams	89
	a) Blue Ridge Mountain	
	b) Coquille-Myrtle Point	

List of Figures (cont.)	Page
5.9 Chondrite normalized REE diagrams	90
a) Jack Creek Anticline	
b) Coos River-Kentucky Slough	
5.10 Chondrite normalized REE diagrams	91
a) Drain anticline	
5.11 Chondrite normalized REE diagrams	92
a) Siletz River basalts	
5.12 Chondrite normalized REE diagrams	93
a) Crescent Fm. basalts	
b) Black Hills basalts	
c) Grays River basalts	
5.13 Chondrite normalized REE diagrams	94
a) Metchosin Fm. basalts	
5.14 (Ce/Yb) _n vs (Ce) _n plot of representative oceanic basalts	96
5.15 (Ce/Yb) _n vs (Ce) _n plot	97
a) Roseburg basalts	
b) Oregon-Washington Coast Range	
5.16 Spider Diagrams	100
a) North Atlantic MORB	
b) Average MORB	
5.17 Spider Diagrams	101
a) Roseburg exposure	
b) Sugarloaf Mountain	
5.18 Spider Diagrams	102
a) Red Hill anticline	
b) Sutherlin Mobil Well # 1	
5.19 Spider Diagrams	103
a) Blue Ridge Mountain	
b) Coquille-Myrtle Point	
5.20 Spider Diagrams	104
a) Jack Creek anticline	
b) Coos River-Kentucky Slough	
5.21 Spider Diagrams	105
a) Hawaiian alkali basalts	
5.22 Spider Diagrams	106
a) Drain anticline	
5.23 Spider Diagrams	107
a) Hawaiian basanites	
5.24 Spider Diagrams	108
a) Siletz River basalts	
b) Average Hawaiian tholeiites	
5.25 Spider Diagrams	109
a) Black Hills basalts	
b) Grays River basalts	
5.26 Spider Diagrams	110
a) Metchosin Fm. basalts	
b) Crescent Fm. basalts	
6.1 Th-Hf/3-Ta ternary plot (representative oceanic basalt systems)	120
6.2 Th-Hf/3-Ta ternary plot (Roseburg basalts and Coast Range)	121
6.3 Th/Yb vs Ta/Yb (Roseburg basalts and Coast Range)	123

LIST OF TABLES

Tables	Page
3.1 Analytical Errors and STD Results	38
4.1 Roseburg Basalt Major Elements Abundances	
a. Roseburg and Sugarloaf Mountain	43
b. Coquille-Myrtle Point and Red Hill	44
c. Blue Ridge, Coos River, and Kentucky Slough	45
d. Jack Creek Anticline and Drain Anticline	46
4.2 Mobil Sutherlin Well #1, Major and Trace Element Abundances, (Core samples)	47
4.3 Washington-British Columbia Coast Range Major Element Abundances, (Black Hills, Grays River, and Metchosin basalts)	48
5.1 Roseburg Basalt Trace Element Abundances	
a. Roseburg and Sugarloaf Mountain	68
b. Coquille-Myrtle Point and Red Hill	69
c. Blue Ridge, Coos River, and Kentucky Slough	70
d. Jack Creek Anticline and Drain Anticline	71
5.2 Mobil Oil Sutherlin Well #1, Trace elements Abundances, (Drilling chip samples)	72
5.3 Washington-British Columbia Coast Range Trace Element Abundances, (Black Hills, Grays River, and Metchosin basalts)	73

Geochemical Evolution of the Roseburg Formation Basaltic Rocks, Southern Oregon Coast Range

CHAPTER 1: INTRODUCTION

I. Purpose

The basaltic rocks of the Oregon-Washington Coast Range represent a significant section of oceanic crust that was emplaced and uplifted to its present position by subduction of the Farallon plate beneath the North American plate during the early Tertiary. Recently, much attention has focused on the plate tectonic history of the continental margin of western North America. Field and laboratory studies have identified allocthonous terrains ("crustal blocks" or "microplates") which have been accreted to the North American plate during translation (right-lateral sense) and convergence with subducting oceanic plates to the west (Simpson and Cox, 1977; Beck, 1980). The Coast Range of Oregon and Washington is one such terrain which is thought to have formed on the Farallon plate and, subsequently, rotated clockwise into its present position during collision with North America. The details of the accretionary history are poorly constrained. Analyses of the timing and geochemical variation of the magmatic events in the Coast Range will provide essential information for understanding the plate tectonic evolution of this province.

Volcanism during the Paleocene and early Eocene produced seven major accumulations of submarine, pillowed and massive tholeiitic basalt flows that are locally interbedded with, and overlain by, subaerially erupted alkali basalts (Figure 1.1). The

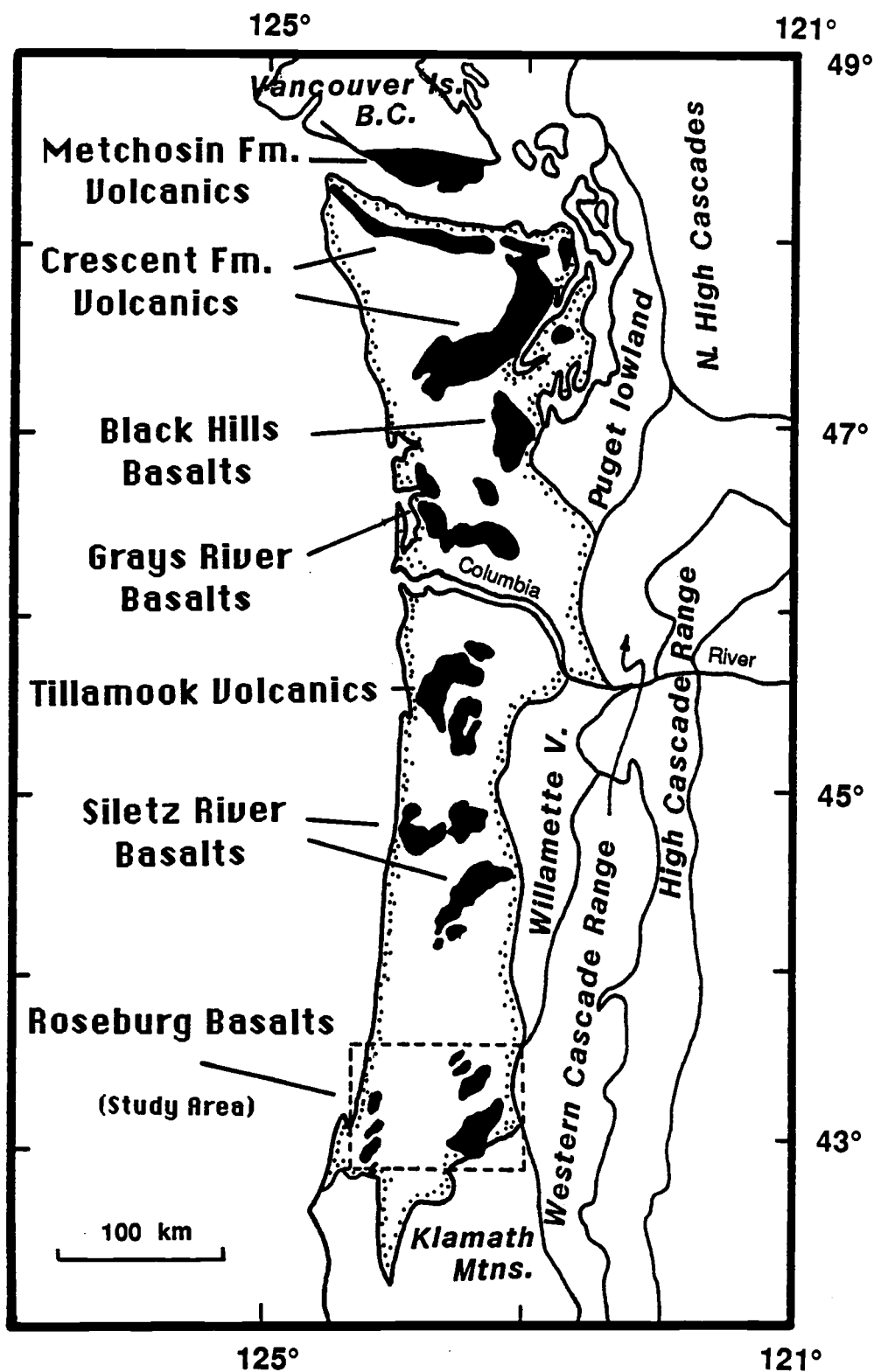


Figure 1.1 Geologic provinces of the Pacific Northwest with the positions of the major Paleocene and lower Eocene volcanic accumulations discussed in this work (modified after Wells et al., 1984). The thesis study area is bordered by dashed lines which approximate the dimensions of the sample location geologic map (Fig. 1.2).

chemical composition and the morphological character of the basalt flows and associated pyroclastic rocks indicate that the rocks of this province represent oceanic type volcanism. Snively and co-workers (1963,1968) first characterized the locally thick sections of basaltic rocks as remnant seamounts erupted along the North American continental margin. The seamount hypothesis is still widely accepted but the exact location and plate tectonic regime in which seamount volcanism occurred has not been satisfactorily resolved. This study contributes to the resolution of this problem by providing an extensive data set of major and trace elements for the Roseburg basalts. These data are used to evaluate the possible plate tectonic environments which could have generated magma with the chemical signature found in these and other early Tertiary basalts of the Oregon-Washington Coast Range.

II. Objectives

This study was conducted to provide a detailed geochemical evaluation of the Paleocene volcanic rocks which crop out along the east and west flanks of the southern Oregon Coast Range synclinorium (Figure 1.1). The study area covers approximately 10,000 km² from the edge of the western Cascades volcanic province near Glide to the Pacific Coast near Coos Bay and from Drain to south of Roseburg (Figure 1.2). Based on age, stratigraphic position, and mineralogical and chemical similarities, this volcanic sequence has been designated as part of the Siletz River Volcanics (Am. Comm. Strat. Nomenclature, 1961) which are exposed 100km to the north (Snively et al., 1968; Baldwin, 1974). The Siletz River Volcanics of the southern Oregon Coast Range is herein referred to as the Roseburg basalts so a clear distinction can be made between the two volcanic centers during discussion of their geochemical characteristics. The Roseburg

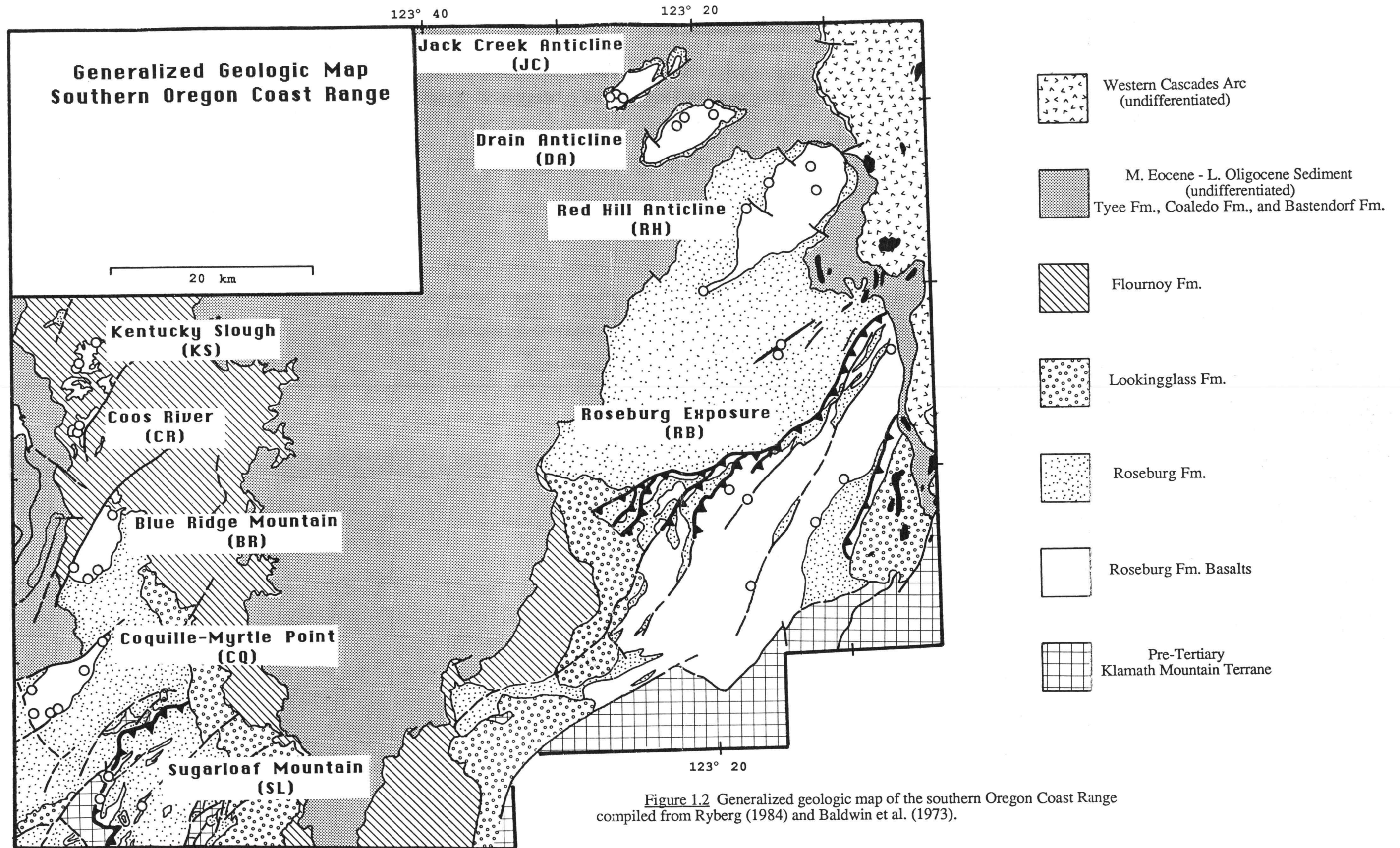


Figure 1.2 Generalized geologic map of the southern Oregon Coast Range compiled from Ryberg (1984) and Baldwin et al. (1973).

basalts represent the southernmost exposure of an early Tertiary volcanic province that now extends approximately 600 km from the southern tip of Vancouver Island, B.C. to southern Oregon.

Understanding the chemistry of these rocks, and particularly their trace element characteristics, is necessary in determining the similarities and differences between the Roseburg basalts and other early Tertiary volcanic centers in the Coast Range. This information is also essential in correlating petrogenetic relationships between the several outcrops of the Roseburg basalt that occur over a 10,000 km² area. Duncan (1982) has shown the Roseburg basalts to be the oldest rocks in the Oregon-Washington Coast Range. Assuming all the volcanic centers in the province are related to a common tectonic and magmatic regime, the chemical composition of the basalt in the Roseburg area should approach most closely an "initial" chemical composition for the mantle source that fed these seamounts. Duncan also demonstrated that the position of the Yellowstone hotspot at 65 ma would have coincided with the inferred location of volcanic activity producing the Coast Range basalts. If this idea is correct, it implies that these rocks are also the earliest preserved expression of the Yellowstone hotspot and that their chemical composition has been influenced by a hotspot-type mantle source composition.

The source regions for mid-ocean ridge basalts, oceanic island basalts (associated with hotspots), and island arc basalts have been shown to be distinguishable by certain trace element characteristics (Gast, 1968; Schilling, 1971; Kay and Gast, 1973; Pearce and Cann, 1973; Wood et al., 1979). "Depleted" basaltic compositions that are characteristic of mid-ocean ridge basalts (MORB) and "enriched" basaltic compositions that are characteristic of oceanic island basalts (OIB) and, possibly, basaltic compositions that have characteristics of island arc basalts (IAB) are all found in the Coast Range province (Hill, 1975; Glassley, 1974; Lytle and Clark, 1975; Loeschke, 1979). The degree of enrichment and depletion of the basaltic rocks and the extent to which these

different magma types are represented at various volcanic centers has not been completely determined. Plate motion models (Atwater, 1970; Simpson and Cox, 1977; Ewing, 1980; Duncan, 1982; Moore et al., 1983; Engebretson, 1983; Wells et al., 1984) for the northeast Pacific ocean basin during the early Tertiary show mid-ocean ridge spreading, hotspot volcanism, and subduction-related volcanism occurring in a relatively confined area. All of these environments could have produced basaltic magmas that directly or indirectly affected basalt compositions in the province. Determining the geographic distribution of magma types is therefore important for resolving the plate tectonic configuration of the region during eruption of the basaltic magmas.

This study is a thorough geochemical characterization of the Roseburg basalts. New major and trace element analyses of the Crescent Formation in Washington and the Metchosin Formation on Vancouver Island, B.C. are also reported. Major data sets from published sources (Snively et al., 1968; Glassley, 1974, 1976; Lytle and Clark, 1975, 1976; Muller, 1980) and from unpublished M.S. theses (Hill, 1975; Globberman, 1980) were also compiled with data of this study to determine the geochemical characteristics of the region. This information will provide a basis for evaluating the magmatic history of the Oregon-Washington Coast Range province. This evaluation will be carried out by:

- (1) determining the distribution of magma types in the southern Oregon Coast Range and their geographic/stratigraphic relationships (i.e. if stratigraphic-chemical correlations can be made between the scattered basalt exposures and if the most evolved basalt compositions occur in the higher stratigraphic units).
- (2) characterizing the chemical composition of the mantle source(s) from which the basaltic melts were extracted to produce the Roseburg basalt sequence.
- (3) assessing the geochemical relationships between the Roseburg basalts and other early Tertiary volcanic centers in the Oregon-Washington Coast Range.

(4) comparing the chemistry of the Coast Range basalts to basaltic magmas from known plate tectonic environments(e.g. Hawaii, Iceland, Mid-Atlantic Ridge, East Pacific Rise, etc.) in an attempt to constrain current models proposed for the origin of this province.

CHAPTER 2: PREVIOUS WORK

I. The Southern Oregon Coast Range

Basaltic Rocks

The basaltic rocks of the Umpqua Group were first mapped and described by Diller(1898) as "diabase" being partly intrusive and partly extrusive. Wells and Waters (1934,1935) published the first detailed petrographic descriptions of these rocks exposed around the Red Hill anticline and in the Roseburg vicinity. They recognized the morphological character of the flows and associated palagonitic tuffs and breccias as evidence for a dominantly extrusive sequence which erupted into a subaqueous environment. Hoover (1963) published a detailed map of the Drain and Anlauf quadrangles and discussed the alkali basalts and associated tuffs in that area. More recently, Hill (1975) reported 6 analyses of the Roseburg basalt in a regional study of the Oregon-Washington Coast Range that included early Tertiary basalts, as well as younger volcanic units. Hill noted a trend from Hawaiian-type tholeiitic compositions in the Siletz, Tillamook, and Roseburg volcanics to more mid-ocean ridge type tholeiites in the Crescent and Metchisin Formations. Loeschke (1979) published an average of ten analyses on samples collected along the North Umpqua River at Horseshoe Bend northeast of Roseburg. This area is located in the lower tholeiitic section of the Roseburg basalt, and based on this limited sample distribution, he concluded the basalts were probably erupted along a mid-ocean ridge spreading center.

Stratigraphy

Other studies of the southern Oregon Coast Range have focused mainly on the stratigraphy and structural relationships in the overlying sediments of the Roseburg, Lookingglass, Flourney, and Tyee Formations. Dr. Ewart M. Baldwin of the University of Oregon has published several articles concerning the general geology of the southern Oregon Coast Range and supervised many unpublished mapping theses on the area (Baldwin, 1964, 1965, 1974 and references therein; Baldwin and Beaulieu, 1973; Ramp, 1972). Ryberg(1984) has recently presented a comprehensive discussion of the geology of southwestern Oregon and a detailed study of the sedimentation, structure, and tectonics of the Umpqua Group. This stratigraphic section is intercalated with and overlies the Roseburg basalts and was simultaneously deposited as volcanism proceeded. A brief summary of the general geology of the area is given below.

The Umpqua Group of Baldwin (1974) is composed of three formations. The Roseburg Formation is the lowermost unit and consists of a lower volcanic section, the Roseburg basalts, that intertongues with and is overlain by turbidites (rhythmically bedded sandstone, siltstone, and mudstone sedimentary unit) which reaches a maximum thickness of over 2.7 km (Baldwin, 1974). The base of the Roseburg Formation has not been identified at any location and it is apparently everywhere in fault contact with older rocks. The Roseburg basalts are believed to represent the remnant oceanic crust upon which turbidites, conglomerates, and massive sandstones of the overlying formations were deposited. Pyroclastic deposits which include hyaloclastites, vitric tuffs, slump breccias, tuff and basalt welded conglomerates, and phreatic explosion breccias, grade into basalt, both vertically and laterally, and in some places make up entire outcrops. Interbedded sediments occur at all levels in the volcanic pile and between all types of magmas. Intercalations of boulder-sized conglomerates composed of plutonic rocks exposed in the

Klamath mountains in the lower tholeiitic basalt sections indicate volcanism probably occurred close to the early Tertiary continental margin of North America.

The Lookingglass Formation is separated from the underlying Roseburg Formation by an angular unconformity in the study region. This unconformity marks a major change in the tectonic processes occurring along this convergent margin during the early Tertiary. Deposition of conglomerate, sandstone, siltstone, and coal-bearing sandstone of the Lookingglass Formation replaced the turbidite sedimentation of the Roseburg Formation.

The Flourney Formation disconformably overlies the Lookingglass Formation. Ryberg (1984) and Miles (1977) has estimated that a million-year hiatus occurred between the two depositional intervals. The Flourney Formation, the uppermost unit of the Umpqua Group, is the non-micaceous equivalent of the overlying Tyee Formation. The Tyee and the Flourney fill the core of the southern Oregon Coast Range synclinorium. The geographic distribution of the Flourney Formation is limited to the southern end of the Oregon Eocene coastal basin. The Tyee extends farther north and onlaps the Siletz River volcanic rocks. A stratigraphic correlation chart for the entire Coast Range province from Snavely et al. (1980) is given in Figure 2.1. The stratigraphic sequence of the Umpqua Group records the depositional transition from deep water, submarine fan-continental slope environment of the Roseburg Formation to a shallow marine continental shelf and alluvial fan-delta environment of the Lookingglass Formation and Flourney Formation (Ryberg, 1984).

Structure

Exposures of the Roseburg basalts are confined to the axes of anticlines and along high angle faults that follow a dominantly NE-SW trend (Figure 1.2). Intense deformation of the Roseburg Formation during the early Eocene records the culmination of Klamath-style thrusting and folding. The structural patterns in the lower section of the Umpqua Group parallel trends established in the Klamath Mountain terrain which lies directly to the south. Middle Eocene strata (Lookingglass and Flournoy Formations) are only gently folded along more northerly-trending fold axes. Folds in the Roseburg Formation north of Roseburg on the east side of the Coast Range Eocene basin are generally broad and open. However, the Roseburg Formation along the western side of the Coast Range is intensely folded and interleaved with melange wedges. The structural differences between the two sides of the basin has been attributed to exposure of deeper levels of the volcanic pile on the west side of the Coast Range (Perttu and Benson, 1980; Ryberg, 1984). Deposition of the Lookingglass Formation records a gradual transition in structural style from NW-SE shortening to more N-S trending gentle folding.

The most striking structural feature in the area is the NE-SW striking Bonanza thrust fault system which has pushed lower tholeiitic basalts of the Roseburg area from the southeast over the upper sedimentary units of the Roseburg Formation (Baldwin, 1964). This thrust has been traced beneath the central basin fill of the Coast Range and reappears along the northwestern edge of Sugarloaf Mountain (Figure 1.2). Ryberg (1984) estimates the age of movement on the fault system to occur at approximately 52 My ago. Faults younger than the Bonanza Fault have more of a N-S or E-W orientation with appreciable right-lateral as well as vertical separations (Ryberg, 1984). The lateral movement on some of the fault systems indicate shearing of the southern Oregon Coast Range during the early Tertiary tectonic history of the province.

II. Oregon-Washington Coast Range, a regional overview

Geologic setting

The Roseburg and the Siletz River basalts are the southernmost exposures of the Oregon-Washington Coast Range province. The Paleocene-lower Eocene basalts of the Siletz River Volcanics of Oregon are equivalent to the lower Eocene Crescent Formation basaltic rocks of Washington and the lower Eocene basaltic rocks of the Metchosin Formation on southern Vancouver Island, B.C. Basalts of the Crescent Formation crop out in several exposures in the western Washington Coast Range. The basalts at these exposures have been named according to local geographic features and these names are used in this report to facilitate discussion of the geochemical features of the region. The Grays River basalts are exposed in southwestern Washington between Grays River Harbor and the Willapa Hills north of the Columbia River. The Black Hills basalts are exposed immediately south of Puget Sound and lie between the Willapa Hills basalt exposure and the Crescent Formation type section to the north. The Crescent Formation name is retained here to refer to the horseshoe shaped exposure of basalt which rims the Olympic Peninsula.

The major accumulations of early Tertiary volcanic rocks in the Oregon-Washington Coast Range are shown in Figure 1.1. The base of these volcanic piles has not been identified at any locality suggesting that they represent the lower basaltic crust which underlies the province. The eastern boundary of this province has been covered by later volcanic events of the Western Cascades and the western boundary marks the present position of active subduction of the Pacific plate beneath the North American plate. This area is technically the forearc of a generalized arc-trench subduction model.

Nature of the Crust

Crustal thickness estimates based on gravimetric surveys (Berg et al.,1966) and seismic refraction profiles(Bromery and Snavely,1964; Couch and Braman,1980; Couch and Pitts,1980) show an approximately 16 km thickness of total crust for the province, 8 to 10 km of which is probably made up of the lower Eocene volcanic flows and associated pyroclastic material (Figure 2.2). These surveys indicate that the Oregon-Washington Coast Range occupies a zone of transition between normal oceanic crust (8 km thick) of the Cascadia Abyssal Plain and average continental crust(30 km thick) located east of the Cascade Volcanic Arc. The crustal thicknesses and the morphological character of the basaltic basement rocks have led to the interpretation that this area represents a slice of remnant early Tertiary oceanic crust (Snavely et al.,1968). Interpretations of gravity measurements suggest that volcanic accumulations thin towards the east and west edges of the basin and that locally thick piles of basaltic flows in the center of the basin represent the volcanic edifices of seamounts (Bromery and Snavely, 1964). Subaqueously-erupted pillowed and massive tholeiitic basalt flows and associated tuffs and breccias dominate the lower sections. Locally, tholeiitic basalts grade upwards into subaqueous and subaerially erupted alkalic basalts. Baldwin (1974) and Snavely et al.(1968) estimate the lower Eocene basalt accumulation to be at least 3 km thick and probably as much as 6-8 km thick near volcanic edifices.

The total amount of erupted material in the province can be estimated by assuming an average crustal thickness of 4 km and approximating the dimensions of the basin at 600 km long by 100 km wide. An accumulation of $240,000 \text{ km}^3$ of basaltic material is thus estimated to make up the province. If eruptions occurred between 65 Ma and 45 Ma

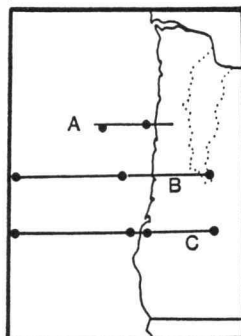
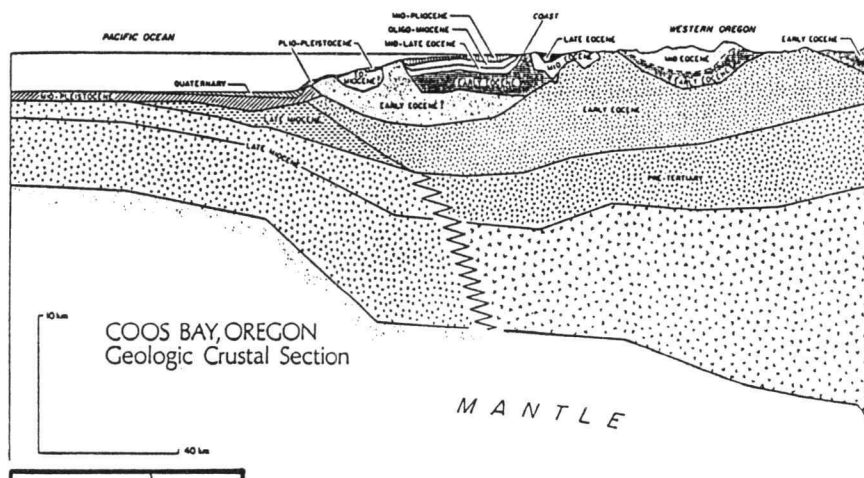
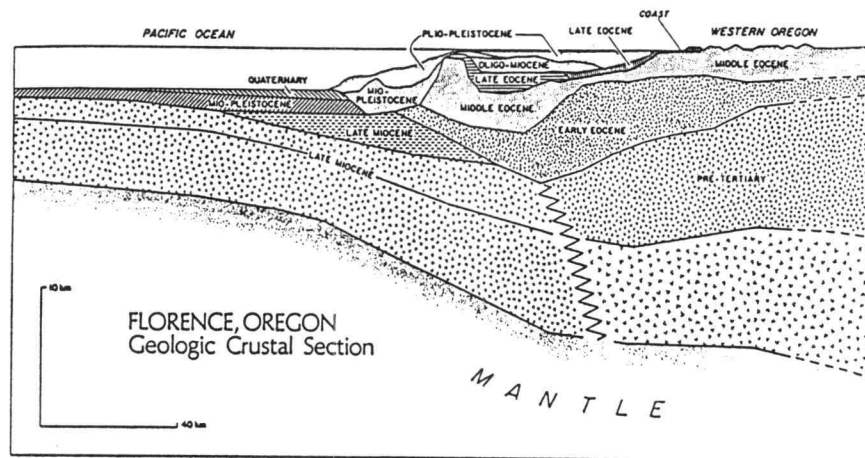
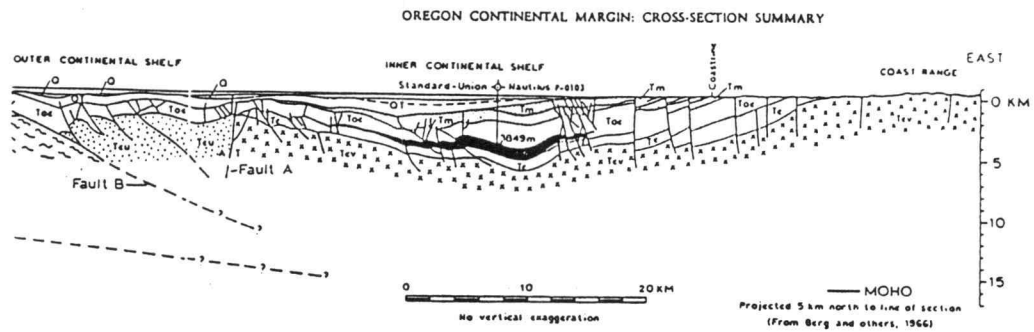


Figure 2.2 Three crustal profiles across the Oregon Coast Range. The inset shows the location of the cross-section traces. The Roseburg basaltic rocks are represented as "early Eocene" in the Florence (B) and the Coos Bay (C) sections (Couch and Braman, 1980; Couch and Pitts, 1980). Equivalent basaltic rocks in section A are the Siletz River volcanics (Snively et al., 1980).

(Duncan, 1982), a magma production rate of $20 \text{ km}^3/\text{km}/\text{M.y.}$ is estimated. Moore et al. (1974) have estimated eruption rates at the FAMOUS area along the Mid Atlantic ridge (36° N lat.) to be approximately $8.6 \text{ km}^3/\text{km}/\text{M.y.}$ compared to $90 \text{ km}^3/\text{km}/\text{M.y.}$ on Iceland (BVSP, 1981). These estimates indicate that the magma production was approximately twice as great in the Pacific Northwest than along a "typical" modern mid-ocean ridge segment and one quarter of the estimated magma production for the ridge-centered Icelandic hotspot.

Geochemistry and Petrology

The origin and emplacement of the Oregon-Washington Coast Range along the western continental margin of North America has been the subject of several investigations. Snively and Wagner (1963) first suggested the lower Eocene basalts in Oregon and Washington represent islands that were extruded in their present position along a N-S trending fissure system adjacent to the North American continental margin. Snively et al. (1968) recognized a lower tholeiitic sequence and an upper alkalic sequence to the Siletz River basalts and pointed out that the eruptive sequence (tholeiites capped by alkalic rocks) and the chemistry of the basalts resembled Hawaiian Island-type volcanism. Glassley (1974, 1976) presented a geochemical study of the Crescent Volcanics in the northern Washington Coast Range and concluded that a lower tholeiitic basalt unit and an upper alkalic basalt unit could be distinguished by trace element characteristics. Glassley noted that the upper and lower units were in fault contact, that the alkali basalts were far less abundant than in the Oregon Coast Range and that they were mostly intrusive. While trace element compositions of the lower tholeiites pointed to a MORB source, he argued that the upper alkalic basalts were "unrelated" to the basal tholeiites. Lyttle and Clark

(1975, 1976) disputed Glassley's interpretation and presented new data which they believed indicated the Crescent Volcanics represent a remnant oceanic island arc. Cady (1975) proposed the "abyssal and Hawaiian-type tholeiitic basalts" of the Crescent Volcanic rocks extruded onto the Juan de Fuca plate near the continental margin, covering continentally derived sediments before and during initiation of subduction in the area. Studies by Muller (1980) of equivalent rocks exposed along southern Vancouver Island (the Metchosin Formation), concluded that trace element discrimination diagrams did not unequivocally differentiate plate tectonic environments but decided that the data could be best explained by an Icelandic type eruptive center (i.e. a hotspot beneath a spreading ridge). Globberman (1980, 1982) reported paleomagnetic data and chemical analyses for the Black Hills basaltic rocks which are exposed immediately south of the Crescent Volcanics. His model, based on the evolution of ocean basin seamounts (Menard, 1972; Batiza, 1976), called upon seamount volcanism at or near a spreading ridge with the eventual eruption of an alkali basalt cap as the seamount was carried farther from the axis of spreading on the diverging plate.

Age of Volcanism

Radiometric ages of the Paleocene to lower Eocene volcanic centers have been reported by Duncan (1982). He has shown that the age of the basalts become progressively younger from the northern Metchosin volcanic rocks (58 My) and the southern Roseburg basalts (62 My) towards the center of the volcanic lineament where the Grays River basalts (45 My) crop out (Figure 2.3). This age trend and the overall trace element "enriched" character of the basalts in the province suggest they may have been erupted on a mid-ocean ridge segment being fed by a hotspot. The Icelandic volcanic

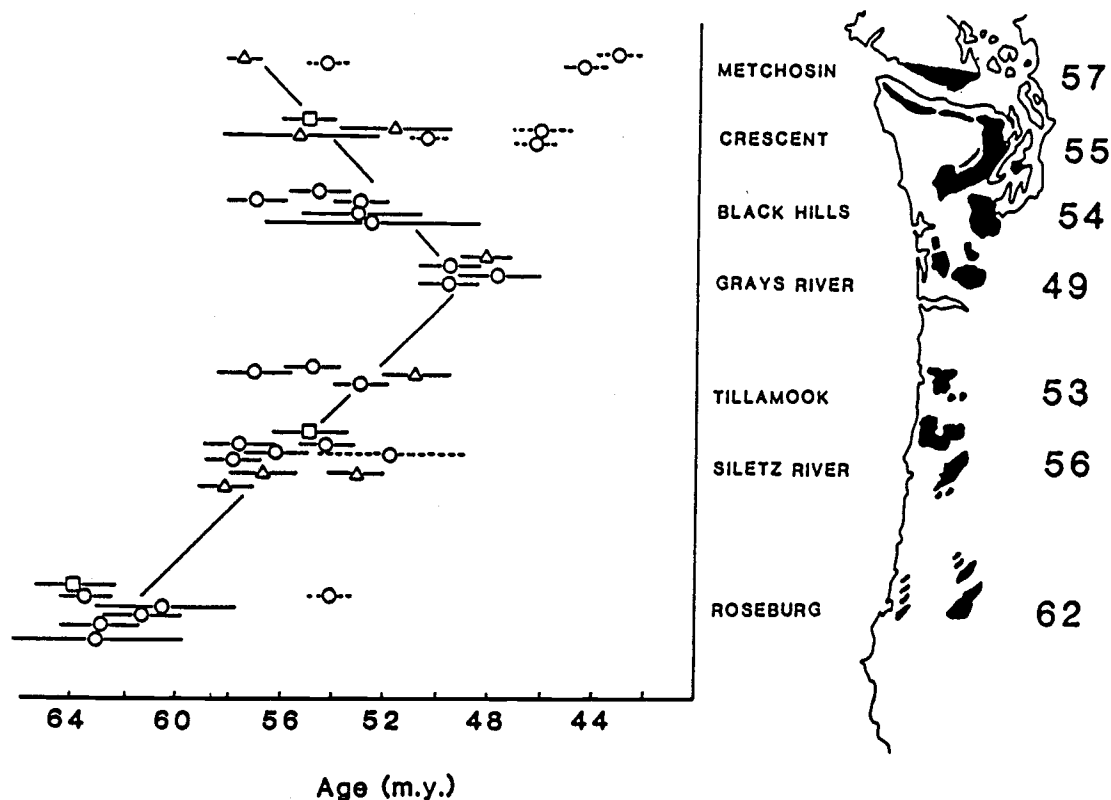


Figure 2.3 The radiometric ages and relative positions of the Paleocene - L. Eocene volcanic rocks in the Oregon-Washington from Duncan (1982). The progressively younger average eruption ages of the basalt exposures toward the center of the province (Grays River basalts) suggests the origin of these volcanic rocks could be explained by a ridge-centered hotspot tectonic setting similar to Iceland.

system is a modern analog for this hypothesis. The large volumes of magma which accompanies hotspot volcanism would produce topographic highs on the ocean floor. The topographic highs would be propagated on either side of the hotspot as the plates spread away from the magma source (cf. Iceland-Faroes Ridge, Rio Grande Rise and Walvis Ridge system). An age progression along the ridge or seamount chain would be "mirrored" on the divergent plates and subsequent accretion of this ridge or line of seamounts could explain the age progression, chemistry, and possibly, the paleomagnetic rotations found in the Oregon-Washington Coast Range.

Paleomagnetism and plate tectonic configuration

Simpson and Cox (1977) first reported paleomagnetic data on the lower, middle, and upper Eocene volcanic and sedimentary rocks in the Oregon Coast Range that indicated these rocks were displaced 50°-70° east of the expected Eocene magnetic field direction. They presented two models (Figure 2.4) which showed that the Roseburg and the Siletz River basaltic basement had been tectonically rotated clockwise as a single crustal block since their eruption. In the first model, a crustal block rotated from a southern pivot point as the Farallon plate subducted beneath the North American plate. In the second model, an oceanic aseismic ridge parallel to the early Tertiary subduction zone clogged the trench and caused subduction to jump seaward in middle Eocene. The second model rotated the crustal block from a northern pivot point as rifting of the Klamath Mountain terrain away from the line of Cretaceous batholiths proceeded.

Subsequent paleomagnetic results from the Washington Coast Range (Beck and Plumley, 1980; Beck, 1980; Beck and Engebretson, 1982; Magill et al., 1982; Globberman et al., 1982) showed the clockwise rotations to be more complicated than the rotation

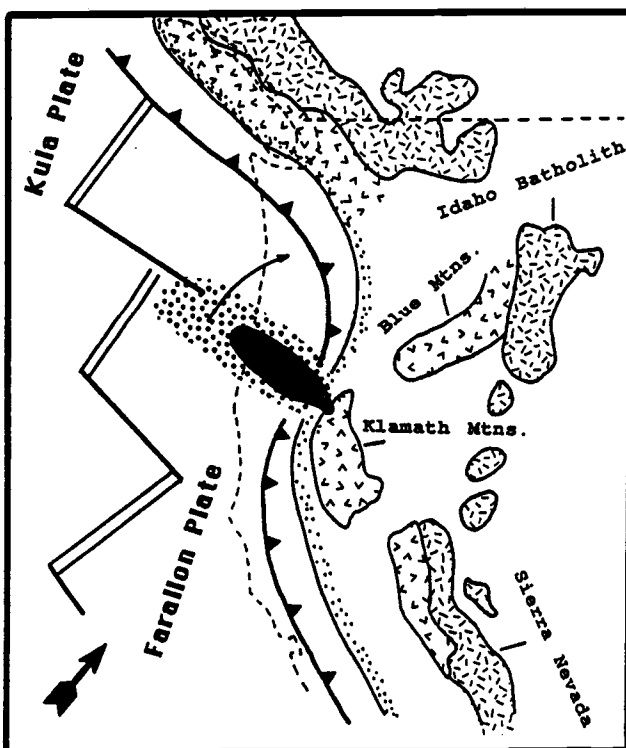
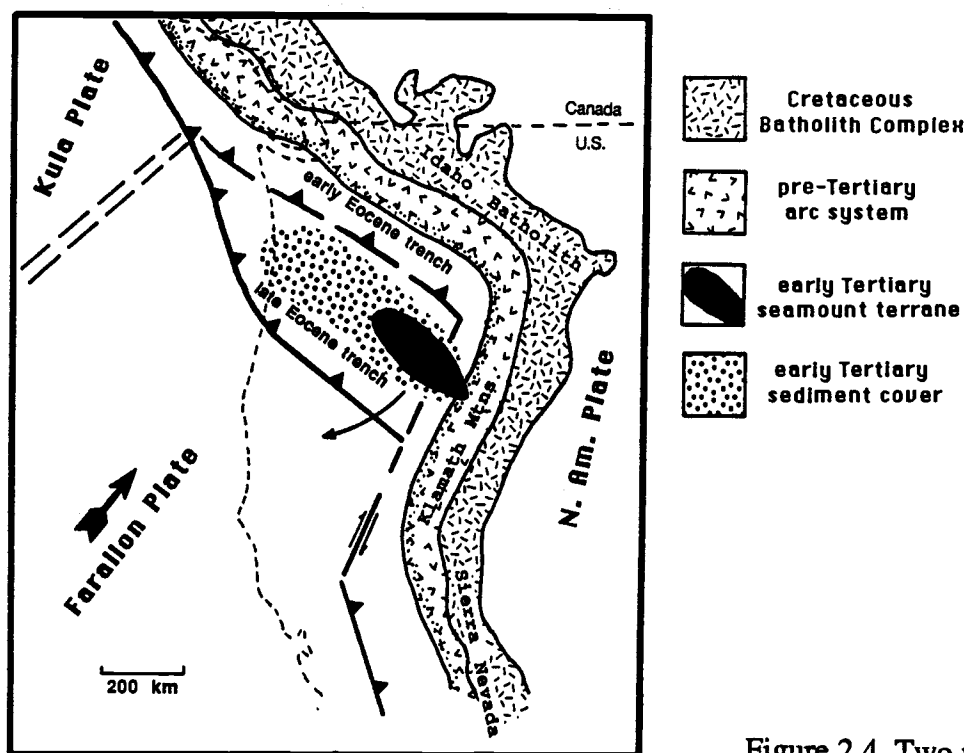


Figure 2.4 Two models proposed by Simpson and Cox (1977) to explain the paleomagnetic displacement of the Oregon-Washington Coast Range rocks. In model 1 rotation is caused by jamming of the early Eocene trench during obduction of the Eocene seamount terrane and outboard jumping of the subduction complex. Rotation about a northern pivot of the province is caused by the subsequent rifting of, and extension behind, the late Cretaceous arc system. In model 2 rotation of the coast range basaltic rocks is caused by the oblique (northeast) subduction of the Farallon plate carrying the early Tertiary seamount province. Collision of the Roseburg volcanic pile occurs against the Klamath Mtns. and the province is subsequently rotated into the continental margin about a southern pivot point.

found in Oregon and that several independent crustal blocks or "microplates" were necessary to explain the differences in paleomagnetic displacements in the two areas. Further paleomagnetic work in the western Cascades (Magill and Cox, 1980; Bates et al., 1981) revealed more evidence for rotations of younger terrains in the western United States.

Magill and Cox (1980), considering the original oceanic setting for the Oregon Coast Range rocks, thought that the observed paleomagnetic rotations could be explained by a first-stage accretion of the Oregon seamount province to North America during the early Tertiary and a later-stage rotation related to extension in the Basin and Range province. The intense folding and thrusting in the Roseburg Formation and the melange nature of the southwestern side of the Oregon Eocene basin has been interpreted as evidence of a fossil subduction zone (Beaulieu, 1971). Subduction at this locality must have stopped abruptly at or near the end of the lower Eocene since the turbidites and conglomerates of the Tyee Formation and Flourney Formation which overlie the Roseburg Formation are only gently folded (Baldwin, 1974; Ryberg, 1985). Magill and Cox (1980) also evoked a westward jump of the subduction zone which they believed occurred between deposition of the Roseburg Formation and Flourney Formation. The trench jump was caused by "jamming" of the subduction zone with large seamounts and associated sediments. The production of young oceanic lithosphere near the trench due to the close proximity of the Kula-Farallon spreading center at this time may have also contributed to the clogging of the subduction zone. The plate being consumed would have been relatively warm, buoyant and not easily subducted. Dickinson (1979) believed the dip of the Farallon plate being subducted beneath North America began to "shallow" in latest Cretaceous time and continued to be nearly horizontal well into the Eocene. The shallow dip of the plate, the buoyancy of the crust, and the presence of an elevated island chain or volcanic ridge all caused a reorganization of the trench system farther to the west.

Collision of the seamount terrain against the Klamath Mountains to the south was completed by about 50 my ago and occurred before deposition of the Tyee Formation (Heller and Ryberg, 1983). The tectonic rotations of the basalts and sediments in the Coast Range may have been caused by the entrapment of this section of oceanic crust between the newly established subduction zone to the west and North American Continent to the east. A possible problem with the accreted terrain model is the gentle folding which characterizes the middle Eocene stratigraphic section. These rocks apparently have undergone nearly as much rotation as the underlying basaltic basement (Wells et al., 1984) but they do not record a deformation event which might be expected if a crustal block was obducted or accreted to the continental margin. These stratigraphic relationships require that most of the rotation occurred following suturing of the basalts to the continental margin in middle Eocene time. Also, the presence of 3 m diameter quartz diorite boulders interbedded within the basalts of the Crescent Formation (Cady, 1975) and similar sized boulders derived from the Klamath Mountains interbedded within the Roseburg basalts (Ryberg, 1984) indicate both ends of the volcanic province remained close to the continental margin as the basalts were extruded. This field evidence suggests that rotations may be mostly due to asymmetric, back-arc spreading behind the Cretaceous volcanic arc. Figure 3.4 shows the pre-Tertiary configuration of the continental margin of the western North America and the presumed trend of the Cretaceous magmatic arc.

Beck (1980) pointed out that northward transport of allochthonous blocks was important south of Cape Mendocino and north of southern Vancouver Island but that only clockwise rotations were found in the Pacific Northwest. He believed this fact indicated that displacements of the Coast Range rocks could be explained by right-lateral shear caused by oblique northeast subduction of the Farallon plate beneath North America. Moore et al. (1983) also called upon a right-lateral shear mechanism along the Oregon-Washington continental margin for the reconstruction of allochthonous Alaskan terranes at

62 My. They showed this terrain to be attached to Oregon at this time and, subsequently, was rifted away as North America overrode the Kula-Farallon ridge and an active Yellowstone hotspot. The high oblique, northward convergence of the Kula plate provided plate tectonic transport for the Alaskan terrains to their present position. The oblique rifting of the continental margin would have opened a back-arc basin in which the Paleocene-lower Eocene basalts of the Coast Range erupted. Snavely (1984) proposed a similar model in which rapid, strongly oblique subduction set up a tensional regime along the Pacific Northwest continental margin. The rift zone initiated spreading that produced the seamount volcanoes that make up the basement of the Coast Range province.

Wells et al. (1984) claimed that the simple ridge-centered hotspot model of Duncan (1982) was problematic based on plate motion models of Engebretson (1983). Engebretson (1983) has determined the relative motions of the Kula-Farallon-North American plates and calculated their rates of convergence for the early Tertiary. His model predicts high convergence rates for the Farallon plate with the North American plate during the time of Coast Range magmatic activity. With the predicted convergence rates, a "seamount chain" produced by a ridge-centered hot spot would form a V-shaped pattern on the diverging plates away from the site of eruption instead of a linear chain (see Wells et al., 1984). Accretion of this terrain would likely juxtapose seamounts of different ages and the preservation of any age progression would be highly fortuitous. A major amount of crustal shortening would also be necessary to fit the estimated length of the volcanic ridges (i.e. high spreading rate) into the Coast Range embayment (~600 km). Wells et al. (1984) proposed a ridge-centered or slightly off ridge hotspot model in which volcanic activity occurred along "leaky" fracture zones that opened in response to minor plate readjustments. The ridge centered hotspot hypothesis is the simplest explanation of the age progression in the Coast Range province and the plate motion models are not constrained enough to rule out this idea (Duncan, 1987 pers. comm.).

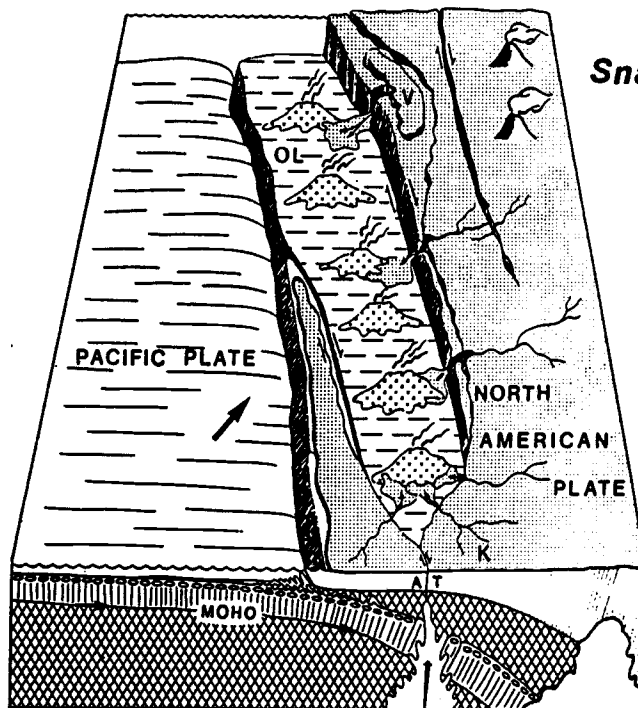
Summary

The geologic, geochemical, and geophysical evidence demonstrates the Coast Range basement to be fundamentally oceanic crust. The presence of ocean ridge spreading (MORB compositions), hotspot volcanism (OIB compositions), and active subduction (IAB compositions) in the northeast Pacific during the early Tertiary suggests that the Coast Range magmas were probably derived from one or more of these tectonic settings. Most investigators have concluded that a mid-ocean ridge and/or oceanic island source is most consistent with the basalt chemistry. The distinctive age progression toward the middle of the province supports the ridge centered hot spot model. The stratigraphic record requires the location of eruption to be near the North American continental landmass in order to receive conglomeritic deposits that could not have been carried appreciable distances from their source. The paleomagnetic data are most consistent with deposition of the sediments before most of the rotation of the Coast Range province began. The gentle folding of Eocene sediments which overlie the basaltic basement support the model of back arc extension of the region during breakup of the Cretaceous volcanic arc and, more recently, Basin and Range extension.

The plate tectonic environment of eruption of the Coast Range basalts can be considered with respect to two models (Figures 2.5 and 2.6). Both models suggest some type of spreading ridge process is involved in magma production but the mechanism for magma production in each case is significantly different.

Model 1) Basaltic volcanism is associated with extension caused by oblique subduction of the Farallon Plate beneath the North American

Subduction-Marginal basin



Snively (1984)

Moore et al. (1983)

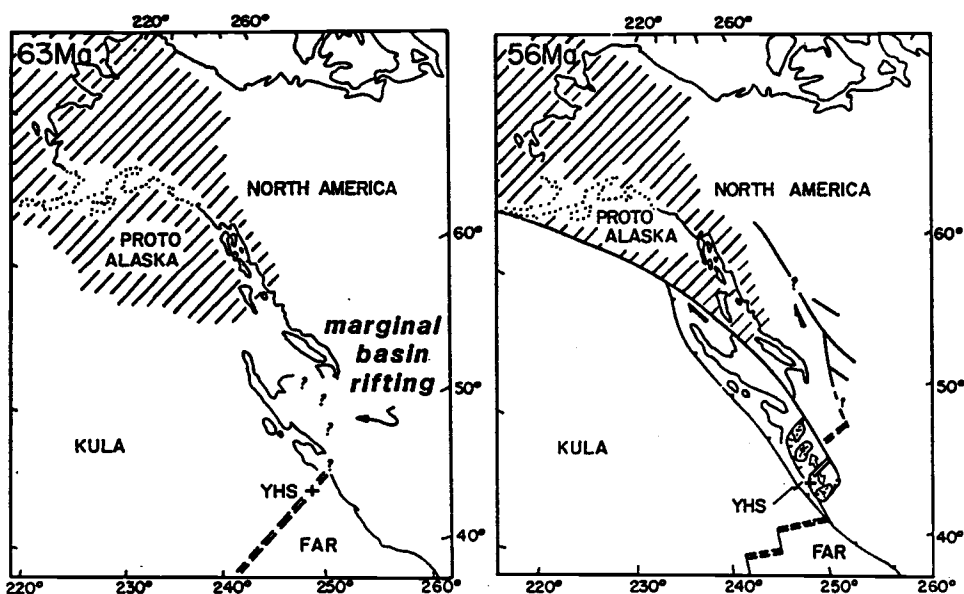


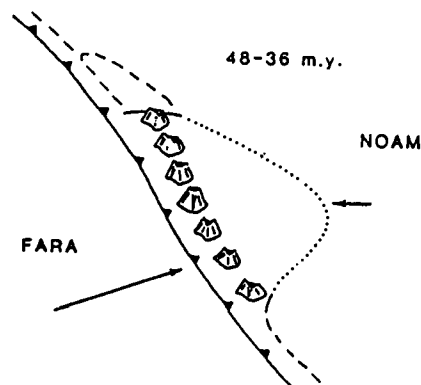
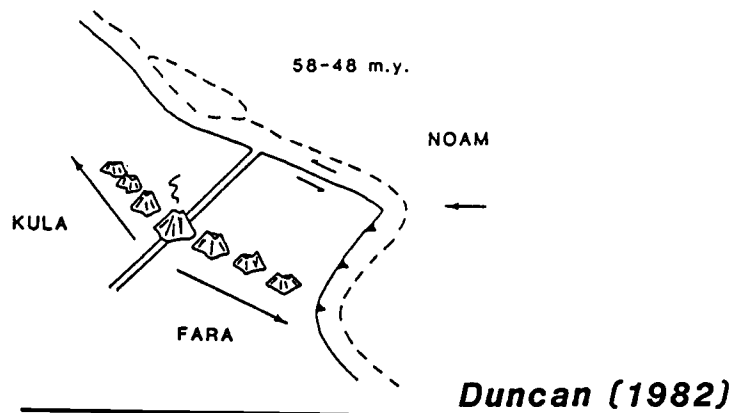
Figure 2.5 Model 1: Subduction related volcanism models proposed for the origin the Oregon-Washington Coast Range province. Upper diagram suggest volcanism occurred along N.-S. trending fissures which opened in response to highly oblique subduction of the Pacific plate beneath the N. American continental margin. Lower diagram proposes marginal basin development along the continental margin also caused by highly oblique plate subduction.

plate. In this case, a short term spreading center may have been set up in an extensional or back arc basin. Magma production and chemistry would presumably reflect the modification of the mantle source by subducted oceanic lithosphere beneath the new spreading system.

Model 2) Basaltic volcanism is associated with a mature mid-ocean ridge spreading center and/or an oceanic island setting. In this case, magma production and chemistry would reflect mantle source(s) that are more typical of melting at diverging plate margins or intraplate sites.

Magma generation within these two environments will impart distinctive trace element characteristics to the erupted basalts. The remainder of this study deals with sorting out the trace element signature found in these rocks and, from these data, interpreting their plate tectonic significance.

Hotspot-Ridge



Wells et al. (1984)

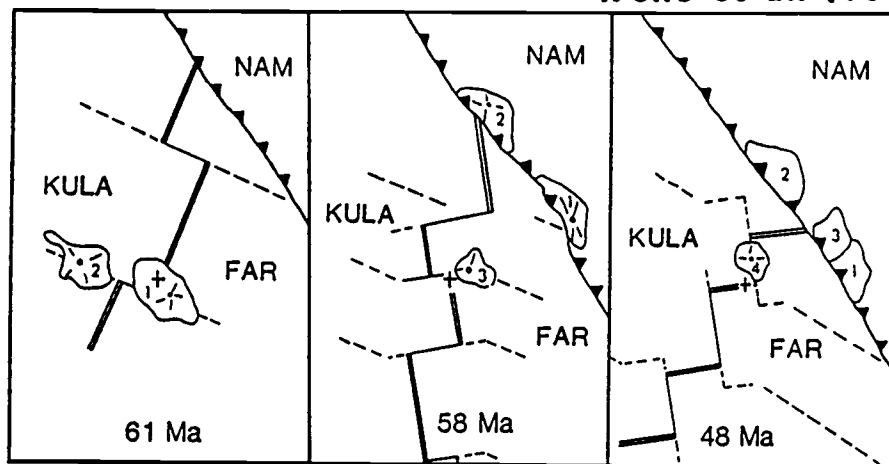


Figure 2.6 Model 2: Hotspot - ridge related volcanism models proposed for the origin of the Oregon-Washington Coast Range province. Upper diagram proposes volcanism is related to a ridge-centered hotspot that produces seamount which diverge on the spreading plates. The lower diagram proposed a ridge-centered or "near" ridge hotspot which creates seamounts at fracture zones during minor plate readjustments.

CHAPTER 3: FIELD AND LABORATORY INVESTIGATIONS

I. Field relationships

Samples were collected during the summers of 1981 and 1982. The limited exposure of most outcrops made correlation of individual flows and interbedded pyroclastic layers between areas impossible. Rarely were significant sections of the volcanic pile observed over areal distances of more than 50 m and only in quarries was there more than 10 or 20 m of vertical exposure of reasonably fresh rock. Most roadcut exposures were much smaller and contained severely weathered basalt as well. The lack of extensive lateral exposure could be somewhat ameliorated by examining numerous road cuts and accessible quarries. These glimpses at the flow type, volcanic detritus and/or pyroclastic debris within each area revealed a general trend that is interpreted as resulting from an eruptive environment that changed from deep water extrusion to shallow water to subaerial volcanism with time.

The lower section of the Roseburg basalt volcanic pile is exposed in the Roseburg and Sugarloaf Mountain areas. This conclusion is based on field work by Baldwin (1974) and Ryberg (1985) in the overlying stratigraphic section, on the morphology of the flows, and on the chemistry of the rocks. The Roseburg and the Sugarloaf rocks are bounded on the northwest by the trace of the Bonanza Fault (Figure 1.2). The basalt flows in the Roseburg region are mostly thick and massive with pillowed margins. Lateral gradation into pillows and pillow breccias is common. Pillows are usually 0.5 to 1.0 m in diameter and, in some areas along the North Umpqua River, they make up entire flows up to 10 m thick. Localized interbeds of basaltic sandstone and conglomerate occur in numerous locations throughout the section. Pebble-sized conglomeritic deposits with well-rounded

clasts are prevalent along the northern edge of the Roseburg outcrop area. A localized, angular, clast-supported basalt breccia, interpreted as a slump feature in the volcanic pile, can be seen along Sunshine road north of Roseburg. Columnar jointing is common in the Roseburg area but only rarely observed in the Sugarloaf area. Pillow basalts are prevalent towards the Sugarloaf area and thin manganese crusts are observed on remnant glass selvages (now weathered to clays) suggesting seafloor hydrothermal circulation.

Alteration is also more pervasive in the Sugarloaf samples. The distribution and nature of the flows in the lower section suggest that the Sugarloaf Mountain area represents the periphery of the basal volcanic pile and the Roseburg area was within the central part of the seamount.

The Red Hill Anticline and the Coquille-Myrtle Point exposure lie to the north of the Roseburg and Sugarloaf areas, respectively. The northeast-southwest structural trend of the area suggests the two sections are equivalent in stratigraphic position even though direct evidence is buried beneath the basin fill of the Tyee Formation. Both of these areas display features which indicate that the flows were subaqueously and subaerially erupted. Pillows are present in each area and massive flows occur as well. These areas also display ropey crusts of "pahoehoe" flow top structure that are characteristic of subaerially erupted fluid basaltic magma. These flow top structures were not seen at any of the other sample localities. Blocky flows which may be of the "aa" type flows were also found in a road cut along Highway 38 between Coquille and Myrtle Point. Alternating layers of lava flows and sediments observed at a quarry in the Coquille-Myrtle Point section may indicate periods in which the crust dilated as magma moved beneath the area, erupted, and then subsided as magma emptied from a magma chamber. Porphyritic augite basalt and feldspar-phyrlic basalt flows similar to rocks described by Snavely et al. (1968) are also found in this basaltic mass. In the Red Hill Anticline no sediment interbeds were observed, but tuffaceous units appear on the periphery of the basalt exposure. Abundant

amygdaloidal basalts are found in this area and alteration is pervasive at some outcrops. At a road cut along the northeast end of the Red Hill section a small erosional gully has been filled with an overlying flow. This outcrop is significant because it is the only evidence found that there may have been a volcanic quiescence before the eruption of the highly alkali, silica undersaturated basalts exposed in the Drain Anticline. These two exposures of basalt, the Red Hill Anticline and the Coquille - Myrtle Point section, are transitional between the dominantly submarine eruptions of the lower tholeiites in the Roseburg and Sugarloaf areas and the dominantly subaerial eruption of the basalts exposed to the northwest. The absence of porphyritic basalt types found in the Coquille-Myrtle Point exposure on the other side of the coast range at Red Hill Anticline indicate that magmatic processes differed within the volcanic pile, but chemical data presented below indicate that these two areas are at equivalent stages of chemical evolution.

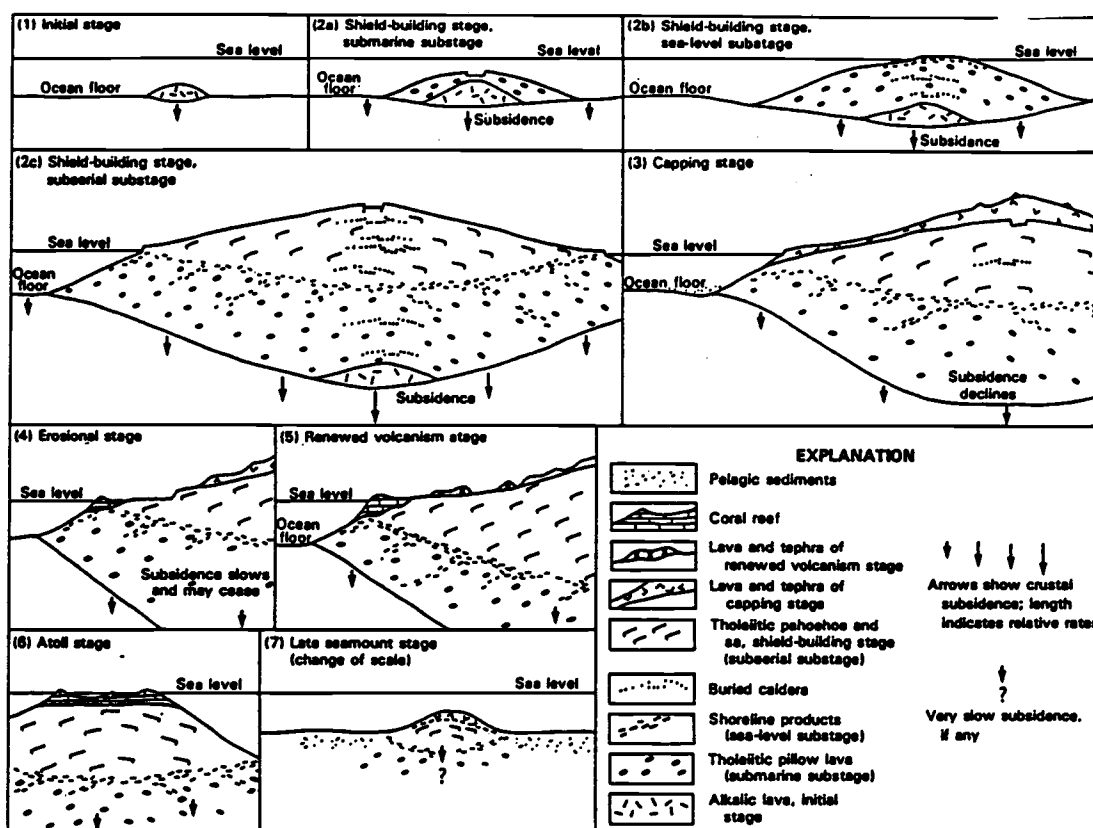
The morphologic and textural differences between flows on the two sides of the Eocene basin become more pronounced in the basalt masses which crop out north of Myrtle Point and Red Hill. This may be partly due to the poor exposure of the outcrops on the west side of the Coast Range, but the rock types and associated pyroclastic material collected from either side of the basin display significant differences, especially in eruptive style. The Drain and Jack Creek Anticlines on the east side of the Coast Range are thinly bedded, aphanitic alkali basalt flows. The flow tops are oxidized to reddish zones that are baked by overlying flows. Fine vitric tuffaceous deposits are abundant in the area. In the Jack Creek Anticline a large section of lapilli crystal tuff is exposed. Hoover (1963) observed "small rounded fragments of basalt" that compose about 20 percent of the lowermost beds of tuff exposed along State Highway 38 (west of Drain) that suggested to him that some of the contacts between pyroclastic rocks and basalt flows were erosional in some places.

In marked contrast to the above sequence, the rocks in the Blue Mountain, Coos River, and Kentucky Slough region on the west side of the Coast Range display highly porphyritic and cumulate textures. The picritic and ankaramitic basalts all were collected from the Blue Ridge area. The volcanic accumulation includes aphanitic and plagioclase porphyritic basalt. The pyroclastic tuffaceous rocks intimately associated with the basaltic flows are highly weathered and field relationships are difficult to establish. An impressive deposit of explosive breccia can be seen along the southern side of the Coos River valley east of Coos Bay. Basaltic boulders in this area range in size from 10 m in diameter to several cm and occur in a red and green tuffaceous matrix. The breccia deposit also incorporates previously consolidated tuffs that are now angular clasts. Most of the basalt clasts are subangular to rounded and many of the "smaller" basalt clasts (< 5 cm) are highly vesiculated. Some of the fragments are encased by thin layers of zeolitic material and the tuffaceous matrix often show signs of alteration due to baking around the clasts. Some of the basalt "ejecta" have bread-crust type textures that were subsequently filled with calcite and zeolite. This type of deposit has been thoroughly discussed by Kokelaar (1986) and is attributed to a volcanic pile building into shallow water depths.

The Kentucky Slough section also displays rock types not found in other parts of the southern Oregon Coast Range. The rocks exposed along the lower part of Kentucky Creek have coarsely crystalline textures which indicate they may be intrusive. Thin sections of the rock show a high abundance of zeolites but the zeolites are incorporated within the texture of the rock and not as vesicle or vein fillings. These zeolites are interpreted as being late stage deuteric minerals that formed as the intrusive body cooled and trapped its volatile constituents. Further up Kentucky creek, aphanitic basaltic flows and tuffaceous deposits similar to material found in the Jack Creek and Drain areas occur.

The volcanic evolution of Hawaiian volcanoes have been recently reviewed by Peterson and Moore (1987). They have defined seven stages in the volcanic history of

GEOLOGIC HISTORY AND EVOLUTION OF GEOLOGIC CONCEPTS, ISLAND OF HAWAII



Diagrams showing successive stages in evolution of a Hawaiian volcano as proposed in this paper. Changes between stages normally are transitional and gradational. For simplicity, feeder conduits and rift zones are omitted. Substantial crustal subsidence caused by volcanic loading occurs throughout growth stages (1) through (3); subsequent sea-level changes may be sporadic, but not subsidence continues into stage (7). Vertical exaggeration varies from approximately 2× to approximately 4×. Only stages (1) through (4) are represented on Hawaii. See text for additional details.

—Revised evolutionary scheme for Hawaiian volcanoes

Stage	Dominant composition of magma	Dominant geologic processes and characteristics ¹
(1) Initial	Alkaline basalt, basanite, transitional basalt	Initial activity of new volcano; rates and frequency of eruption and duration of stage not known; edifices may be steep sided (because only a single example is recognized, this stage is considered provisional).
(2) Shield-building	Tholeiitic basalt, tholeiitic picrite	Frequent voluminous eruptions from central vent and rift zones, historic examples suggest eruptive rates of 1–3 km ³ /100 yr, frequency about 5–50 eruptions/100 yr; shield-shaped edifice built; caldera may form and be refilled repeatedly during any substage.
(2a) Submarine	-- do -----	Products pillow lava and pillow fragments; moderately steeply sloping edifice.
(2b) Sea level	-- do -----	Products hyaloclastites—the result of explosive interaction between sea water and molten lava, and wave abrasion.
(2c) Subaerial	-- do -----	Products chiefly pahoehoe and aa lava flows, interspersed with sporadic tephra produced by occasional explosions; dominantly fluid lava builds gently sloping edifice; processes of 2a and 2b continue.
(3) Capping	Alkaline basalt, transitional basalt, other alkaline rocks ²	Products initially pahoehoe and aa lava flows, increasing proportions of tephra-built cinder cones, gradual or abrupt change to smaller briefer eruptions; increasing lava viscosity (block flows); declining eruptive rates and frequency of eruptions, eventually at intervals exceeding 10 ³ yr; capping structure steeper sided than stage 2c.
(4) Erosional	None	Lack of eruptions allows fluvial and marine erosion to carve valleys, canyons, cliffs, and so on; reefs may develop along some shorelines (erosion operates during all stages, but effects offset by repeated eruptions).
(5) Renewed volcanism	Alkaline basalt, basanite, nephelinite, nepheline melilitite	Sporadic eruptions, generally from vents not related to central conduit or rift zones, commonly explosive though some are effusive. Eruptions are of low volume and widely spaced in time. Erosion and reef building continue.
(6) Atoll	None	Abetted by regional subsidence, fluvial and marine erosion reduce volcano to sea level. Reef building continues, may form ring-shaped group of islands with interior lagoon.
(7) Late seamount	None	Rate of regional subsidence eventually exceeds rate of reef building and island sinks below sea level to become a seamount; gradually mantled by pelagic sediments; subducted edifice may survive for millions of years.

¹In addition to processes listed, regional crustal subsidence caused by weight of growing volcanoes is nearly continuous, resulting in apparent rise in sea level. Episodes of glaciation cause a worldwide drop in sea level, temporarily offsetting steady regional subsidence.

²Other alkaline rocks may include hawaiite, mugearite, basanite, nephelinite, trachyte.

Figure 3.1 Summary of the successive stages in the evolution of a Hawaiian-type volcanic island (reproduced from Peterson and Moore, 1987).

oceanic islands (summarized in Figure 3.1). The Hawaiian-type morphological development of an oceanic island is displayed in the Roseburg volcanic sequence. The lower tholeiites of the southern Coast Range, the Sugarloaf and Roseburg exposures, represent the initial shield-building stage that is dominated by pillow lava (stages 1-2a). The thrust faulting that separates this area from the basalt sections to the north probably marks a zone of weakness in the shield volcano. Detachment of the upper, subaerially erupted flows from the lower pillow basalt pile was facilitated by deposits of pyroclastic material that would have been erupted as the pillowed shield built towards shallower water depths and eventually breached the sea water surface. The Red Hill and Coquille-Myrtle Point sections are the first evidence of emergent volcanic activity (stages 2b-3 and maybe 4). The Blue Ridge, Coos River, Kentucky Slough, Jack Creek and Drain rocks are related to the post-erosional events (stage 5). The last stages of the ocean island scenario results in regional subsidence which in the Oregon case is displayed by the basin development in the Oregon-Washington Coast Range and filling of the basin by middle Eocene sediments such as the Tyee Formation. This characterization is simplified but the specific rock types are represented in the southern Coast Range. An extensive field mapping program in the basalts is needed to determine the regional variation in rock types and their exact relationships to the pyroclastic deposits.

II. Methods

Sampling Procedure

Basalt samples were selected from thirty-seven localities among the several large outcrops (or groups of outcrops) of Roseburg basalt that rim the southern Oregon Eocene coastal basin. The outcrop areas were designated by geographic names and samples taken at those locations were prefixed with abbreviations of those names. The prefixes and corresponding geographic locations are as follows: JC = Jack Creek Anticline, DA = Drain Anticline, RH = Red Hill Anticline, RB = Roseburg Exposure, SL = Sugarloaf Mtn. Exposure, CQ = Coquille to Myrtle Point Exposure, BR = Blue Ridge Exposure, CR = Coos River Exposure, and KS = Kentucky Slough Exposure (see Figure 1.2). Thirty-four major and trace elements have been determined on fifty-four samples. An additional thirteen samples from three lower Eocene volcanic centers in the Washington Coast Range have been analyzed for a similar number of major and trace elements.

Geologic field work in the Oregon Coast Range is almost exclusively limited to stream valleys, road cuts, and rock quarries because of the dense cover of vegetation and the deep soil profile produced by the large annual rainfall. Sampling for this study was conducted primarily to determine the major and trace element characteristics of the major basalt exposures and secondarily, to sample a range of possible magma types found at these different locations. Several samples were usually taken from all the outcrops but only the "least" altered from each area were selected for analyses. Quarries provided the greatest amount of stratigraphic exposure of the lava flows, but reasonable limits to the number of samples which could be analyzed dictated that only one quarry section could be sampled in detail. A stratigraphic section of flows from the Hayhurst quarry near Drain

was sampled because preliminary trace element results showed these highly silica undersaturated alkali basalts to be extremely enriched. Basaltic chemical compositions of this type had not been reported in any other part of the Coast Range. Individual flows were also well defined by baked, reddish-oxidized soil horizons, tuffaceous layers, and in one instance, a red tuffaceous sandstone layer which contains leaf fossils. The distinction of the flows assured that the samples recorded pulses of different magma batches.

Mobil Oil Corporation drilled a test well near Sutherlin, Oregon in an attempt to test an anticlinal structure thought to lie below the Roseburg volcanic rocks which they believed to be composed of lower Eocene Roseburg sediments and possibly natural gas. This well penetrated approximately 4000 m of basalt before drilling was stopped. Well-cuttings were sampled at 150 m intervals and five drill cores were taken at the bottom of the hole. These drilling chips and cores were obtained from Mobil by R. Duncan who kindly provided them for this study.

Nine well-cutting intervals were selected for trace element analyses and basalt fragments were hand picked from the sample bags under a binocular microscope. Because of the small fragment size (usually <3 mm) and the homogenization caused by drilling, each interval represents an "average" chemical composition for ~150 meters of basalt flows (Mobil Sutherlin well chip samples - MSW 5 thru 13; Table 5.2). The number of flows sampled within each interval could not be determined and eruptions of chemically distinct, though volumetrically insignificant, magma types were consequently undetectable. Three drill cores from the lower 10 m of the well were also selected for analyses (MSWC-29,30,31; Table 4.2). Trace element variation in the bottom cores lies within the field of total variation for the 4000 m section and no differentiation trend was observed with depth.

Samples of the Crescent Formation in the central and southern Washington Coast Range (BH = Black Hills basalts and GR = Grays River basalts) and from the Metchosin

Formation (MT) on Vancouver Island, B.C., were selected for analyses because these areas lacked a full suite of trace element data (especially REE) that could be directly compared with the Roseburg data set. This information fills gaps in the chemical data between other more thoroughly studied volcanic centers such as the Crescent Formation in the northern Washington Coast Range and the Siletz River Basalts in the Oregon Coast Range. Conventional K-Ar and $^{40}\text{Ar}/^{39}\text{Ar}$ stepwise heating ages and some $^{87}\text{Sr}/^{86}\text{Sr}$ values have also been reported for these samples (Duncan, 1982). Further trace element work on them seemed appropriate to determine if an age related petrogenetic evolution was present in the Coast Range province.

Sample Preparation

Samples selected for major and trace element analyses were the "freshest" possible rocks available from outcrop sites in the area. In some locations all of the basalt was completely altered to chlorite and clay. Highly weathered basalts were analyzed only if no other basaltic rocks could be found in the area. Most samples exhibited some amount of surface weathering. When possible, weathered surfaces were removed from the hand samples with a trim saw. The interiors of the hand samples were then crushed in a jaw crusher with aluminum oxide plates. The pulverized rocks were then sieved to remove rock powder and size fractions less than 30 mesh (0.6mm). This step helps to avoid contamination by small fragments and powder from samples previously run through the crusher. Large amounts of rock were processed (approx. 10-20 grams) to insure the final powder represented the bulk rock sample. Crushed rock was then rinsed with doubly distilled water and sonic washed to further remove rock powder. The cleaned rock chips were then powdered in a high purity stainless steel ball mill. A stainless steel ball mill was

used because it produces a very fine powder which is necessary to dissolve the sample in acid for atomic absorption analyses. Significant Cr contamination can occur from a stainless steel ball mill but the amount of Cr added to the samples (2-5 ppm) becomes less significant as the amount of Cr in the rock increases. Use of a tungsten carbide ball mill was avoided because of the unmanageable contamination by Ta to the sample. Sample powders from the Metchosin Formation analysed in this study were clearly powdered in a tungsten carbide mill. Tantalum values in these samples were 7 to 10 ppm when other trace constituents indicated the samples should have less than 1 ppm Ta. The stainless steel mill was cleaned between each run by washing with distilled water and rinsing with ethanol. Altered rocks tended to "cake" on the sides of the ball mill which made it necessary to run quartz glass through the mill to remove this remnant powder.

Analytical methods

The final powders were then prepared for major and trace element analyses by atomic absorption spectroscopy (AA), instrumental neutron activation analyses (INAA), and x-ray fluorescence (XRF). Dissolution of the 100-300 mg of sample for AA was carried out according to the procedure of Robbins et al. (1984). INAA procedures were followed from Laul (1979). Si, Al, Ti, Fe, Mn, Mg, Ca, Na, K, Rb, Sr, and Ba were determined by AA. La, Sm, U, Yb, Lu, Nd, Th, Cr, Ce, Hf, Zr, Tb, Sc, Ta, Cs, Co, and Eu were determined by INAA. Ni, Cu, and Zn were determined by XRF.

Two irradiations using the rotating rack assembly in the OSU TRIGA reactor were conducted for this study. The principle standards used were CRB-3, an Oregon State University College of Oceanography in-house standard collected at the same quarry site as the U.S. Geological Survey standard BCR-1, and the National Bureau of Standard NBS

Table 3.1: Comparison of standard reference material elemental abundances determined in this study with values obtained from published compilations.

	CRB-3 OC STD This study		BCR-1 USGS STD Gladney et al. (1983)		BHVO-1 USGS STD This study		BHVO-1 USGS STD Gladney and Goode (1981)		JB-1 GSJ STD This study		JB-1 GSJ STD Ando and Terashima (1985)	
	(n=9)				(n=1)				(n=2)			
SiO ₂ (wt.%)	55.27	(±0.37)	54.3	(±0.51)	-	-	49.9	(±0.8)	-	-	52.17	
TiO ₂	2.49	(±0.04)	2.22	(±0.1)	-	-	2.65	(±0.09)	-	-	1.34	
Al ₂ O ₃	13.54	(±0.19)	13.62	(±0.25)	-	-	13.8	(±0.2)	-	-	14.53	
FeO(t)	12.28	(±0.14)	12.07	(±0.28)	-	-	11.21	(±0.18)	-	-	8.07	
MnO	0.193	(±0.006)	0.182	(±0.011)	-	-	0.166	(±0.005)	-	-	.16	
MgO	3.55	(±0.06)	3.45	(±0.17)	-	-	7.14	(±0.20)	-	-	7.73	
CaO	7.31	(±0.12)	6.95	(±0.15)	-	-	11.4	(±0.2)	-	-	9.29	
Na ₂ O	3.21	(±0.04)	3.28	(±0.11)	-	-	2.21	(±0.09)	-	-	2.79	
K ₂ O	1.76	(±0.02)	1.69	(±0.08)	-	-	0.55	(±0.08)	-	-	1.42	
P ₂ O ₅	-	-	.37	(±0.2)	-	-	0.29	(±0.4)	-	-	.28	
-H ₂ O	-	-	.78	(±0.26)	-	-	.05	-	-	-	.95	
+H ₂ O	-	-	.78	(±0.20)	-	-	.23	-	-	-	1.02	
LOI	-	-	-	-	-	-	-	-	-	-	-	
total	-	-	99.96	-	-	-	99.60	-	-	-	99.73	
	(n=5)				(n=5)				(n=5)			
Sc (ppm)	32.6	(±0.78)	32.8	(±1.7)	30.5	-	30	(±2)	27.9	(±1.3)	27.4	
Cr	15.7	(±4.7)	18	(±4)	264	-	300	(±30)	460	(±38)	469	
Co	37.6	(±0.14)	36.3	(±1.8)	45	-	45	(±1)	38	(±1.3)	38.7	
Ni	15	-	13	(±4)	-	-	117	(±18)	-	-	139	
Cu	-	-	-	-	-	-	-	-	-	-	56.3	
Zn	-	-	-	-	-	-	-	-	-	-	83	
Rb	51	(±3)	47.1	(±0.8)	-	-	10	(±2)	-	-	41.2	
Sr	380	(±59)	330	(±5)	-	-	440	(±70)	-	-	435	
Cs	1.1	-	0.97	(±0.13)	-	-	0.086	-	-	-	1.19	
Ba	760	(±13)	678	(±18)	-	-	142	(±18)	-	-	490	
Zr	160	(±47)	191	(±5)	182	-	180	(±30)	133	(±33)	143	
Hf	4.61	(±.27)	4.9	(±0.3)	4.6	-	4.2	(±0.2)	3.73	(±0.15)	3.4	
Ta	0.82	(±0.04)	0.79	(±0.09)	1.16	-	1.1	(±0.2)	2.45	(±0.07)	3.6	
Th	6.1	(±0.07)	6.04	(±0.6)	1	-	1.1	(±0.2)	9.4	(±0.49)	9.2	
U	1.7	(±0.06)	1.71	(±0.16)	0.6	-	0.42	(±0.06)	2.1	(±0.4)	1.7	
La	26	-	25.0	(±0.08)	15.6	-	16.7	(±0.8)	37.1	(±1.5)	38	
Ce	55.1	(±0.14)	53.7	(±0.8)	37.7	-	41	(±4)	67.4	(±6)	67	
Nd	29.7	(±1)	28.7	(±0.8)	26.4	-	24	(±6)	29	-	27	
Sm	6.58	(±0.11)	6.58	(±0.17)	5.9	-	6.1	(±0.7)	4.75	(±0.35)	5	
Eu	1.90	(±0.04)	1.96	(±0.05)	1.94	-	2	(±0.4)	1.43	(±0.84)	1.52	
Tb	1.03	(±0.04)	1.05	(±0.09)	0.97	-	1	(±0.2)	0.73	(±0.014)	1.2	
Yb	3.4	(±0.03)	3.39	(±0.08)	1.85	-	2.1	(±0.5)	2.68	(±0.11)	2.1	
Lu	0.53	-	0.51	(±0.03)	0.29	-	0.32	-	0.37	(±0.05)	0.31	

Coal-Fly Ash. A CRB-3 standard was also run in each irradiation as an unknown along with either the Geological Survey of Japan basalt JB-1 or the U.S. Geological Survey Hawaiian Basalt BHVO-1, or both. Elemental abundances for these standards from this study and "consensus" values are given in Table 4.1. Sample duplicates were run in each irradiation and two samples from the first irradiation were run in the second irradiation to determine if an analytical bias was present between runs; none was detected. Trace element abundance values between sample duplicates were usually within counting statistic errors and some results were better than expected from counting statistics. The estimated errors for INAA were based on duplicate samples or on counting statistics, whichever was greater.

A similar procedure for assuring data quality was followed when analyzing for major element abundance by AA. Two to three splits of CRB-3 and sample duplicates were dissolved along with the unknowns. Nine splits of CRB-3 were dissolved and run during the course of the study and some of these dilutions were analyzed more than once for nine major elements. The mean and standard deviation of 12 different AA runs on CRB-3 are given in Table 4.1. All the major element results fall within the error limits of the consensus values reported by Gladney et al. (1983) except for Ti. Ti was consistently higher than the reported BCR-1 values throughout all of the AA runs. The precision was less than 2% for the higher Ti value (2.49%). This consistently high value indicated the digested rock solutions may have had signal interferences which were not present in the standard solutions. A practical normalization factor (observed value/consensus value) was applied to all the unknowns to reduce the observed TiO₂ value of CRB-3 (2.49%) to the accepted value (2.22%).

Chapter 4: Major Element Geochemistry

I. Basalt Classification

A number of classification schemes have been proposed for the subdivision of basaltic rock types (Kennedy, 1933; Tilley, 1950; Yoder and Tilley, 1962; Kushiro and Kuno, 1963; MacDonald and Katsura, 1964; Miyashiro, 1978). The most accurate determination of basalt type relies on both the mineralogical and chemical constitution of the rock. The major subdivision of basaltic rocks as alkali or tholeiite is essentially based on a reaction relationship between olivine and Ca-poor pyroxene (orthopyroxene). Tholeiite is a silica saturated rock in which magnesian olivine reacts with the magma and is converted to an equilibrium orthopyroxene. Alkali basalt is a silica undersaturated rock in which both olivine and clinopyroxene crystallized in equilibrium with each other. So, essentially, the presence of low Ca-pyroxene (pigeonite) in a basalt would designate the rock as a tholeiite.

Tilley (1950) first proposed using a dividing line on an silica (SiO_2) versus total alkalis ($\text{Na}_2\text{O} + \text{K}_2\text{O}$) diagram to categorize basaltic rocks as either alkali basalt or tholeiite basalt. MacDonald and Katsura (1964) expanded this idea and derived a classification scheme that used an alkali-tholeiite field boundary on Tilley's diagram as a first order designation of Hawaiian basaltic rocks into the tholeiitic suite or alkalic suite. Further refinement of the rock type names were defined according to their modal mineral content. Hart (1970) showed that seawater alteration of a tholeiitic basalt removes silica and adds alkalis to the rock. This process could move compositions that lie close to the tholeiite-alkali dividing line from the tholeiite field into the alkali field. Some Roseburg tholeiites may plot in the alkali field on this diagram due to the variable degrees of alteration which

most of the Roseburg basalts have undergone. The designation of basalt in the southern Oregon Coast Range as alkali or tholeiite is loosely based on the alkali-tholeiite dividing line proposed by MacDonald and Katsura (1964) but other considerations, such as trace element composition of the rock, have been used to classify the basalts.

The nomenclature used in this study is based on the above guidelines and on normative mineral content rather than by modal mineral content. This procedure was followed because thin sections were not available for all of the samples and modal analyses of the available thin sections were not performed. Secondary alteration phases of the mafic minerals (olivine and pyroxene) have obscured or completely replaced much of the original crystalline texture of the rocks and the magmatic relationships between olivine and pyroxene and/or the host liquid are not determinable. In the following discussion, tholeiite generally refers to basalt lying below the dividing line on the alkali vs. silica diagram and alkali basalt generally refers to basalts that plot above this line. Further subdivision is given below:

Tholeiite - normative quartz and normative hypersthene

Olivine Tholeiite - normative hypersthene and > 5% normative olivine

Alkali basalt - < 5% normative hypersthene or < 5% normative nepheline

Basanite - > 5% normative nepheline

Ankaramite - abundant phenocrysts of olivine and augite, >15% normative olivine

Picrite - abundant phenocrysts of olivine, >20% normative olivine

Hypersthene normative rocks are technically tholeiites according to the classification of Yoder and Tilley (1962). This would suggest that the definition of alkali basalt given above is wrong. MacDonald and Katsura (1964) point out that the presence or absence of normative hypersthene depends on the oxidation state of iron and that the degree of alkali enrichment is a better criterion for separating alkalic from tholeiitic basalt. Classifications based on normative mineral content suffer from uncertainties in the oxidation state of the original melt and oxidation of the basalt after eruption by post consolidation alteration. The ferrous to ferric iron ratio of a rock sample is an indicator of this oxidation state, but it may not reflect the actual initial oxidation state of the melt. Higher amounts of ferrous iron (more oxidized) result in the calculation of a more saturated normative mineral content for the rock sample (greater amounts of hypersthene and quartz)

Normative mineral contents of the Roseburg basalt were calculated using an oxidation ratio of $\text{Fe}_2\text{O}_3 = 30\%$ of FeO(t) . This high oxidation ratio was chosen because ferric and ferrous iron determination on samples from the Roseburg area (Wells and Waters, 1935; Snively, 1986 unpublished data) and the Siletz River basalts (Snively et al., 1968) were similar or higher than this value. The lowest $\text{Fe}_2\text{O}_3/\text{FeO(t)}$ ratio measured from these two areas probably approaches the true oxidation state of the original magma but undoubtedly is high due to alteration. Using a $\text{Fe}_2\text{O}_3/\text{FeO(t)}$ ratio similar to the Siletz River basalts facilitates comparison of the normative mineralogies between the two areas. This procedure was followed to insure that the rock names assigned to the samples would not overstate their alkaline affinities. The normative mineral contents listed in Tables 4.1a-e and 4.2 are actually more "saturated" than should be expected from normal mantle oxidation states. $\text{Fe}_2\text{O}_3/\text{FeO(t)}$ ratios in MORB magmas are 10% or less (BVSP, 1980; Christie et al., 1986) and the oxidation state of the most reduced alkali basalts are approximately $\text{Fe}_2\text{O}_3/\text{FeO(t)}=20\text{-}25\%$ (Sun and Hanson, 1975; Clague and

Table 4.1a: Major element compositions and normative mineral content of the Roseburg basalts.

Sample	RB 1	RB 622	RB 2	RB 16	RB 611	RB 7	RB 22	SL 5	SL 4	SL 2	FMP 1
Rock Type	thol†	thol	thol	thol	thol	thol	thol	thol	thol	thol	ol thol
Roseburg ††								Sugarloaf Mountain			
Wt% Oxide											
SiO2	47.72	46.79	48.25	48.03	47.72	48.01	50.05	48.05	48.22	48.63	45.83
TiO2	1.75	1.68	1.93	1.85	2.02	1.77	2.44	1.75	1.77	1.85	2.01
Al2O3	13.83	13.27	13.61	13.86	13.19	13.14	13.55	13.86	13.35	14.28	13.58
FeO(t)	11.65	11.39	12.72	12.86	13.05	12.09	11.29	11.96	11.98	11.77	11.47
MnO	0.20	0.19	0.21	0.22	0.22	0.19	0.24	0.19	0.23	0.24	0.39
MgO	7.54	7.00	6.81	6.71	6.35	6.33	5.27	7.15	7.13	6.80	7.27
CaO	12.98	11.23	12.36	10.99	11.92	12.12	10.98	11.84	10.66	11.95	12.41
Na2O	2.13	2.06	2.20	2.41	2.27	2.07	2.87	2.33	2.53	2.52	2.51
K2O	0.11	0.37	0.21	0.51	0.22	0.10	0.17	0.17	0.48	0.09	0.12
P2O5	0.14	0.15	0.17	0.17	0.19	0.16	0.23	0.16	0.16	0.17	0.19
LOI	1.54	4.16	1.94	1.72	1.36	3.11	1.77	2.20	2.42	1.46	4.92
total	99.59	98.28	100.41	99.33	98.51	99.09	98.86	99.66	98.93	99.76	100.70
Mg*	39.3	38.1	34.9	34.3	32.7	34.4	31.8	37.4	37.3	36.6	38.8
Wt% NORM											
Qtz	-	1.68	1.35	0.48	1.82	3.63	5.04	0.77	0.53	0.95	-
Or	0.66	2.32	1.26	3.09	1.34	0.62	1.03	1.03	2.94	0.54	0.74
Ab	18.37	18.51	18.89	20.88	19.76	18.24	25.00	20.22	22.17	21.68	22.16
An	28.39	27.47	27.04	26.11	25.88	27.36	24.28	27.55	24.49	27.85	26.54
Ne	-	-	-	-	-	-	-	-	-	-	-
Di	29.42	24.83	27.75	23.34	27.51	27.87	24.65	25.70	23.74	25.46	29.51
Hy	13.57	15.73	13.50	15.90	12.97	12.48	9.19	15.18	16.41	13.91	4.02
Ol	-	-	-	-	-	-	-	-	-	-	6.93
Mt	5.55	5.65	6.03	6.15	6.27	5.88	5.43	5.73	5.80	5.59	5.59
Il	3.39	3.39	3.72	3.60	3.95	3.50	4.77	3.41	3.48	3.57	3.98
Cr	0.04	0.04	0.03	0.03	0.02	0.03	0.03	0.04	0.03	0.03	0.04
Ap	0.33	0.37	0.40	0.40	0.45	0.39	0.55	0.38	0.39	0.40	0.46
Zr	-	0.01	0.03	0.02	0.03	0.01	0.02	-	0.02	0.02	0.03
total	99.72	100.00	100.00	100.00	100.00	100.01	99.99	100.01	100.00	100.00	100.00

† thol=tholeiite, ol thol=olivine tholeiite, alk=alkali basalt, alk ol=alkali olivine basalt, bas=basanite, ank=ankaramite, pic=picrite.

†† Sample collection location given in appendix A.

Table 4.1b: Roseburg major elements (cont.).

Sample	CQ 5	CQ 11	CQ 6	CQ 4	CQ 3	RH 1	RH 7	RH 4	RH 303	RH 283	DCLP 1
Rock Type	ol thol	thol	alk	thol	alk ol	alk ol	alk ol	thol	thol	thol	thol
Coquille-Myrtle Point						Red Hill					
Wt% Oxide											
SiO2	47.59	47.25	47.48	48.22	47.54	44.37	46.57	48.26	46.48	47.72	49.00
TiO2	1.77	1.77	1.95	2.65	1.77	2.25	2.62	2.26	2.56	2.98	2.19
Al2O3	13.43	14.04	13.43	13.75	18.86	15.00	13.35	14.15	14.14	13.19	14.78
FeO(t)	11.51	10.12	11.91	13.08	10.12	12.29	13.85	12.67	13.10	13.25	11.77
MnO	0.20	0.19	0.24	0.19	0.18	0.17	0.20	0.22	0.19	0.21	0.18
MgO	8.38	7.53	7.21	5.52	4.38	6.97	6.91	6.68	6.15	6.10	6.17
CaO	11.89	12.56	11.01	11.48	12.68	11.03	9.50	11.76	11.56	11.68	11.98
Na2O	2.36	2.12	3.28	2.53	2.70	1.87	3.51	2.26	2.42	2.46	2.52
K2O	0.22	0.09	0.43	0.30	0.52	1.10	0.07	0.19	0.30	0.55	0.13
P2O5	0.13	0.14	0.15	0.23	0.20	0.21	0.23	0.21	0.23	0.32	0.22
LOI	2.47	2.80	2.44	1.28	1.02	5.74	3.17	0.73	1.60	1.00	0.97
total	99.95	98.61	99.53	99.23	99.97	101.00	99.98	99.39	98.21	99.46	99.91
Mg*	42.1	39.7	37.7	29.7	30.2	36.2	33.3	34.5	31.9	31.5	34.4
Wt% NORM											
Qtz	-	0.61	-	2.73	-	-	-	1.97	0.14	1.25	2.18
Or	1.33	0.55	2.61	1.81	3.10	6.82	0.43	1.14	1.82	3.30	0.78
Ab	20.47	18.71	27.73	21.83	23.08	16.60	30.65	19.37	21.07	21.12	21.53
An	26.04	29.76	21.25	25.79	38.19	30.73	21.12	28.27	27.61	23.67	28.92
Ne	-	-	0.45	-	-	-	-	-	-	-	-
Di	27.12	27.64	27.79	25.19	19.76	20.48	21.29	23.98	24.37	26.93	24.19
Hy	11.74	13.88	-	10.66	3.06	6.31	5.58	14.38	13.09	10.86	12.06
Ol	3.95	-	10.24	-	4.14	7.98	8.51	-	-	-	-
Mt	5.51	4.93	5.73	6.24	4.78	6.03	6.68	6.00	6.30	6.28	5.55
Il	3.45	3.51	3.81	5.13	3.40	4.48	5.14	4.35	5.00	5.74	4.20
Cr	0.07	0.06	0.03	0.04	0.01	0.03	0.03	0.02	0.02	0.02	0.05
Ap	0.31	0.34	0.36	0.55	0.47	0.51	0.55	0.49	0.55	0.75	0.52
Zr	0.01	-	-	0.02	0.02	0.03	0.02	0.02	0.01	0.05	0.03
total	100.00	99.99	100.00	99.99	100.01	100.00	100.00	99.99	99.98	99.97	100.01

Table 4.1c: Roseburg major elements (cont.).

Sample	BR 22	BR 24	BR 24 a	BR 3	BR 2	CR 25	CR 1	KS 3	KS 1
Rock Type	pic	ank	ank	alk ol	alk ol	alk ol	alk ol	bas	alk
Blue Ridge Mountain						Coos River		Kentucky Slough	
Wt% Oxide									
SiO2	44.84	45.23	47.18	46.07	48.08	47.29	47.87	46.34	46.04
TiO2	1.25	0.78	1.34	1.65	1.80	1.44	1.84	1.36	1.85
Al2O3	8.77	9.62	12.33	14.90	15.25	15.81	16.30	15.32	17.09
FeO(t)	9.42	9.60	10.44	10.88	10.13	9.50	10.17	9.80	11.55
MnO	0.16	0.19	0.18	0.19	0.19	0.18	0.19	0.17	0.23
MgO	17.60	15.70	13.94	8.08	7.43	9.74	8.03	9.52	6.52
CaO	13.44	14.16	11.72	11.68	13.28	10.93	10.02	10.22	10.21
Na2O	0.92	2.10	1.83	2.50	2.24	2.65	3.05	3.54	3.26
K2O	0.26	1.09	0.41	0.43	0.62	0.40	0.54	0.65	1.06
P2O5	0.20	0.57	0.17	0.15	0.23	0.19	0.28	0.17	0.30
LOI	2.18	1.64	0.98	3.71	1.15	1.74	1.47	3.57	1.30
total	99.04	100.68	100.32	100.22	100.40	99.87	99.76	100.66	99.41
Mg*	65.1	62.1	57.2	42.7	42.3	50.6	42.8	49.3	36.1
Wt% NORM									
Qtz	-	-	-	-	-	-	-	-	-
Or	1.58	6.49	2.43	2.63	3.69	2.41	3.24	3.95	6.38
Ab	8.01	0.53	13.86	21.91	19.08	22.82	26.23	21.18	21.82
An	19.59	13.71	25.24	29.17	29.92	30.59	29.67	24.68	29.40
Ne	-	9.41	-	-	-	-	-	5.22	3.39
Di	37.88	42.66	25.67	24.13	28.31	18.81	15.43	21.25	16.67
Hy	1.56	-	9.22	1.64	4.72	3.46	6.11	-	-
Ol	23.53	19.67	15.51	11.63	5.47	14.01	10.19	15.83	12.52
Mt	4.53	4.52	4.90	5.26	4.76	4.52	4.83	4.71	5.50
Il	2.44	1.49	2.56	3.25	3.44	2.78	3.55	2.66	3.58
Cr	0.39	0.18	0.21	0.02	0.05	0.12	0.06	0.10	0.03
Ap	0.48	1.33	0.40	0.36	0.54	0.45	0.66	0.41	0.71
Zr	-	-	-	0.02	0.02	0.02	0.04	0.02	-
total	99.99	99.99	100.00	100.02	100.00	99.99	100.01	100.01	100.00

Table 4.1d: Roseburg major elements (cont.).

Sample	JC 2a	JC 223	JC 1	JC 2	DA 1	DA 252a	DA 252b	DA 252c	DA 252e	DA 221a	DA 232
Rock Type	alk ol	alk ol	alk ol	alk ol	alk	bas	bas	alk	alk ol	alk ol	alk ol
Jack Creek					Drain						
Wt% Oxide											
SiO2	47.71	47.00	46.98	46.92	43.09	42.80	43.57	43.06	45.22	45.28	49.18
TiO2	1.25	2.03	1.86	2.73	3.76	3.22	3.05	3.60	2.88	2.34	2.48
Al2O3	18.51	16.05	17.49	14.25	15.30	14.03	15.50	15.57	16.53	16.71	17.16
FeO(t)	8.96	12.11	10.82	14.55	14.37	14.00	12.94	14.07	12.83	12.71	12.57
MnO	0.14	0.21	0.19	0.27	0.22	0.29	0.24	0.24	0.26	0.22	0.22
MgO	8.96	6.42	6.04	4.71	6.97	6.88	6.90	5.89	4.96	5.72	3.69
CaO	12.42	11.74	11.77	9.80	9.11	10.08	9.85	9.61	8.24	10.85	6.97
Na2O	1.86	2.49	2.63	3.18	3.17	3.57	3.52	2.82	3.29	2.44	4.48
K2O	0.03	0.57	0.71	0.78	1.21	1.37	1.19	1.20	1.14	0.68	1.26
P2O5	0.11	0.26	0.29	0.34	0.58	0.80	0.62	0.60	0.64	0.30	0.57
LOI	1.56	1.20	1.72	1.29	2.15	2.38	1.96	2.36	2.68	2.19	1.96
total	101.51	100.08	100.50	98.82	99.93	99.42	99.34	99.02	98.67	99.44	100.54
Mg*	50.0	34.6	35.8	24.5	32.7	33.0	34.8	29.5	27.9	31.0	22.7
Wt% NORM											
Qtz	-	-	-	-	-	-	-	-	-	-	-
Or	0.18	3.40	4.24	4.72	7.30	8.32	7.21	7.32	7.01	4.13	7.54
Ab	15.73	21.29	22.51	27.57	20.20	15.06	17.92	21.26	28.96	21.21	38.41
An	42.05	31.26	34.21	22.86	24.45	18.72	23.56	27.13	28.06	33.53	23.30
Ne	-	-	-	-	3.89	8.67	6.83	1.83	-	-	-
Di	15.24	21.21	18.80	20.47	14.81	22.82	18.56	15.33	8.67	16.32	6.89
Hy	14.79	6.59	2.30	8.06	-	-	-	-	4.48	6.63	3.71
Ol	5.12	5.98	8.51	3.19	13.75	11.40	12.24	11.79	9.30	6.75	8.03
Mt	4.18	5.72	5.11	6.97	6.86	6.73	6.20	6.79	6.24	6.10	5.95
Il	2.37	3.90	3.57	5.31	7.29	6.29	5.94	7.06	5.69	4.57	4.77
Cr	0.08	0.01	0.03	-	-	-	0.01	-	-	-	-
Ap	0.26	0.61	0.68	0.81	1.38	1.91	1.48	1.44	1.55	0.72	1.34
Zr	-	0.03	0.04	0.04	0.05	0.08	0.06	0.06	0.06	0.04	0.05
	100.00	100.00	100.00	100.00	99.98	100.00	100.01	100.01	100.02	100.00	99.99

Table 4.2: Major and trace element compositions of core samples from the Mobil Sutherland test well.

Sample	MSWC 28	MSWC 30	MSWC 31
Rock Type	thol	ol thol	thol
Wt% Oxide			
SiO ₂	47.35	46.29	48.20
TiO ₂	2.50	2.27	2.80
Al ₂ O ₃	14.24	14.11	11.94
FeO(t)	13.21	13.20	14.30
MnO	0.22	0.21	0.23
MgO	5.67	8.43	6.73
CaO	10.40	10.94	11.14
Na ₂ O	2.68	2.46	2.02
K ₂ O	0.36	0.12	0.12
P ₂ O ₅	0.21	0.20	0.27
LOI	1.91	2.69	1.41
total	98.75	100.92	99.16
Mg*	30.0	39.0	32.0
Wt% NORM			
Qtz	1.34	-	5.02
Or	2.20	0.72	0.73
Ab	23.40	21.17	17.47
An	26.58	27.57	23.68
Ne	-	-	-
Di	20.71	21.34	25.32
Hy	13.94	10.79	14.82
Ol	-	7.19	-
Mt	6.37	6.27	6.83
Il	4.90	4.39	5.44
Cr	0.03	0.05	0.02
Ap	0.50	0.47	0.64
Zr	0.04	0.03	0.04
	100.01	99.99	100.01
Sc	37.2	37.9	37.0
Cr	126	232	94
Co	49.5	54.5	51.6
Ni	83	121	83
Cu	-	-	-
Zn	-	-	-
Rb	3	2.7	0.9
Sr	339	290	222
Cs	-	-	-
Ba	100	45	74
Zr	174	133	195
Hf	4.65	3.91	4.87
Ta	0.85	0.63	0.89
Th	1.14	0.83	1.08
U	0.2	0.2	0.9
La	14.3	9.8	12.9
Ce	32.8	25.2	34.0
Nd	21	17	-
Sm	5.77	4.70	6.20
Eu	1.93	1.61	2.07
Tb	0.87	0.75	0.91
Yb	2.78	2.43	3.13
Lu	0.48	0.41	0.47
*t REE	79.9	61.9	-

Table 4.3: Major element compositions and normative mineral contents of Washington and British Columbia Coast Range Basalts.

Sample	MT 2	MT 3	MT 4	BH 23	BH 19	BH 18	BH 7	BH 6	GR 1	GR 2	GR 3	GR 4	GR 5
Rock Type	thol	thol	thol	thol	thol	thol	thol	thol	thol	thol	thol	thol	thol
	Metchosin Basalts			Black Hills Basalts					Grays River Basalts				
Wt% Oxide													
SiO ₂	49.52	51.08	53.59	47.90	49.39	48.67	47.85	48.01	48.68	48.02	47.96	48.20	49.06
TiO ₂	1.52	1.49	1.33	2.16	2.36	2.47	3.16	3.15	2.79	2.48	3.00	2.41	2.78
Al ₂ O ₃	13.92	13.87	14.62	14.02	13.91	13.66	13.08	13.15	12.68	14.39	13.46	15.27	15.15
FeO(t)	12.56	13.33	10.68	11.73	11.40	12.38	13.93	14.11	14.13	13.34	14.09	12.25	11.88
MnO	0.22	0.27	0.13	0.20	0.18	0.16	0.21	0.21	0.25	0.24	0.22	0.22	0.19
MgO	7.22	6.20	5.64	7.19	6.68	6.57	5.77	5.73	6.44	5.65	5.73	5.51	4.64
CaO	10.52	9.69	9.43	12.00	12.46	11.88	10.94	10.91	10.35	11.17	10.85	11.16	9.51
Na ₂ O	2.38	2.51	3.71	2.28	2.53	2.51	2.69	2.73	2.45	2.48	2.55	2.53	3.07
K ₂ O	0.22	0.07	0.07	0.35	0.35	0.32	0.33	0.41	0.35	0.09	0.12	0.30	0.80
P ₂ O ₅	0.14	0.18	0.23	0.20	0.25	0.23	0.32	0.31	0.30	0.26	0.33	0.26	0.42
LOI	1.50	0.90	0.90	1.20	0.85	0.59	0.03	0.32	0.99	1.05	1.04	1.00	1.68
total	99.71	99.59	100.33	99.23	100.36	99.44	98.31	99.04	99.59	99.17	99.35	99.11	99.18
Mg*	36.5	31.7	34.5	38.0	36.9	34.7	29.3	28.9	31.3	29.8	28.9	31.0	28.1
Wt% NORM													
Qtz	2.64	6.17	4.73	0.40	1.38	1.43	2.18	1.82	3.58	2.96	3.41	2.38	2.84
Or	1.32	0.42	0.42	2.11	2.08	1.91	1.98	2.45	2.10	0.54	0.72	1.81	4.84
Ab	20.20	21.51	31.56	19.67	21.50	21.47	23.15	23.38	21.05	21.37	21.93	21.81	26.62
An	27.12	26.71	23.15	27.52	25.68	25.34	23.03	22.69	22.92	28.38	25.34	29.98	25.82
Ne	-	-	-	-	-	-	-	-	-	-	-	-	-
Di	20.41	17.05	18.22	25.82	28.17	26.60	24.57	24.60	22.23	21.57	22.25	20.18	16.28
Hy	18.73	18.50	13.76	14.20	10.71	12.05	11.58	11.54	15.27	13.35	13.02	12.71	11.44
Ol	-	-	-	-	-	-	-	-	-	-	-	-	-
Mt	5.97	6.31	5.02	5.59	5.35	5.85	6.62	6.67	6.70	6.35	6.69	5.83	5.69
Il	2.94	2.87	2.54	4.18	4.50	4.74	6.10	6.06	5.38	4.80	5.79	4.66	5.41
Cr	0.02	0.02	0.03	0.04	0.03	0.03	0.02	0.02	0.04	0.03	0.02	0.02	0.04
Ap	0.33	0.42	0.54	0.47	0.58	0.54	0.76	0.73	0.71	0.62	0.78	0.62	1.00
Zr	0.01	0.01	0.03	-	0.02	0.03	0.02	0.04	0.03	0.03	0.03	-	0.01
	99.69	99.99	100.00	100.00	100.00	99.99	100.01	100.00	100.01	100.00	99.98	100.00	99.99

Frey, 1982). Normative quartz in some of the Roseburg tholeiites is likely an artifact of the assumed oxidation state used for the normative calculation. This point is particularly important for comparing the Roseburg basalts with the Siletz River basalts to the north.

The Roseburg basalts are plotted in the Ne-Ol-Di-Hy-Qtz system of Yoder and Tilley (1962) in Figure 4.1. Snavely et al. (1968) stated that the lower unit of the Siletz River Volcanics is predominantly oversaturated tholeiitic basalts with olivine tholeiites less common. The normative mineralogy of the Roseburg basalts is more undersaturated than the Siletz River basalts and indicates that a distinction between the two areas can be made from the major element contents of the two volcanic centers. According to the classification outlined above the basalts from the Roseburg and Sugarloaf areas are predominately tholeiites. Tholeiites are also present in the Red Hill and Coquille-Myrtle Point exposures but they are interbedded with more differentiated rock types. Both these areas contain tholeiite, olivine tholeiite, and alkali basalt compositions. The association of the different rock types at these locations exemplifies the transitional nature of the Red Hill and Coquille-Myrtle Point basaltic exposures. Generally, picrites, ankaramites, and alkali basalt occur in the Blue Ridge, Coos River, and Kentucky Slough regions, although basanitic compositions are present in the Kentucky Slough area. Alkali and undersaturated basanitic basalt crop out in the Jack Creek and the Drain anticlines, respectively. These groups of highly undersaturated basalts are believed to be the last stage of magma generation in the southern Oregon Coast Range.

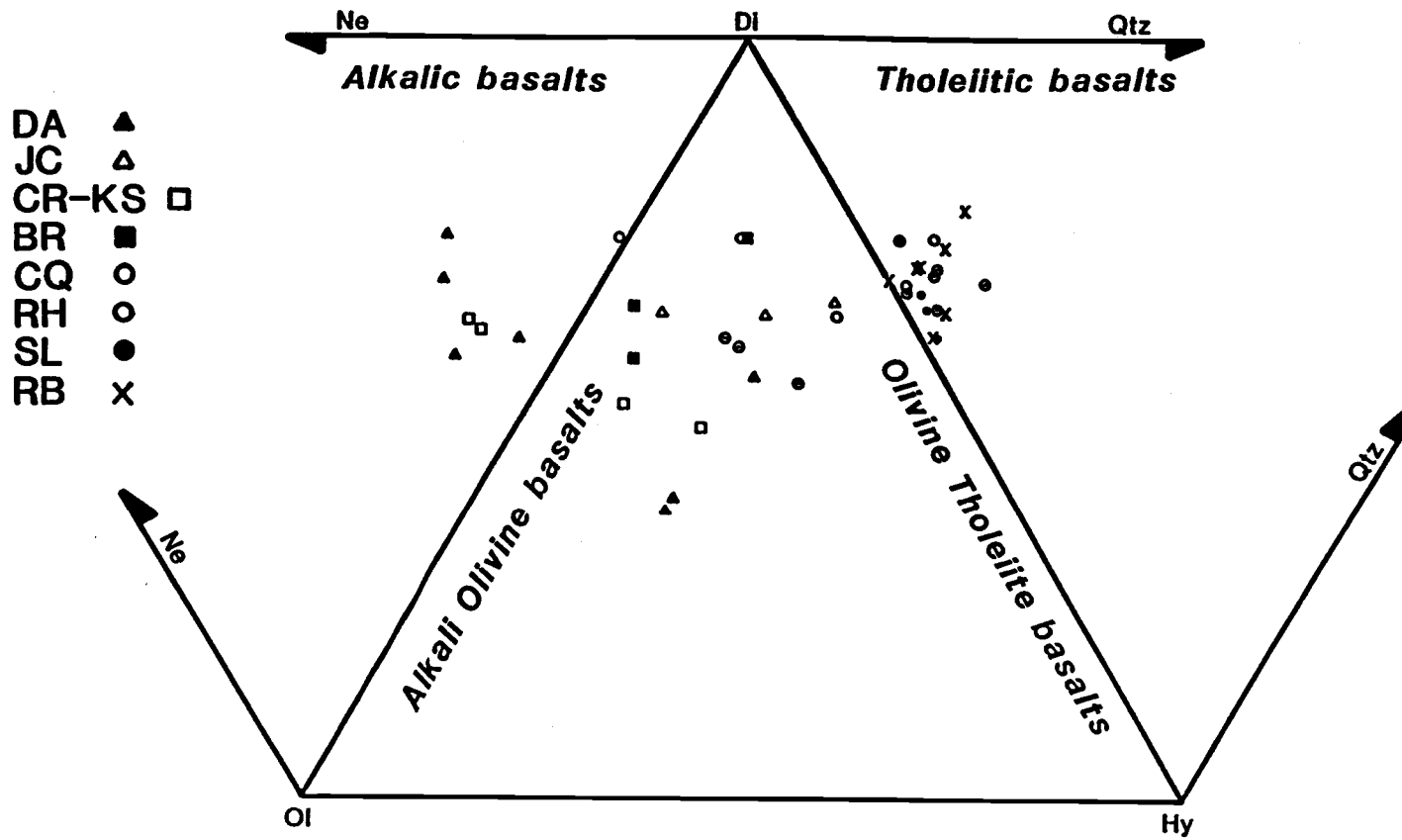


Figure 4.1 The Roseburg basalts plotted in the Ne-Ol-Hy-Qtz normative mineral system of Yoder and Tilley (1962).

II. Major Element Variation

Silica vs total Alkalies Scatter Plot

A silica versus total alkalies plot of the Roseburg basalt is given in Figure 4.2b. A companion plot with all the Oregon-Washington Coast Range data is given for comparison in Figure 4.2a. From these two plots the trend towards silica undersaturation in the Roseburg basalts is clearly distinct from the silica enrichment trends in the rest of the Coast Range. A tholeiitic trend or an alkalic trend typical of the evolution of Hawaiian basalts are not well developed in the Roseburg basalt suites. Only one sample (DA-232) from the Drain anticline exposure plots towards the Hawaiian alkali trend. The lack of an appreciable tholeiitic trend and alkalic trend may be the result of insufficient sampling or, as in the case of the Drain area, the alkalic suite may not be well exposed. The Siletz River basaltic rocks exhibit an alkalic trend as does the Crescent Volcanics, but the other volcanic groups mostly fall below the MacDonald and Katsura (1964) dividing line along a tholeiitic trend. The Metchisin Formation basalts are the least alkali enriched group in the Coast Range province. The Crescent Volcanic rocks seem to display a variation in alkali content that lie between the Metchisin tholeiitic basalts and the Siletz River alkali basalts.

AFM diagram

The Roseburg tholeiites and alkali basalts are plotted on AFM diagrams in Figure 4.3. The Hawaiian tholeiite and alkali trends are shown for comparison. Both the

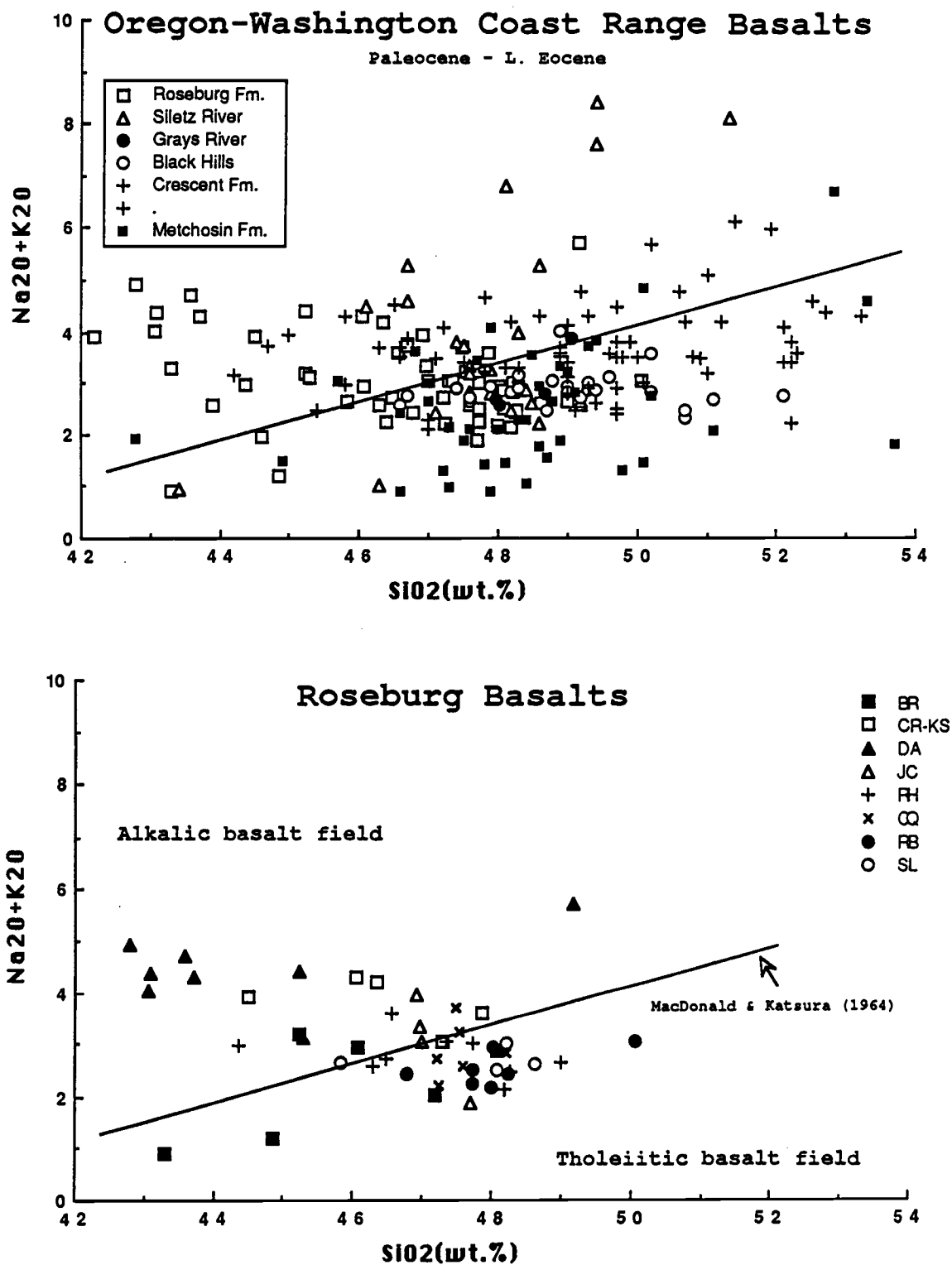


Figure 4.2 a) Silica vs total alkalis plot of the Paleocene to E. Eocene Oregon-Washington Coast Range Basalts (Snively et al., 1968; Globberman, 1980; Glassley, 1974; Lytle and Clark, 1975; Muller, 1980; and this study). b) Roseburg basalts from this study plotted separately to show the chemical relationships between the scattered exposures of these basalts.

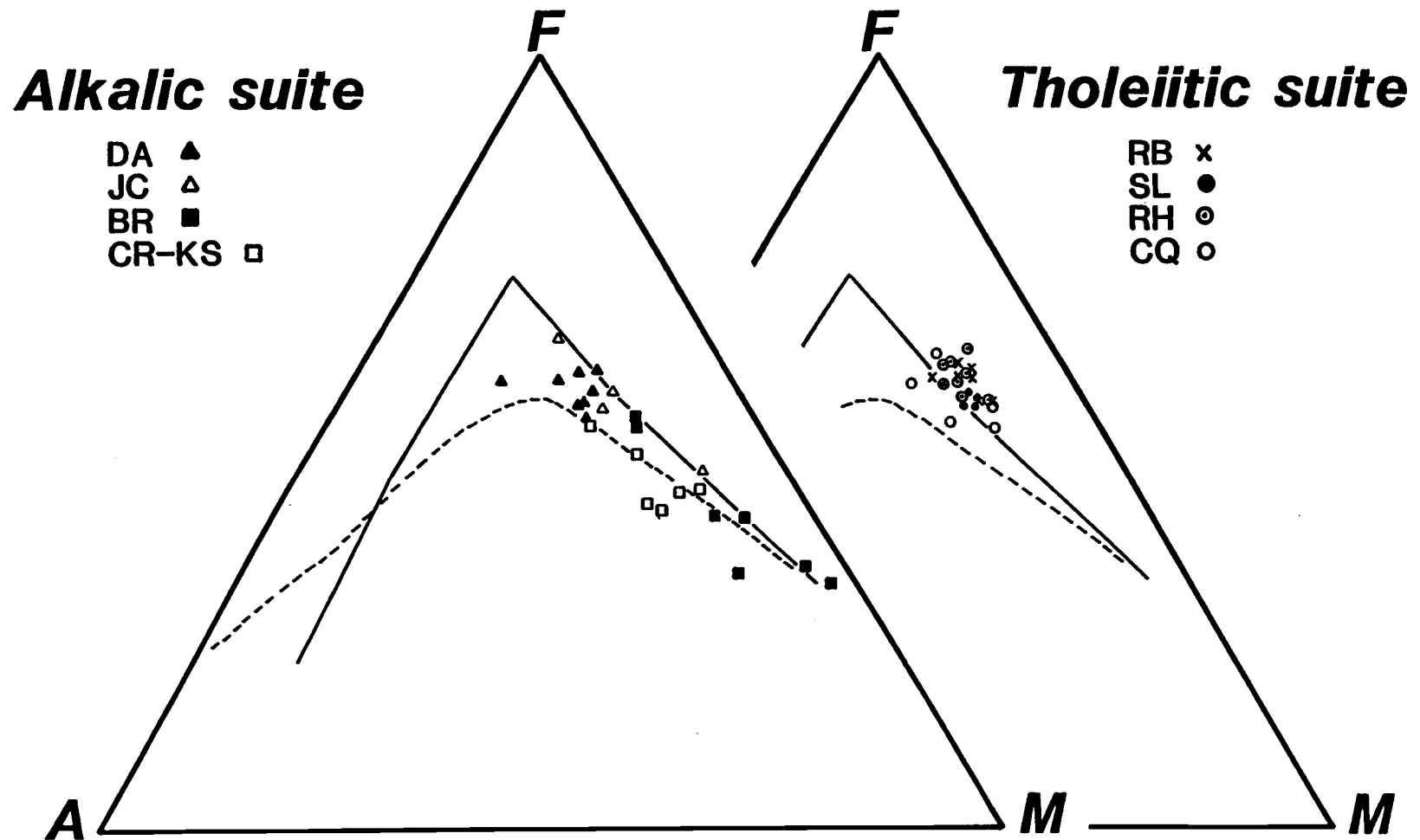


Figure 4.3 AFM diagram of the Roseburg basalts. A=Na₂O+K₂O, F=FeO(t)+MnO, and M=MgO

tholeiite trend and the alkali trend of the Roseburg basalts parallel the Hawaiian trends but they plot above the "average" trend lines. This shift is attributed to a greater FeO(t) content in the Roseburg basalts. Snavely et al. (1968) also noted FeO(t) contents somewhat higher than Hawaiian basalts for the Siletz River volcanic rocks. The alkali trend in the Roseburg basalt does not show a well defined differentiation path away from the iron apex towards alkali enrichment as is seen in the Siletz River alkali basalts. The same sample which showed silica and alkali enrichment on the silica versus total alkalies diagram (DA-232) also plots towards the alkali apex on the AFM ternary plot, but the rest of the alkali suite seems to continue towards FeO(t) enrichment. This illustrates the dominate differentiation trend toward silica undersaturation rather than towards alkali enrichment. The total alkali content of DA-232 is only 5.5 % compared to alkali contents greater than 8 % in the Siletz River basalts.

MgO scatter plots

The major element concentrations of the Roseburg basalts are plotted against MgO which is used as a index of differentiation (Figures 4.4 a-e). Different plot symbols have been assigned to the data points according to their geographic location as discussed in chapter 3. Some unpublished analyses of Roseburg basaltic rocks which appear on the major element plots, but do not appear in the data tables, were kindly provided by P.D. Snavely, Jr. (written comm., 1986).

The Roseburg basalts can be divided into a tholeiite suite and an alkali suite based on their normative mineral content and their trace element characteristics. The distinction of the two groups is not readily apparent on most of the major element variation diagrams, although P₂O₅ (Figure 4.4e) clearly shows two trends and K₂O shows two and possibly

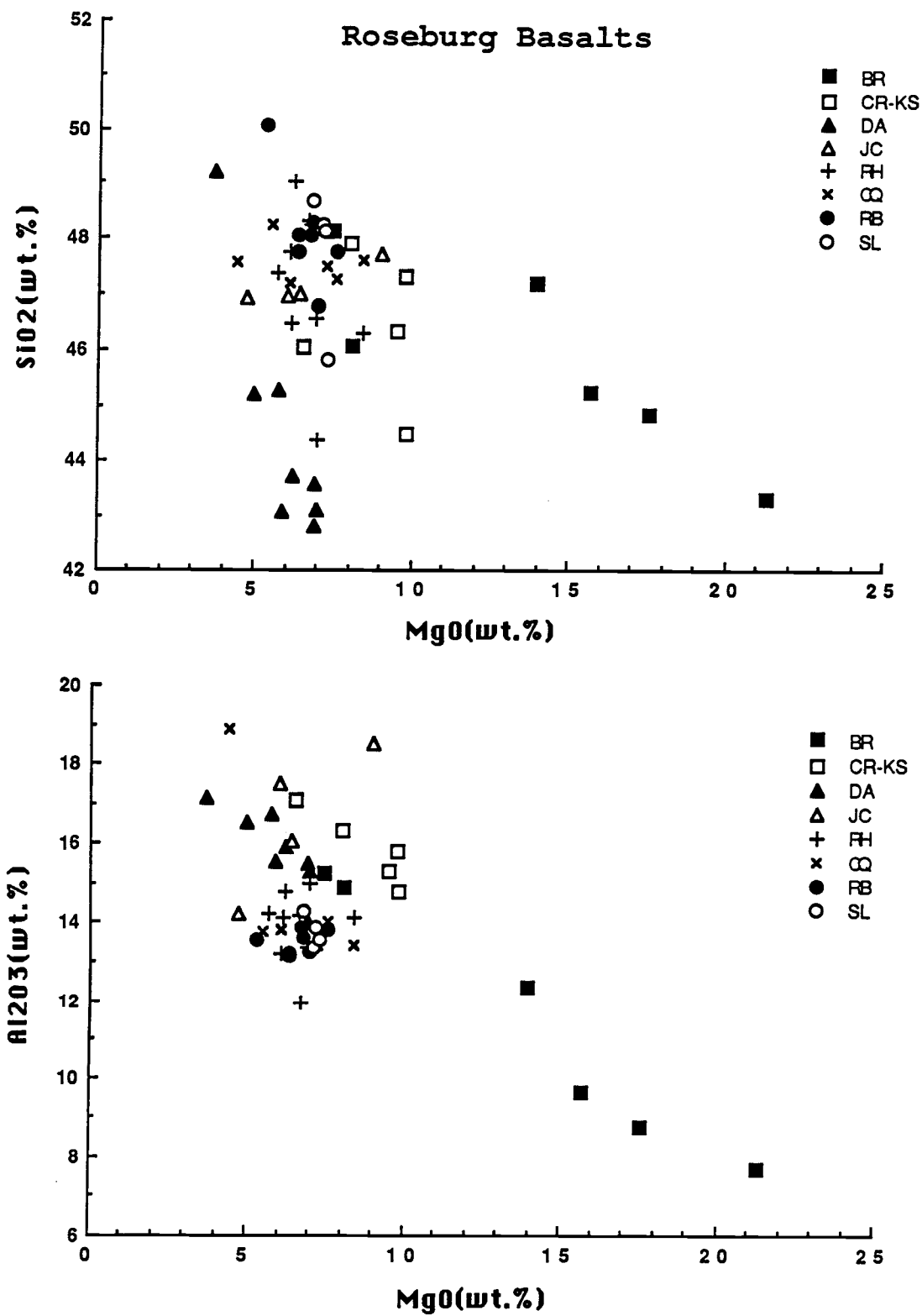


Figure 4.4a Major element variation diagrams for the Roseburg basalts.

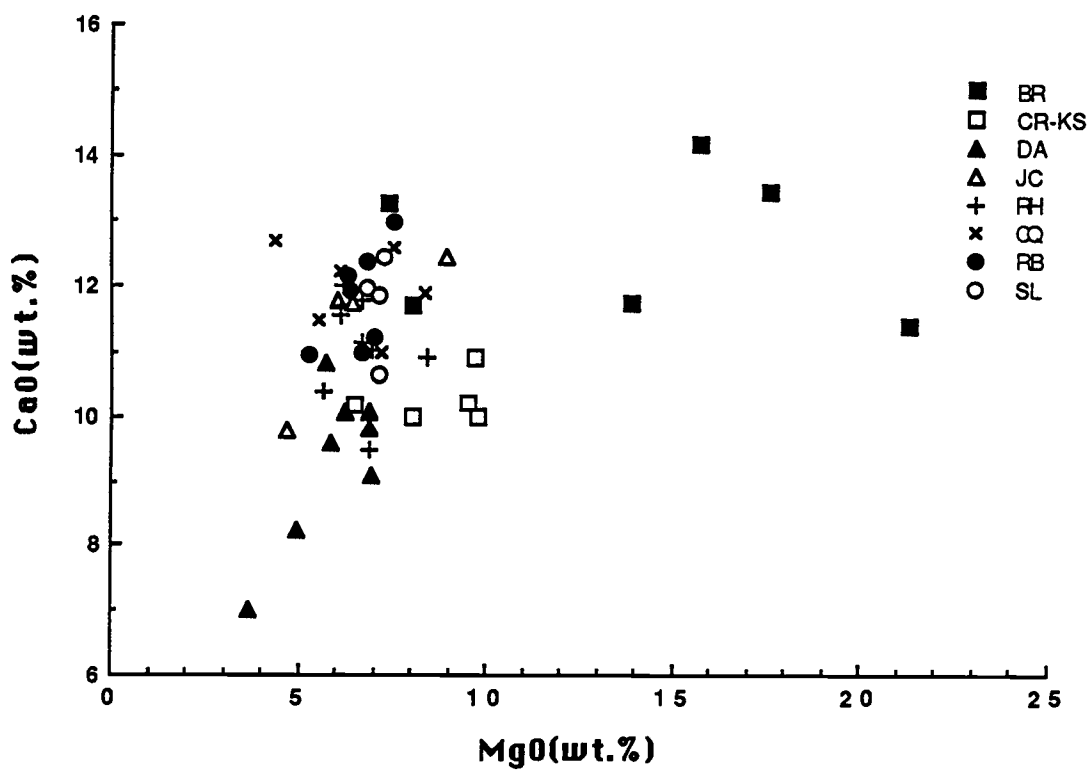
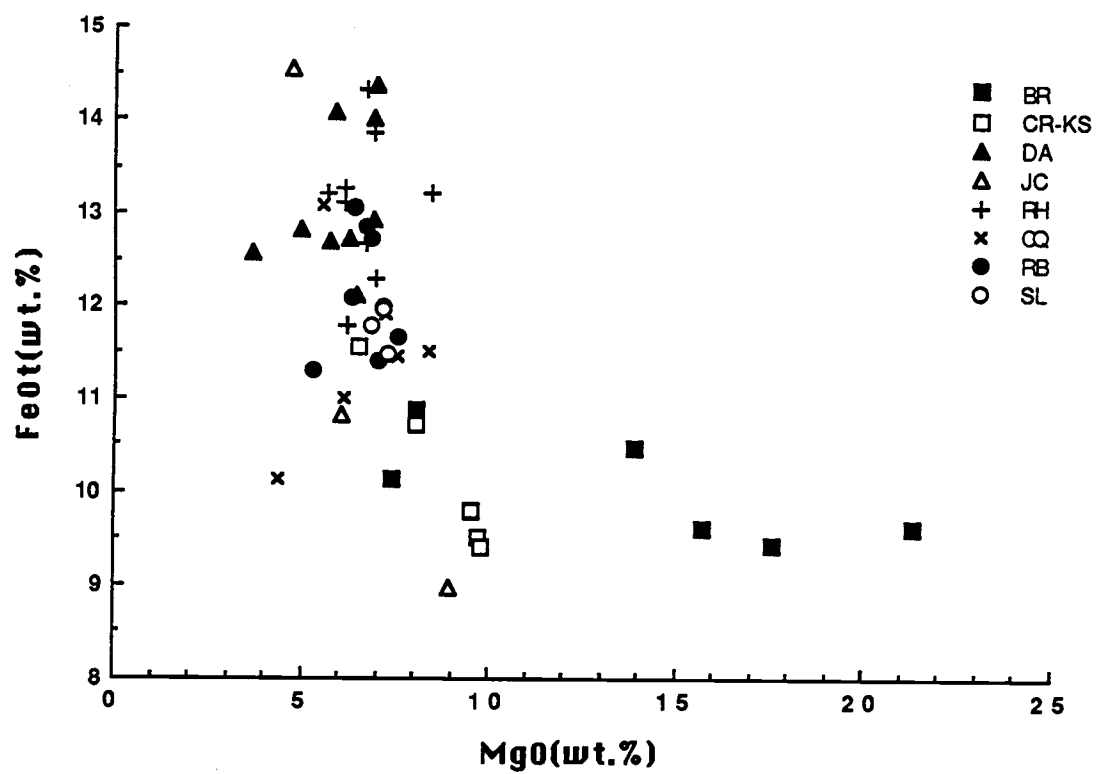


Figure 4.4b Major element variation diagrams cont.

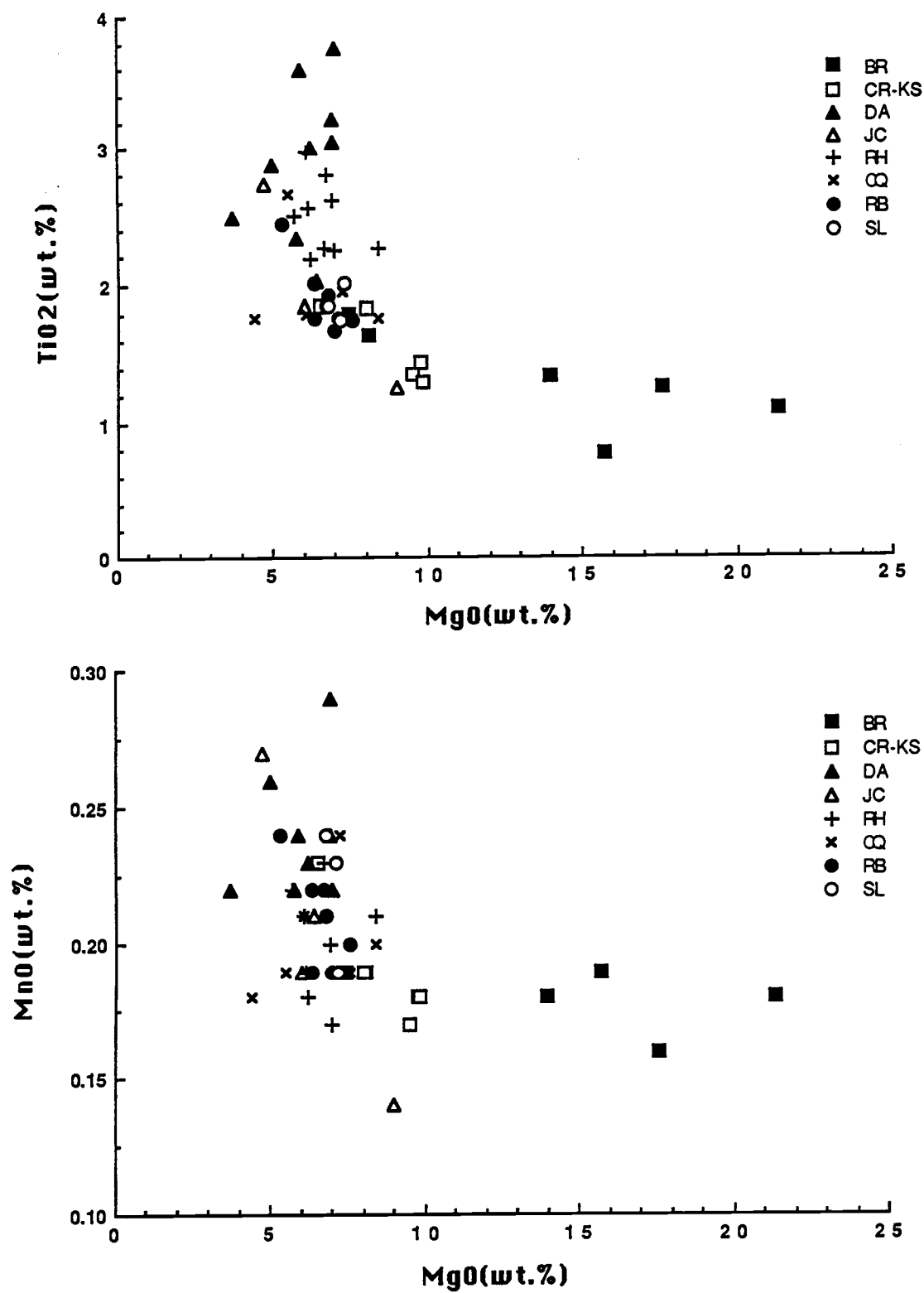


Figure 4.4c Major element variation diagrams cont.

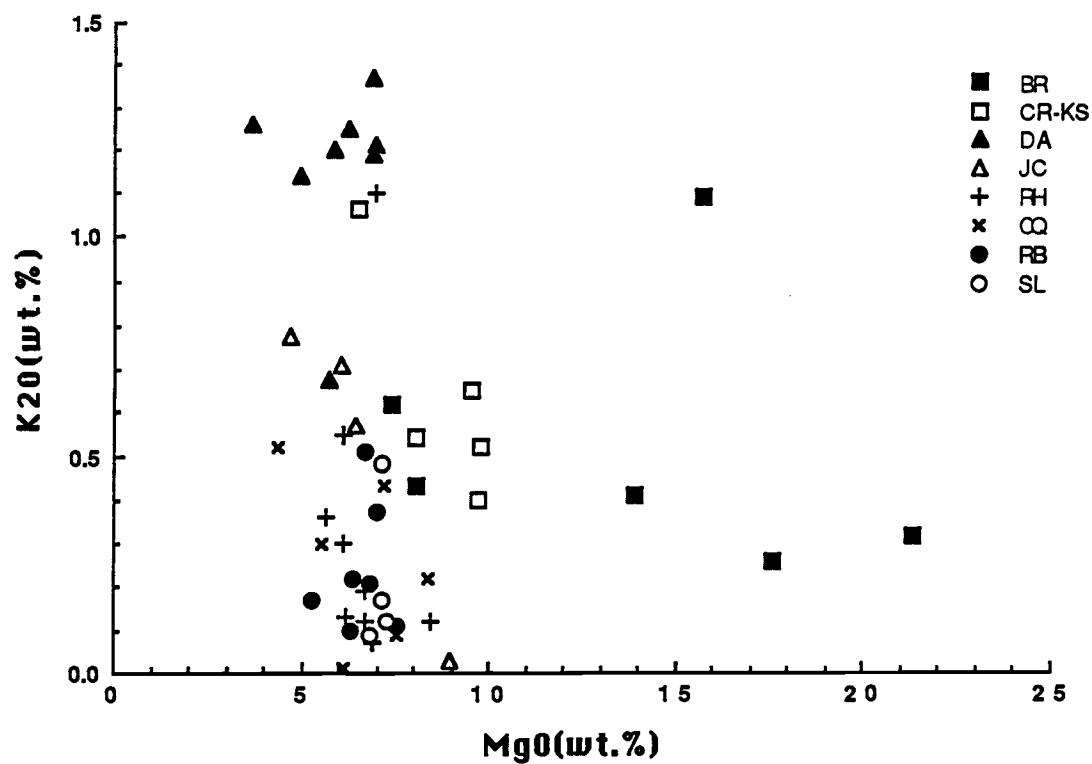
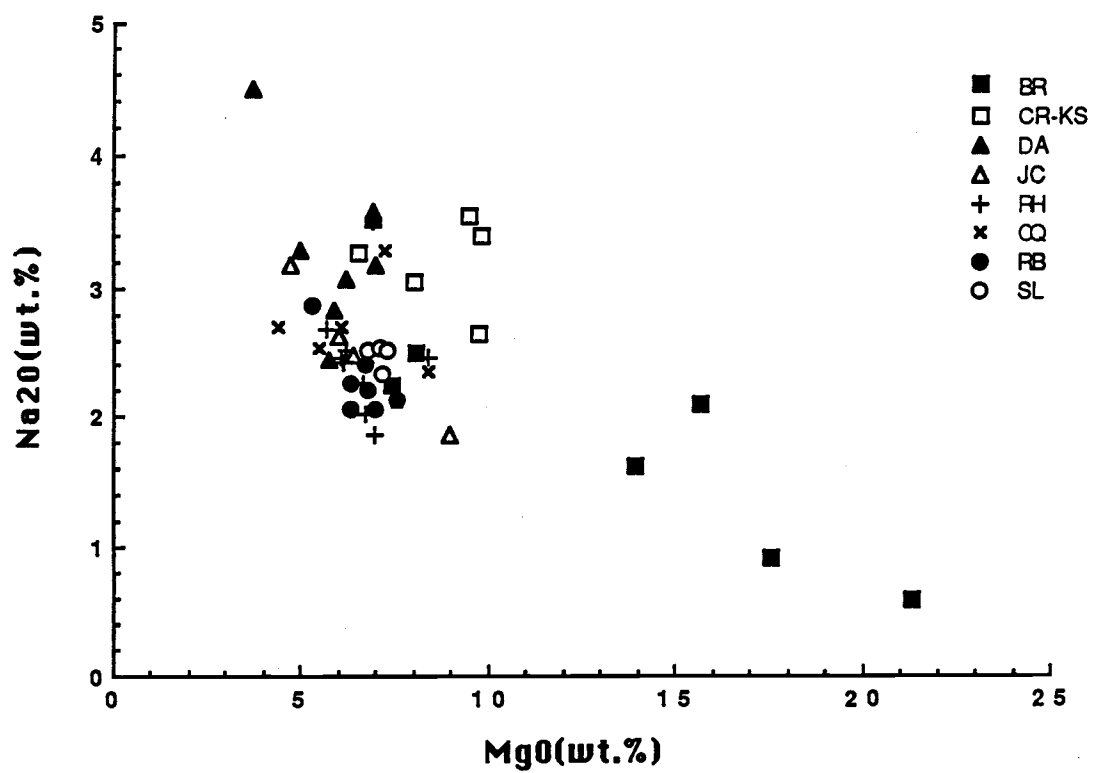


Figure 4.4d Major element variation diagrams cont.

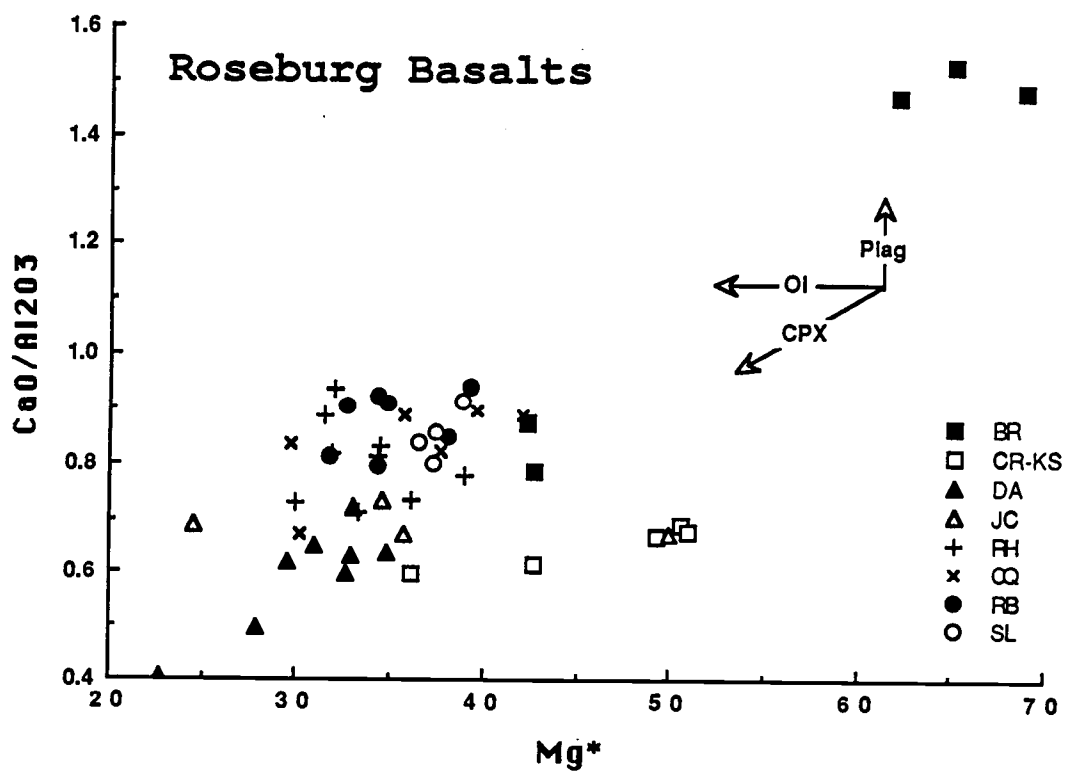
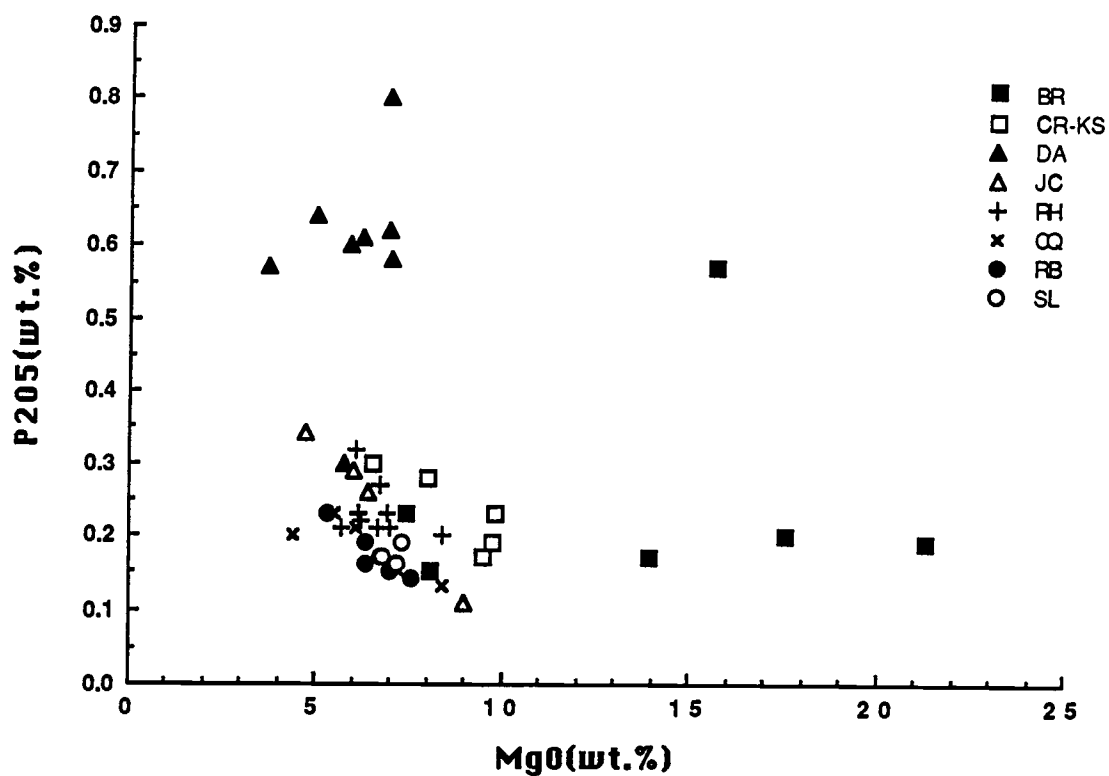


Figure 4.4e Major element variation diagrams cont.

three different trends in the data (Figure 4.4d). Plots of FeO, CaO, Al₂O₃, TiO₂, and Na₂O versus MgO (Figures 4.4a-d) demonstrate variations that might be misinterpreted as fractional crystallization trends if all of the points were plotted as one group. The alkali basalts show the widest variation on these diagrams while the tholeiites have relatively restricted compositions. The SiO₂ composition of the basalts ranges from 42.8 to 50.0% with most of the samples falling between 46 and 48 %. The scatter in the SiO₂ versus MgO diagram is the first indication that the basalts from different locations in the southern Coast Range are not related by crystal fractionation. Some of the scatter in the data may be due to the presence of phenocryst phases but most of it is probably caused by variations in parental magma compositions (i.e. the wide variation in SiO₂ concentrations at low MgO concentrations). Fractional crystallization may play a role in the differentiation of basaltic rock types within individual exposures. The occurrence of plagioclase, olivine, and pyroxene porphyritic rocks in some areas is obvious evidence for this process.

The variations in the essential constituents of olivine, pyroxene, and plagioclase (Mg, Fe, Ca, and Al) reflect the relative proportions in which these major phases contribute to the evolution of the magmatic system. An increase in CaO is observed at the higher MgO concentrations (15-22% MgO) which suggests that olivine was the primary fractionating phase at this stage of differentiation. Al₂O₃ variation in the alkali basalts show a steady increase as MgO declines while CaO reverses its increasing trend with a corresponding decrease. This variation would indicate the control of olivine and clinopyroxene in the evolution of the alkali suite below 15% MgO. Also, the Al₂O₃ contents of the tholeiites are lower and the CaO contents are higher than the alkali basalts at corresponding MgO values. The restricted Al₂O₃ variation (13-14%) and the increase in the CaO content in the lower MgO concentration range would indicate some plagioclase control on the evolution of the tholeiites.

FeO(t) and TiO₂ show identical steady enrichment trends in both the alkali and tholeiite basalts as the MgO content decreases from 22% to 8%. At this point their concentrations drastically increase as MgO drops another 3%. The range of variation in TiO₂ and FeO(t) of both tholeiite and alkali basalt is approximately the same in contrast to the restricted range of the tholeiites on other MgO variation diagrams. Similar trends are observed in Hawaiian Island basalts (BVSP, 1981). The enrichments in TiO₂ and FeO(t), and depletion in Al₂O₃ relative to mid-ocean ridge basalts are a characteristic of intraplate (oceanic island) type volcanism. Chemical differences between abyssal tholeiites (MORB) and oceanic island basalts (OIB) are not related by low-pressure fractionation effects, so the high FeO(t), TiO₂, and low Al₂O₃ must be a consequence of their different mantle source region compositions (BSVP, 1981).

A CaO/Al₂O₃ vs Mg* (Mg*=MgO/FeO(t)+MgO) scatter plot is given in Figure 4.4e. The variation of CaO/Al₂O₃ in a suite of basalts is useful for determining qualitative fractionation relationships between basalts because fractional crystallization of olivine, plagioclase, and clinopyroxene have different effects on this ratio. Olivine control does not affect the CaO/Al₂O₃ ratio of the liquid but it does decrease the Mg*. Plagioclase crystallization increases the CaO/Al₂O₃ ratio but does not affect the Mg*. Clinopyroxene crystallization decreases both the CaO/Al₂O₃ ratio and the Mg*. The CaO/Al₂O₃ ratios of the picrites and ankaramites is thought to be too high to be a primary feature of the magma from which they formed (Fisk, 1987 pers. comm.). Secondary calcite observed in the thin sections of these rocks would account for the excess CaO content of the rocks resulting in high CaO/Al₂O₃ ratios. The overall trend to lower CaO/Al₂O₃ ratios with decreasing Mg* is still evident although the slope of the trend may be steeper in the high Mg* range due to the increased Ca from secondary calcite. From these diagrams olivine and clinopyroxene control seems to be responsible for most of the differentiation trends in the Roseburg basalts. Some plagioclase participation in the evolution of the tholeiitic

basalts is indicated by variations in the $\text{CaO}/\text{Al}_2\text{O}_3$ ratios at similar Mg^* (e.g. Red Hill, Sugarloaf Mountain, and possibly Roseburg), but olivine is also an important constituent controlling the evolution of this group.

Primary and Parental Magmas

One way to determine the evolution of the basalts in the southern Oregon Coast Range is to identify a possible "primary" or "parental" magma composition for the volcanic sequence. "Primary" is defined as a basaltic liquid whose composition has been unmodified by differentiation processes following segregation from its mantle source and eruption on the surface. "Parental" is defined as a liquid composition from which other associated magmas can be derived by processes of crystal fractionation, contamination, magma mixing, or other igneous processes (BVSP, 1981). Several lines of evidence (e.g. mantle xenoliths, high pressure peridotites, harzburgites in ophiolite complexes) indicate that the least refractory upper mantle peridotite compositions have Mg-values ($100 \text{ Mg}/(\text{Mg}+\text{Fe}^{++})$) in the range 88-89 and "primary" basaltic magmas derived from such a source peridotite must have Mg-values of approximately 69-75 (Frey et al., 1978). Ni concentrations in primary magmas are relatively insensitive to extent of partial melting and range between 200-400 ppm depending on assumptions about mantle mineralogy and Ni content (BVSP, 1981). Conversely, Ni is extremely sensitive to olivine fractionation and minor modification of a primary magma (e.g. separation of 5% ol and 5% cpx) will reduce the Ni content by 50% of the original concentration (Sun and Hanson, 1975).

Most of the Roseburg basalts have Ni concentrations below 100 ppm and Mg^* values between 20-40 (Mg^* is roughly equivalent to Mg-value discussed above) which would indicate all have undergone differentiation before they were erupted at the surface.

The picrites and ankaramites from the Blue Ridge area have Ni contents within the range of primary compositions (300-400 ppm) but the Mg^* too low (65 compared to 69). These characteristics probably reflect accumulation of olivine rather than equilibration with a mantle peridotite source region. This evidence leads to the conclusion that no "primary" magma compositions have been sampled in the southern Oregon Coast Range.

Rocks with intermediate Ni concentrations of 150-250 ppm and Mg^* values of 40-50 could be possible "parental" magma types for the Roseburg basaltic sequence. Parental magmas have higher liquidus temperatures than associated derivative magmas and, subsequently, crystallize phases with high melting points. These phases are Mg-rich olivines and pyroxenes and Ca-rich plagioclases and, consequently, parental magmas have the highest Mg^* and $Ca/(Ca+Na)$ ratios within a given basaltic suite (BVSP, 1981). These magmas are also characterized by high Ni and Cr contents and low incompatible element abundances. Generally, the alkali basalts along the western side of the southern Coast Range (Blue Ridge, Coos River, and Kentucky Slough) have higher Mg^* , higher Ni concentrations, and higher $Ca/(Ca+Na)$ ratios than the tholeiitic basalts to the east. BR-2 and CR-2 could be possible parental magmas for the alkali suite according to the conditions outlined above. The most primitive tholeiitic basalts include CQ-5, CQ-11, and RB-1. These samples should represent end member compositions on chemical variation diagrams if they are truly parental magmas from which the more differentiated rock types in the two suites are derived. The parental nature of these samples will be examined further by considering the trace element composition and variation of the Roseburg basaltic rocks within the igneous sequence.

CHAPTER 5: Trace Element Geochemistry

I. Introduction

The major element abundances and variations in the early Tertiary basaltic basement of the Oregon-Washington Coast Range are very uniform throughout the province. Some minor element concentrations display a regional variation (e.g. Ti, total alkalis), but essential elemental constituents of the major fractionating phases, olivine, pyroxene, and plagioclase, do not. Regional variations in the major element content of these rocks are subtle, if they exist at all, and are probably not discernable from the available data. Average or mean basalt compositions for the different volcanic centers can be biased by inadequate sampling and could mislead interpretation of the regional magmatic history of the province. Defining the trace element characteristics of the basalts is the most effective way to resolve the differences between the groups of basalts in the Coast Range and to determine if regional or time dependent variations occur in their petrogenesis.

Trace elements exhibit specific petrogenic behavior in magmatic systems which can be used to constrain the mantle source(s), partial melting of the source(s), fractionation of the melt by residual phases or crystallization enroute to the surface, contamination of the melt, and mixing of sources and/or derivative melts. Mathematical modeling of the trace constituents would provide the most quantitative assessment of the factors controlling the composition of the basalts, but no modelling has been done on these rocks at this time. Some important qualitative conclusions can be drawn from the figures presented below. The remaining sections of this study are concerned with the trace element evolution of the Oregon-Washington Coast Range, with emphasis on the

Roseburg basalts. The trace element composition of the Roseburg basalts is an important end member in the history of the Coast Range because they are the oldest rocks of the province and they have experienced the greatest amount of tectonic displacement.

The northeast Pacific was the location of both hotspot and mid-ocean ridge volcanic environments during the early Tertiary according to the plate models discussed above. Presently, the basalt compositions in the North Atlantic are influenced by the same magma generating processes. The geochemical variability in MORB compositions discovered along the Mid-Atlantic ridge system has been attributed to the mixing of basalt from the different mantle sources which produce MORB and hotspot magmas (Schilling, 1975). To facilitate the discussion of the chemical characteristics of basalts from such areas, a brief explanation of the terminology that has been used to describe these hybrid MORB types and their mantle source regions is necessary.

Hotspot or plume type magmas - tholeiitic and alkalic - generally have higher concentrations of "incompatible" or large ion lithophile elements (e.g. U, Th, Pb, Sr, Rb, K, Cs, Ba, Ta, Nb, LREE,) than MORB and are believed to be generated in mantle reservoirs that are "enriched" or "undepleted" in these incompatible constituents. The geochemical properties of incompatible elements dictate removal of these constituents during the earliest stages of mantle melting. These elements are "incompatible" with the residual mantle mineralogy and are concentrated in the melt. "Enriched" or "undepleted" refers to the mantle source region of hotspot or plume magmas which have high concentrations of these incompatible elements. Enrichment implies that the incompatible element abundance in the mantle source for these magmas is a secondary feature and that the source may or may not have been melted in a previous magma generation event. Undepleted refers to a source region that has not undergone a melting event which would deplete the mantle in incompatible elements since accretion of the earth and removal of the core from the mantle. MORB magmas are typically "depleted" in incompatible elements.

The depletion is attributed to the extraction of the incompatible element component from their upper mantle source to form the continental crust (Gast, 1968; Kay and Hubbard, 1978).

Basalts from the ocean basin display a continuous gradation in trace element compositions that are a product of the various mantle processes which enrich and deplete the magma source regions for these rocks. Basalts which have been dredged or sampled by a submersible from an ocean ridge setting are obviously mid-ocean ridge basalts (MORB) but their trace element abundances can vary between rock types similar to alkali oceanic island basalts and the tholeiitic rock types more commonly erupted at mid-ocean ridges. Schilling (1975) subdivided the mid-ocean ridge system into three types of ridge segments based on topography, heat flow, gravity, and geochemical criteria and designated them as "normal", "anomalous", or "transitional" type basalts. Normal MORB (N-type) are characterized by normal ridge elevations (i.e. water depths greater than 3500 m), well developed magnetic lineations, and typical oceanic crustal thicknesses. They are also the most abundant type of ocean ridge basalt and are invariably light rare earth (LREE) depleted (i.e. chondrite normalized $\text{La/Sm} < 1$). Anomalous ridge segments (plume P-type or enriched E-type MORB) are characterized by elevated ridge topography, thicker oceanic crust, and higher heat flow which is consistent with the greater amounts of basalt erupted along this type of ridge segment. Tholeiitic basalts are the predominate rock type, but alkali basalts are common and the chemical variability in both rock types is greater than at normal ridge segments. These basalts have LREE enriched patterns (chondrite normalized $\text{La/Sm} > 1$) and higher abundances of other incompatible element than N-type MORB that suggest the two basalt types are derived from distinct mantle sources (Saunders, 1984, and references therein). Transitional ridge segments (T-type MORB) are intermediate between the N-type and E-type ridge segments and may be either LREE depleted or LREE enriched.

The trace element abundances of the Roseburg basalts are given in Table 5.1a-d and 5.2. Analyses of other early Eocene Coast Range basalts from the Willapa Hills, Black Hills, and Metcoshin Formation are given in Table 5.3. Much of the previous trace element work in the Coast Range has concentrated on trace element discrimination diagrams to determine the tectonic environment which could have produced the magma types found in the region (Muller, 1980; Globberman, 1980; Lyttle and Clark, 1975, 1976; Glassley, 1974; Loeschke, 1980). Particular attention has been placed on the concentrations of Ti, Zr, Nb, Y in these rocks because of their apparent immobility during alteration processes and because they are useful indicators of magma generation in different tectonic regimes (Pearce and Cann, 1973). Typical discrimination diagrams were avoided in this study because Nb and Y were not determined and the Zr results by INAA have errors (30-50%) which preclude it from being used to determine subtle differences in the basaltic compositions from each volcanic center. Rare-earth element abundances have been determined for basalts from the other volcanic centers in the province, but their potential for tracing petrogenic processes have been sparingly discussed (Glassley, 1974; Hill, 1975). The discrimination diagrams and REE results from previous studies have shown that the Coast Range basalts range from N-type MORB to oceanic island basalt (OIB) based on REE patterns and trace-element tectonic discrimination diagrams. Chondrite normalized REE plots, primitive mantle normalized spidergrams, and incompatible element scatter plots are presented below to determine the trace element evolution of the Roseburg basalts and the geochemical variation within the early Tertiary basalts of the Coast Range. The following discussion relies heavily on the unpublished data of Hill (1975). Trace element comparisons between the Roseburg and Siletz River basalts could not have been made without his work.

Table 5.1a: Trace element abundances for the Roseburg basalts.

Sample	RB 1	RB 622	RB 2	RB 16	RB 611	RB 7	RB 22	SL 5	SL 4	SL 2	FMP 1
ppm											
Sc	29.0	43.6	44.0	37.4	43.0	45.0	35.0	44.0	41.0	45.0	42.4
Cr	203	160	127	118	88	144	116	170	139	130	166
Co	50.0	45.7	48.4	43.4	45.6	48.1	46.0	50.0	50.7	48.8	43.7
Ni	105	108	90	91	78	86	92	100	85	93	70
Cu	117	182	242	152	287	259	-	253	239	239	-
Zn	72	79	90	71	110	85	-	92	82	88	-
Rb	1.3	5.8	2.7	6.1	4.6	2	1	2.3	8	1.5	3
Sr	179	385	174	170	171	205	210	221	154	214	204
Cs	-	-	-	0.1	-	-	-	-	-	-	0.3
Ba	36	30	30	152	46	49	50	29	192	73	74
Zr	-	46	135	114	145	32	99	-	114	84	122
Hf	2.84	2.71	3.12	2.54	3.34	3.10	4.43	2.93	3.06	3.29	3.41
Ta	0.63	0.52	0.59	0.48	0.69	0.59	0.89	0.47	0.53	0.51	0.70
Th	0.53	0.48	0.69	0.51	0.82	0.44	0.84	0.61	0.57	0.67	0.59
U	0.1	0.6	0.7	0.3	0.4	0.8	0.5	0.1	0.1	0.2	1.2
La	6.9	7.4	8.7	7.8	9.1	8.0	12.4	8.1	7.4	8.6	10.2
Ce	18.2	18.4	20.0	17.2	19.9	21.8	30.8	21.0	19.2	21.4	25.4
Nd	9	12	-	12	12	14	-	17	-	12	15
Sm	3.40	3.55	4.10	3.94	4.40	3.94	5.30	3.97	3.50	4.20	5.05
Eu	1.29	1.31	1.43	1.33	1.51	1.38	1.82	1.36	1.40	1.43	1.71
Tb	0.61	0.58	0.69	0.63	0.71	0.67	0.79	0.62	0.66	0.72	0.78
Yb	2.48	2.43	2.87	2.68	3.12	2.63	2.68	2.71	2.56	2.91	2.88
Lu	0.36	0.40	0.50	0.45	0.53	0.43	0.36	0.43	0.41	0.46	0.45
*t REE	42.2	46.1	51.3	46.0	51.3	52.9	72.8	55.2	47.5	51.7	61.5

*t REE=total of the eight REE listed. Missing data concentrations were estimated by extrapolation between elements on the REE diagrams.

Table 5.1b: Trace element abundances for the Roseburg basalts (cont.).

Sample	CQ 5	CQ 11	CQ 6	CQ 4	CQ 3	RH 1	RH 7	RH 4	RH 303	RH 283	DCLP 1
ppm											
Sc	49.0	44.9	46.0	45.0	32.0	36.4	39.0	35.2	40.0	20.9	37.0
Cr	316	283	150	201	45	123	125	98	102	170	214
Co	51.6	49.2	49.8	50.0	43.0	51.0	53.0	41.0	49.8	48.0	47.0
Ni	114	113	87	87	62	104	98	77	77	97	58
Cu	245	248	263	389	192	22	105	139	246	381	-
Zn	87	81	79	100	78	89	92	78	99	91	-
Rb	3.5	0.6	11.6	4.5	13.3	1.8	0.7	1.7	3.3	12.3	-
Sr	211	210	585	240	347	115	648	227	244	300	369
Cs	-	-	-	-	-	-	-	-	-	-	0.5
Ba	129	30	949	75	167	23	75	88	90	187	195
Zr	71	-	-	89	96	128	86	117	71	264	127
Hf	2.74	2.83	3.05	4.61	3.54	4.05	4.60	3.50	4.08	5.69	3.87
Ta	0.43	0.50	0.51	0.89	2.19	0.68	0.80	0.57	0.73	1.61	0.71
Th	0.46	0.47	0.71	1.03	2.87	0.85	0.91	0.70	0.85	2.05	1.07
U	0.1	0.3	0.1	0.2	0.7	0.1	0.3	0.1	0.1	0.8	0.3
La	6.4	7.1	8.0	11.9	27.3	10.2	13.1	10.4	10.6	20.9	10.8
Ce	16.0	19.1	21.0	30.3	54.1	29.0	27.8	22.8	26.1	49.2	27.4
Nd	-	21	14	11	21	20	-	15	-	22	16
Sm	3.20	3.67	3.80	5.30	4.70	4.90	5.80	5.00	5.40	6.70	4.70
Eu	1.28	1.33	1.43	1.91	1.58	1.73	1.87	1.57	1.87	2.23	1.62
Tb	0.57	0.68	0.64	0.88	0.78	0.78	0.84	0.78	0.85	1.00	0.64
Yb	2.23	2.21	2.56	3.02	2.81	2.48	2.97	2.64	3.08	2.87	2.46
Lu	0.33	0.36	0.40	0.50	0.48	0.42	0.45	0.45	0.43	0.50	0.38
*t REE	40.5	55.5	51.8	64.8	112.8	69.5	71.4	58.6	65.7	105.4	64.0

Table 5.1c: Trace element abundances for the Roseburg basalts (cont.).

Sample	BR 22	BR 24	BR 24 a	BR 3	BR 2	CR 25	CR 1	KS 3	KS 1
ppm									
Sc	71.8	41.5	42.4	44.0	44.4	32.0	28.0	33.0	25.4
Cr	1760	851	951	76	217	554	275	442	120
Co	65.6	63.2	68.9	48.0	43.8	49.6	43.9	49.8	46.0
Ni	437	313	336	79	92	201	114	168	67
Cu	210	237	115	163	146	88	35	88	21
Zn	58	61	60	67	67	68	64	57	59
Rb	7	35	11.6	9.8	12.3	6.1	7.3	13.8	24.1
Sr	349	433	460	278	753	438	444	433	726
Ce	-	0.2	-	-	-	0.4	-	0.2	-
Ba	336	1038	155	142	309	307	281	251	560
Zr	-	-	-	86	112	118	177	88	109
Hf	1.88	1.05	2.73	2.85	3.71	3.80	4.20	2.86	3.53
Ta	1.75	0.89	2.85	1.34	3.32	3.02	2.94	1.59	4.54
Th	1.88	0.86	2.54	1.60	3.90	5.00	3.90	2.10	6.11
U	0.7	1.0	0.9	0.4	2.4	0.4	0.9	0.5	1.9
La	25.1	10.2	38.1	15.3	38.1	35.2	35.5	17.4	56.9
Ce	26.7	21.7	49.2	32.5	74.8	64.7	70.0	32.0	94.7
Nd	16	9	20	12	33	20	24	13	23
Sm	2.79	2.03	4.01	3.64	5.25	4.20	6.50	3.40	5.40
Eu	1.02	0.65	1.20	1.33	1.60	1.38	1.75	1.20	1.70
Tb	0.41	0.31	0.58	0.67	0.78	0.72	0.92	0.61	0.83
Yb	1.35	1.26	1.80	2.53	3.05	2.56	3.24	2.17	2.94
Lu	0.24	0.20	0.27	0.42	0.47	0.41	0.53	0.37	0.46
*t REE	73.6	45.4	115.2	68.4	157.1	129.2	141.5	70.2	185.9

Table 5.1d: Trace element abundances for the Roseburg basalts (cont.).

Sample	JC 2a	JC 223	JC 1	JC 2	DA 1	DA 252a	DA 252b	DA 252c	DA 252a	DA 221a	DA 232
ppm											
Sc	38.5	34.0	28.8	36.8	19.5	20.1	21.6	20.4	13.9	26.0	9.7
Cr	378	28	122	12	11	21.7	35.6	8.2	6.4	12	8
Co	50.5	49.8	44.7	48.8	46.0	43.6	43.9	47.2	34.8	54.0	27.0
Ni	224	72	81	52	47	51	61	45	29	55	28
Cu	20	-	40	1128	88	22	22	92	24	21	35
Zn	58	-	99	108	68	68	54	84	74	55	64
Rb	9.4	11.5	17.2	17.3	27.6	44	32.3	27.5	25.7	16.2	29.4
Sr	439	530	556	283	1030	1895	1222	2063	1050	569	789
Cs	-	-	0.2	0.2	-	0.2	0.3	0.2	0.1	-	0.3
Ba	399	222	301	281	538	807	634	536	506	281	420
Zr	-	127	180	173	268	382	312	270	269	194	268
Hf	1.61	3.87	3.71	5.76	7.20	10.40	8.12	7.43	7.48	3.84	6.72
Ta	0.69	2.12	2.76	2.93	6.20	13.58	9.14	6.47	5.65	5.01	4.00
Th	0.69	2.67	3.90	3.54	8.00	17.66	11.80	8.11	7.50	5.50	5.30
U	-	0.8	0.6	0.5	2.4	6.2	3.2	2.1	2.4	2.8	2.1
La	11.0	27.0	35.9	30.5	79.8	173.8	114.8	80.4	72.4	56.8	50.5
Ce	14.9	53.8	69.6	64.9	149.3	308.0	206.0	151.8	135.4	103.9	96.5
Nd	8	24	23	27	49	102	74	60	57	-	48
Sm	2.43	5.00	5.20	7.25	9.80	14.30	11.06	10.22	9.60	6.30	8.10
Eu	0.92	1.66	1.62	2.54	2.84	3.96	3.11	3.02	2.98	1.90	2.54
Tb	0.52	0.85	0.82	1.24	1.15	1.50	1.08	0.90	0.87	0.94	1.23
Yb	1.38	2.47	2.60	4.57	2.64	3.51	2.92	2.74	2.81	2.77	2.92
Lu	0.22	0.40	0.40	0.65	0.41	0.51	0.41	0.39	0.36	0.43	0.45
*t REE	39.7	115.2	139.1	138.7	294.9	607.6	413.4	309.4	281.4	223.0	210.2

Table 5.2: Trace element concentrations from the Mobil Sutherland test well drilling chip samples.

Sample	MSW 5	MSW 6	MSW 7	MSW 8	MSW 9	MSW 10	MSW 11	MSW 12	MSW 13	RANGE
Drilling Interval depth (km)	1.4-1.5	1.7-1.8	2.0-2.1	2.3-2.4	2.6-2.7	2.9-3.1	3.2-3.4	3.5-3.7	3.8-4.0	1.4-4.0
Sc	40.1	40.2	32.7	37.1	33.7	37.8	38.5	32.8	37.3	40.1-32.7
Cr	170	210	158	143	181	150	219	223	188	150-223
Co	45.6	52.9	42	46.2	40.7	46.5	47.2	40.8	45.9	40.7-52.9
Ni	76	102	78	95	98	76	99	76	86	76-102
Cu	-	-	-	-	-	-	-	-	-	-
Zn	-	-	-	-	-	-	-	-	-	-
Rb	-	7	5	6	7	6	-	-	6	5.0-7.0
Sr	126	131	191	307	249	295	212	189	264	126-307
Cs	0.12	0.25	-	-	-	-	0.14	-	-	.12-.25
Ba	167	320	272	297	308	346	164	147	186	164-346
Zr	48	134	84	140	119	70	89	-	102	48-140
Hf	3.95	3.54	3.23	3.84	3.58	3.39	3.57	3.34	4.31	3.23-4.31
Ta	0.77	0.64	0.58	0.77	0.62	0.68	0.6	0.62	0.86	.58-.86
Th	0.87	0.76	0.65	0.72	0.57	0.65	0.68	0.59	0.91	.57-.91
U	1.3	0.6	-	1.2	1.8	0.8	-	2.5	0.6	.6-2.5
La	11.2	9.5	9.6	10.9	9.5	8.9	8.8	9.2	11.4	8.8-11.4
Ce	27.5	25.1	19.4	26.7	22.7	23	23.4	21	29.5	19.4-29.5
Nd	16	22	9	13	15	16	7	18	25	7.0-25.0
Sm	5.23	4.86	4.53	4.87	4.94	4.44	4.71	4.48	5.52	4.44-5.52
Eu	1.76	1.65	1.54	1.74	1.58	1.54	1.63	1.53	1.9	1.53-1.90
Tb	0.88	0.81	0.68	0.72	0.69	0.68	0.8	0.71	0.98	.68-.98
Yb	2.62	2.33	2.48	2.42	2.41	2.18	2.56	2.18	2.37	2.18-2.62
Lu	0.30	0.34	0.46	0.33	0.37	0.27	0.33	0.32	0.32	.27-.37
∑ REE	65.5	66.6	47.7	60.7	57.2	57.0	49.2	57.4	77.0	-

Table 5.3: Trace element abundances for Washington and British Columbia Coast Range basalts.

Sample	MT 2	MT 3	MT 4	BH 23	BH 19	BH 18	BH 7	BH 6	GR 1	GR 2	GR 3	GR 4	GR 5
ppm													
Sc	49.3	45.5	38.9	36.2	38.7	37.7	36.5	40.9	48.2	42.7	39.5	35.3	29.0
Cr	105	113	148	193	143	148	84	94	167	131	113	92	164
Co	52.2	78.3	82.8	41.3	40.7	43.8	41.7	48.3	51.9	46.5	41.1	35.2	41.1
Ni	53	-	71	66	66	66	66	58	20	69	38	16	82
Cu	-	-	-	-	-	-	-	-	-	-	-	-	-
Zn	-	-	-	-	-	-	-	-	-	-	-	-	-
Rb	5	3	4	5.9	4.6	3.5	4.3	5.9	6	22	-	5	27
Sr	112	63	-	239	256	265	276	267	109	191	145	141	563
Cs	-	0.2	0.2	-	-	-	0.2	-	0.2	-	0.2	0.2	0.2
Ba	58	42	22	90	69	53	72	126	103	55	88	69	213
Zr	66	48	162	-	123	168	98	221	141	168	165	140	67
Hf	2.60	3.82	4.32	3.34	3.93	3.68	5.19	5.76	5.53	4.78	5.10	4.22	6.06
Ta	2.43	7.64	10.64	0.71	0.82	0.86	1.15	1.21	1.24	0.91	1.15	1.02	2.14
Th	0.30	0.52	1.59	0.89	0.90	0.98	1.45	1.47	1.36	1.11	1.30	1.14	2.85
U	0.4	0.8	1.8	0.6	0.2	0.6	0.8	0.5	0.9	1.1	0.0	0.4	1.6
La	5.5	9.8	7.9	12.1	14.2	13.2	18.5	18.1	15.2	13.2	15.8	13.2	27.7
Ce	12.7	20.8	18.0	24.6	27.6	26.3	36.8	43.9	34.7	30.0	33.6	25.7	59.3
Nd	9	13	18	15	18	16	24	26	16	21	23	12	21
Sm	3.37	3.98	4.67	4.73	5.48	5.28	7.18	7.01	6.78	6.06	6.93	5.72	7.71
Eu	1.23	1.30	1.65	1.38	1.63	1.64	2.06	2.27	2.15	1.83	2.02	1.63	2.45
Tb	0.61	0.79	0.89	0.71	0.87	0.81	1.00	1.05	1.01	0.86	0.99	1.02	0.92
Yb	2.98	3.66	4.45	2.48	3.01	2.76	3.47	3.29	3.74	3.36	4.40	3.51	3.15
Lu	0.50	0.59	0.68	0.46	0.57	0.47	0.62	0.49	0.56	0.49	0.75	0.64	0.47
*t REE	36.1	53.9	55.7	61.6	71.4	66.9	93.1	101.6	79.6	76.8	87.6	63.1	122.8

II. Trace element variations

Incompatible elements

Establishing the compositional similarities and differences in the mantle source for the Roseburg tholeiitic and alkalic basalt suites, as well as for the different volcanic centers, is an important step in determining the geochemical evolution of the region. This can be done by plotting various incompatible trace element pairs which possess different degrees of incompatibility (Bougault et al., 1979, 1980; Tarney et al, 1979). Bougault et al. (1979) have shown that some trace element pairs with identical partition coefficients (e.g. Y-Tb, Zr-Hf, and Nb-Ta) have not been observed to be fractionated in basalts sampled from 22° N to 63° N along the Mid-Atlantic ridge. Jochum et al. (1986) argued that the consistency in the ratios of Zr-Hf and Nb-Ta element pairs in oceanic basalts and in C1-chondrites suggested that the relative abundances of these elements are chondritic in the bulk earth. In short, no mantle or magmatic process can fractionate the ratios of these element pairs. So, it is reasonable to assume that all the early Tertiary basalts of the Coast Range province share this same chondritic mantle source with respect to these element ratios.

Variations in the ratios of highly incompatible element pairs such as La-Ce, Th-Ta, La-Th, and La-Ta (i.e. elements with solid/liquid partition coefficients $< .01$) are observed in basalts from different locations along the Mid-Atlantic Ridge because slight differences exist between their relative partition coefficients (Bougault et al., 1979). Differences in these ratios cannot be accomplished even at very low degrees of partial melting in the mantle because their partition coefficients are "nearly " identical. Therefore, different values for these ratios reflect heterogeneous mantle source compositions. La/Th, Ce/La,

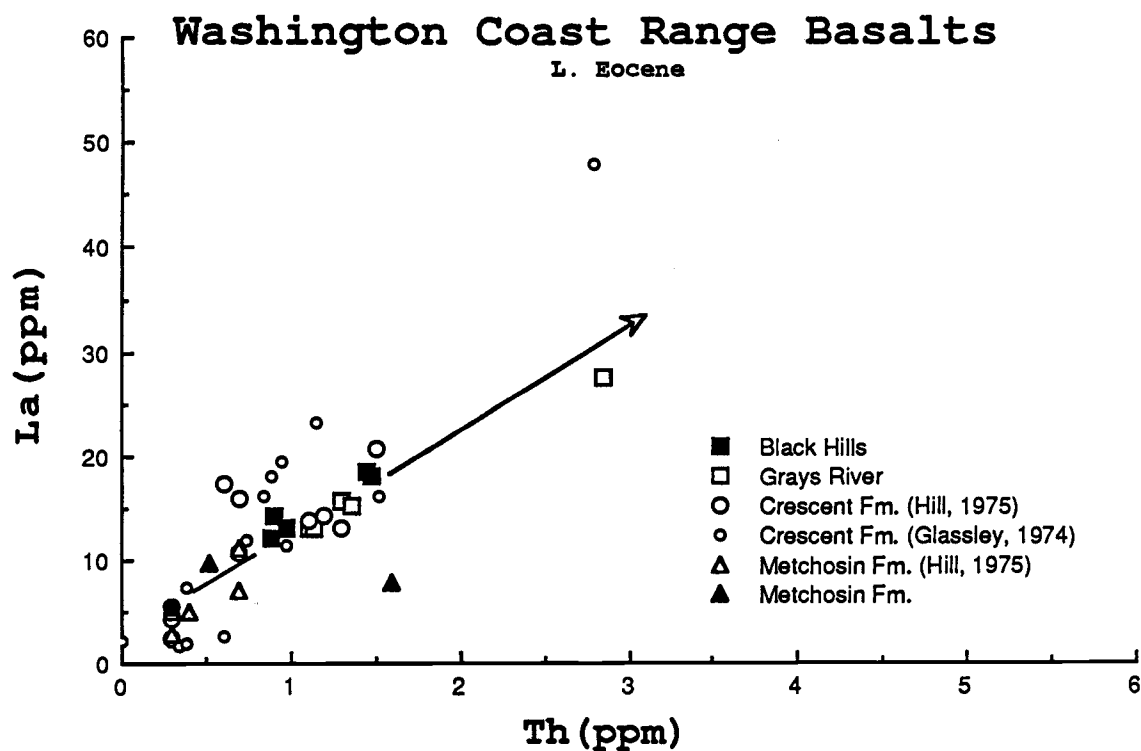
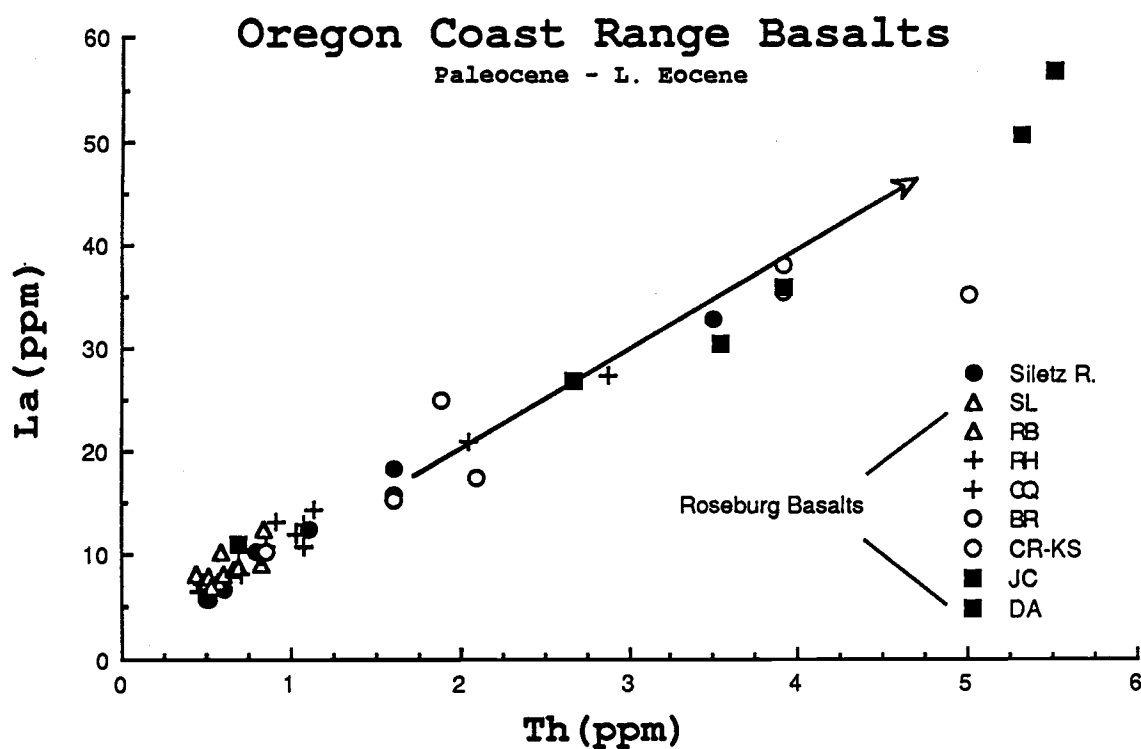


Figure 5.1 La/Th scatter plot: a) Oregon Coast Range basalts. b) Washington Coast Range basalts.

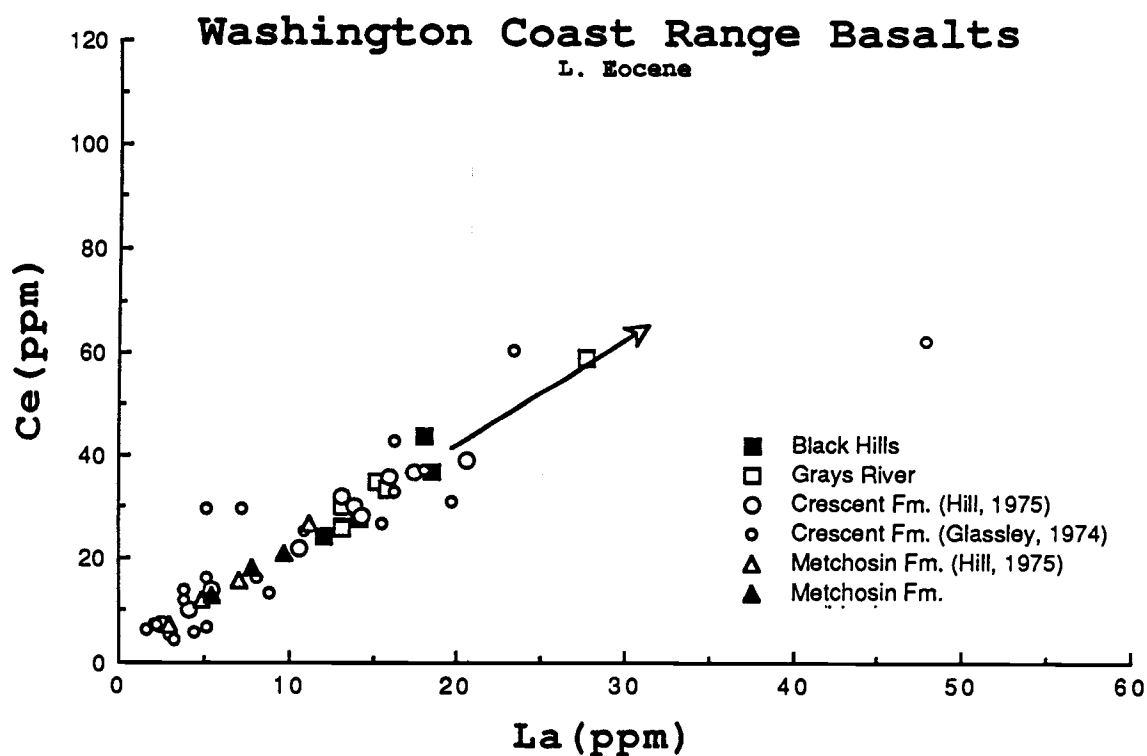
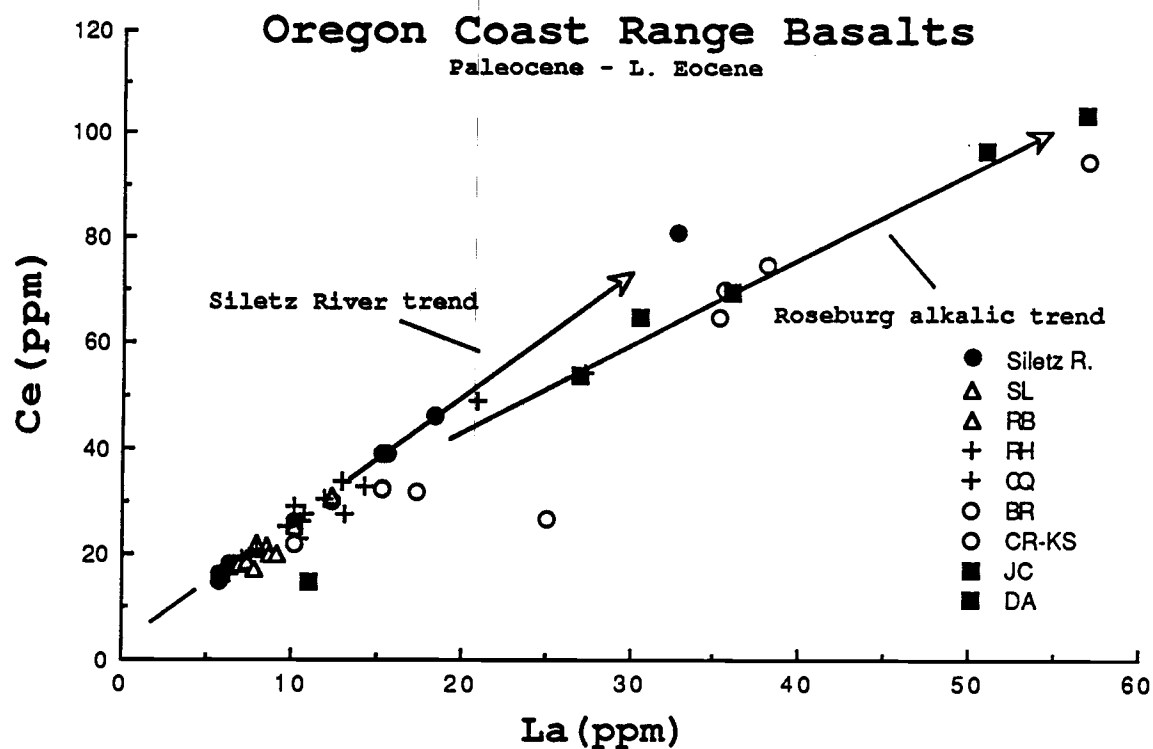


Figure 5.2 Ce/La scatter plots: a) Oregon Coast Range basalts. b) Washington Coast Range basalts.

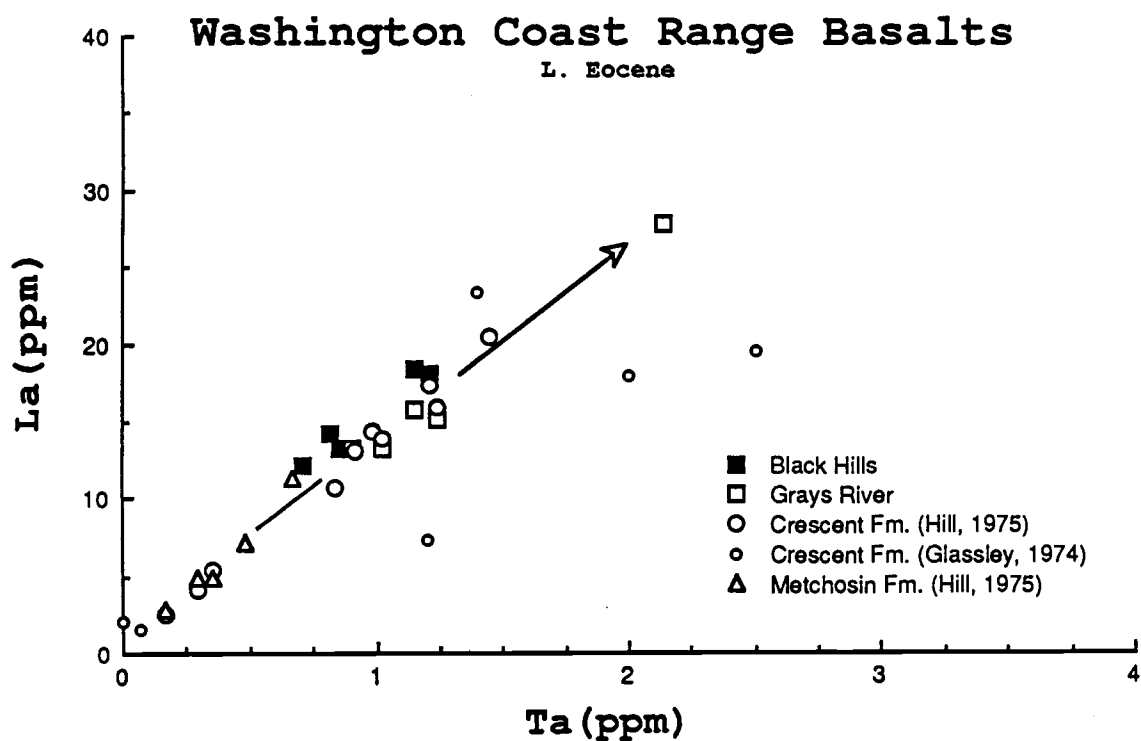
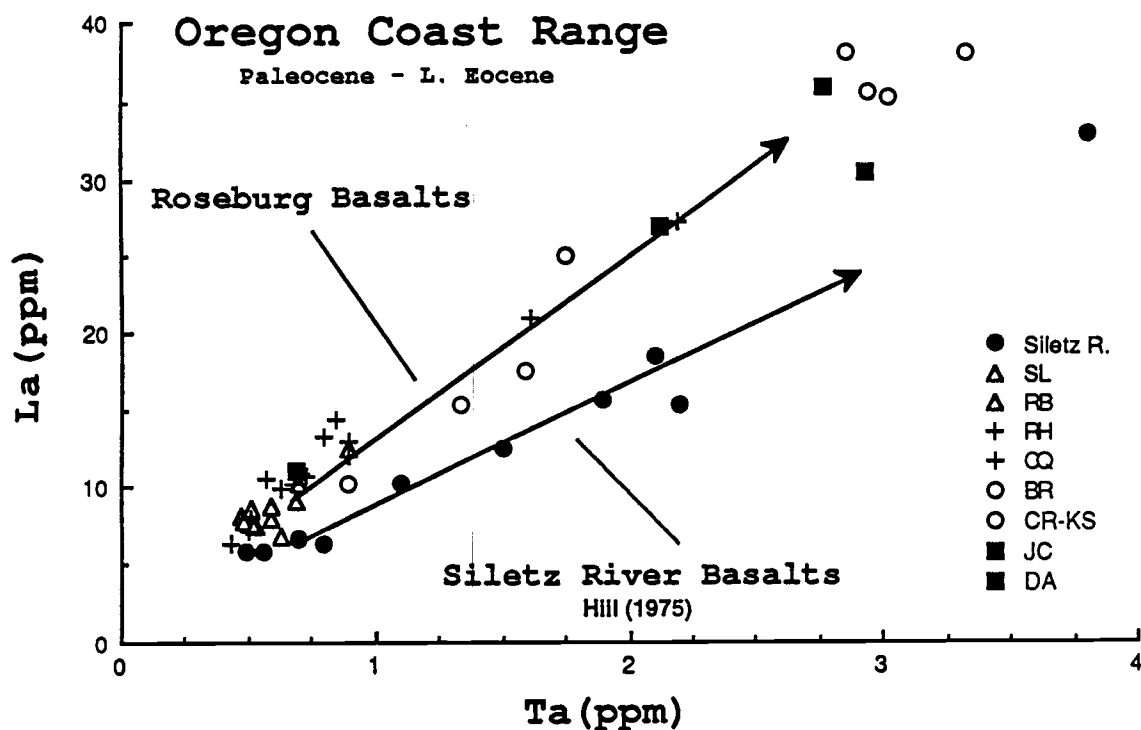


Figure 5.3 La/Ta scatter plot: a) Oregon Coast Range basalts. b) Washington Coast Range basalts.

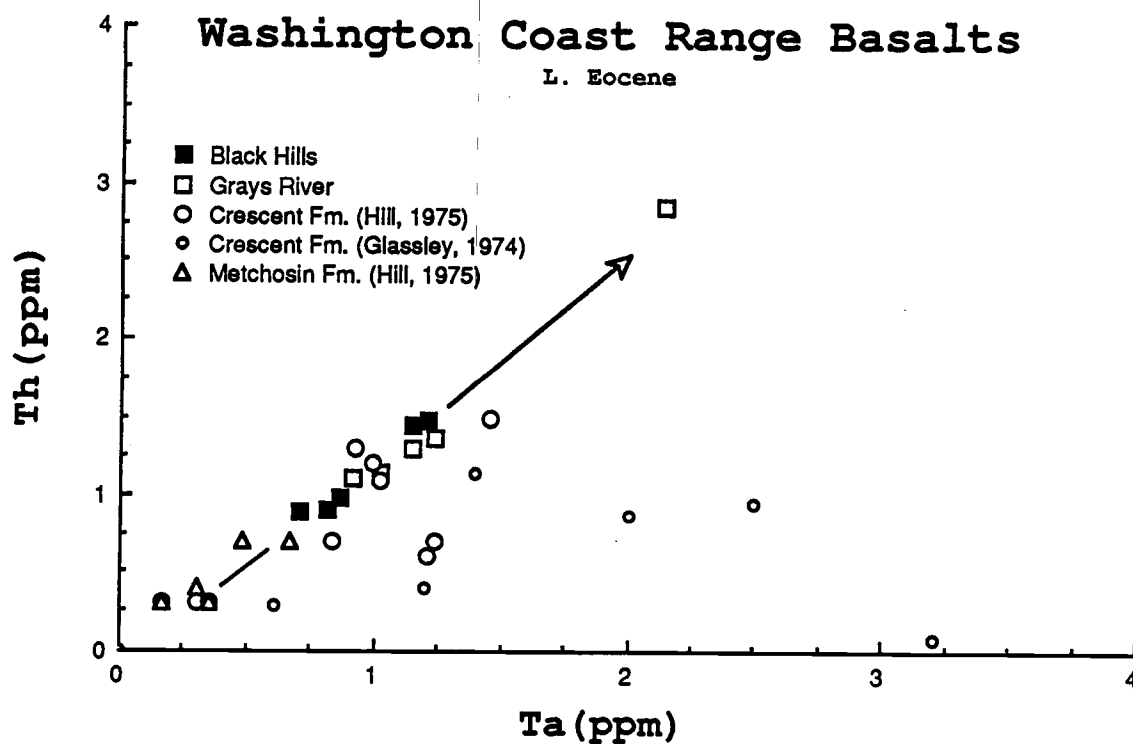
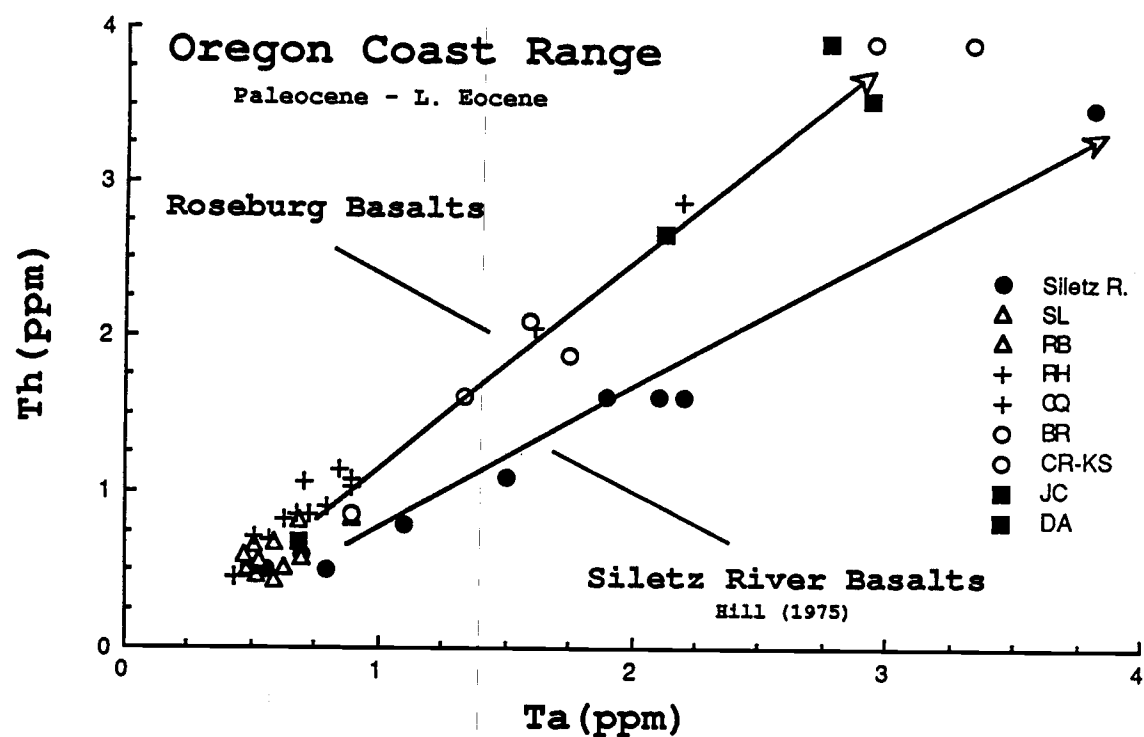


Figure 5.4 Th/Ta scatter plot: a) Oregon Coast Range basalts. b) Washington Coast Range basalts.

La/Ta, and Th/Ta plots of the Oregon Coast Range (Roseburg and Siletz River) basaltic rocks and the Washington Coast Range basaltic rocks (Black Hills, Grays River, Crescent Fm., and Metchosis Fm.) are shown in Figures 5.1a and b, 5.2a and b, 5.3a and b, and 5.4a and b respectively. On these plots the Roseburg tholeiitic and alkalic basalts lie along a straight line which indicates their mantle source compositions are indistinguishable. The Siletz River basalt samples also lie along a straight line suggesting a common mantle source for the tholeiitic and alkalic basalts in that region, but comparison of the two basaltic sequences reveals slight difference in these highly incompatible trace element ratios may exist between the two volcanic sequences (e.g. Th/Ta, and La/Ta). Subtle distinctions between the two areas is difficult to ascertain because the data were collected during different investigations (e.g. Ce/La). Plots of these element pairs for the Washington Coast Range shows that most of the other early Tertiary basalts generally fall along the trend lines of the Roseburg basalts, but small difference in their relative abundances may exist between these other early Tertiary volcanic centers. Undoubtedly some of the scatter on the diagrams is due to analytical uncertainties. On the other hand, the Siletz River basalts and some of the Crescent basalts are notable exceptions to the bulk trends (Figure 5.3b and 5.4b). A larger sample set from these other areas is needed to determine if these slight variations in the La/Ta ratio are real. A first approximation of the differences in these element ratios would suggest that the Siletz basalts and some Crescent basalts are derived from a mantle that is distinctly different from the mantle which produced the other Coast Range basalts. The enrichment of the Siletz in Ta might also be explained by contamination if these rocks were powdered for analysis in a tungsten carbide ball mill. The lack of significant scatter along the Siletz River La/Ta trend would argue against the latter explanation.

If the Siletz River basalts are derived from a compositionally different mantle source, then this difference should be observed in some of the other highly incompatible

element ratios (e.g. La/Th). Average La/Th ratios for the different volcanic centers of the Coast Range were calculated by fitting a least squares line through the data points from samples from each basaltic accumulation. The slope of this line was taken as the average ratio for the volcanic center. The ratios for these areas range from 8.5 to 13.4. The highest ratios were found in the Metcovich and Crescent basalts and the lowest ratios were found in the Siletz and Grays River samples. The low La/Th and La/Ta in the Siletz River basalts lead to the conclusion that its mantle source is compositionally different from the Roseburg basalts. Conclusive evidence for determining if the Siletz River, Roseburg, and other early Tertiary basalts are derived from different mantle source compositions is not presently available. More data (preferably from one comprehensive study) are needed from each volcanic center to confirm or exclude the possibility of mantle heterogeneity in the source(s) of the early Tertiary Oregon-Washington Coast Range basalts.

The geochemical discussion that has been followed to this point is based on the relative differences in the partition coefficients of incompatible trace elements which reflect different petrogenetic process in mantle source regions (Bougault et al., 1979). The highly incompatible element scatter plots indicate that the Roseburg tholeiites and alkali basalts are derived from a compositionally homogeneous mantle source. Their compositional differences must be the result of some process other than an initial mantle source heterogeneity to produce basalts with distinctly different trace element abundances. The percentage of partial melting in the mantle will affect incompatible element abundances according to their partitioning properties between the melt and the residual mantle mineralogy. The greater the difference between the partition coefficients, the greater is the fractionating effect of partial melting on the relative abundances of the incompatible elements. Plotting "slightly" incompatible elements (partition coefficient of ~ 0.1) against "highly" incompatible elements (partition coefficient of ~ 0.01 or less) will accentuate the effects of partial melting on the relative trace element abundance patterns. Incompatible

element pairs with partition coefficients which differ by an order of magnitude are La-Sm, Ti-Th, Hf-Ta, and Hf-La. Hf-La for the Oregon and Washington basalts are plotted in Figures 5.4a and b. The differences between the Roseburg tholeiites and alkali basalts are immediately evident from this figure (the same trends are observed on plots of Ti/Th, Hf-Ta, and La/Sm). The tholeiites have consistently higher "less" incompatible/"more" incompatible trace element ratios. High concentrations of the "less" incompatible constituent in the melt is favored by higher degrees of partial melting which releases more of the "less" incompatible element from the mantle source. The concentrations of the "more" incompatible elements will be higher (thus decrease the less/more incompatible element ratio) if the degree of partial melting is low because they are the first constituents to enter the melt.

Linear slopes of data points on these figures represent fractional crystallization trends. The Roseburg tholeiitic basalts represent one such fractionation trend on all the diagrams. The tholeiites have all been derived by similar degrees of partial melting and their compositional variation is likely due to fractional crystallization after the melt was segregated from its mantle source. The scatter in the Roseburg alkali basalt suite indicates that much of the chemical variation is due to small and variable degrees of partial melting. The basanitic alkali basalts form a well defined fractionation trend which follows a low slope. This trend is consistent with generation of basanitic rock types by less than 5 % partial melting (Sun and Hanson, 1975; Frey et al., 1978). The other alkali basalts were produced by higher degrees of partial melting than the basanites but still significantly less than the tholeiitic basalts.

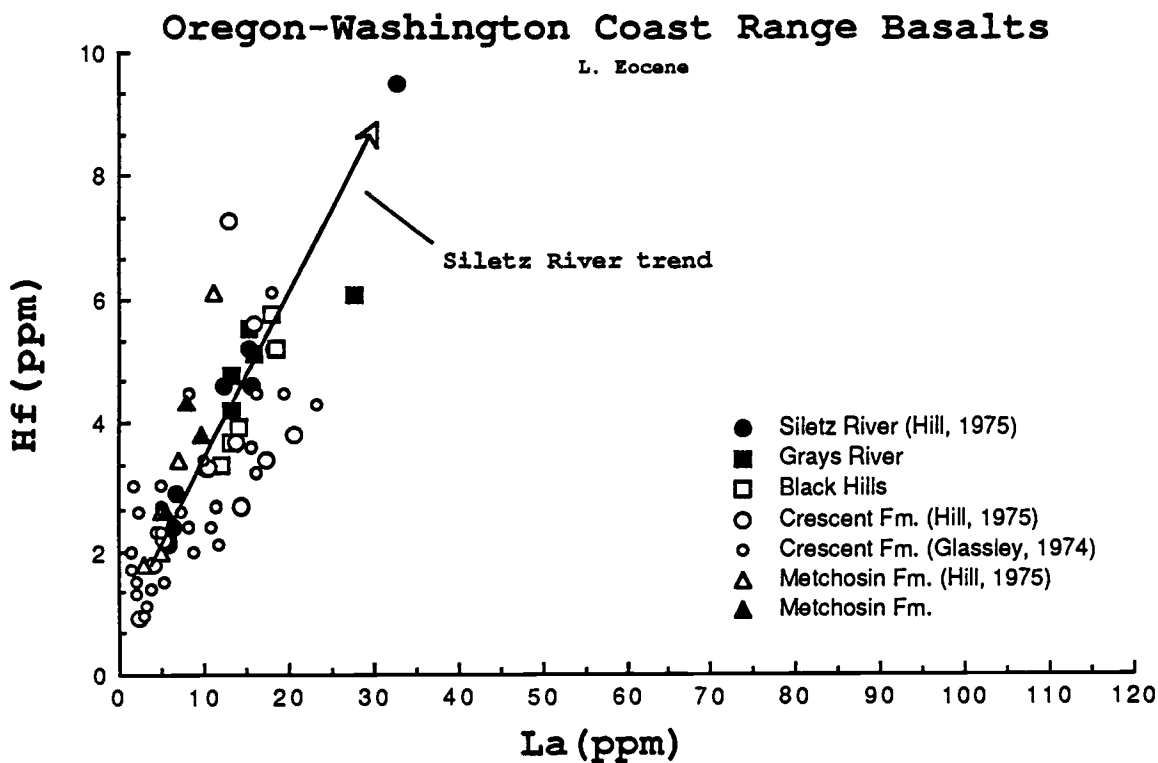
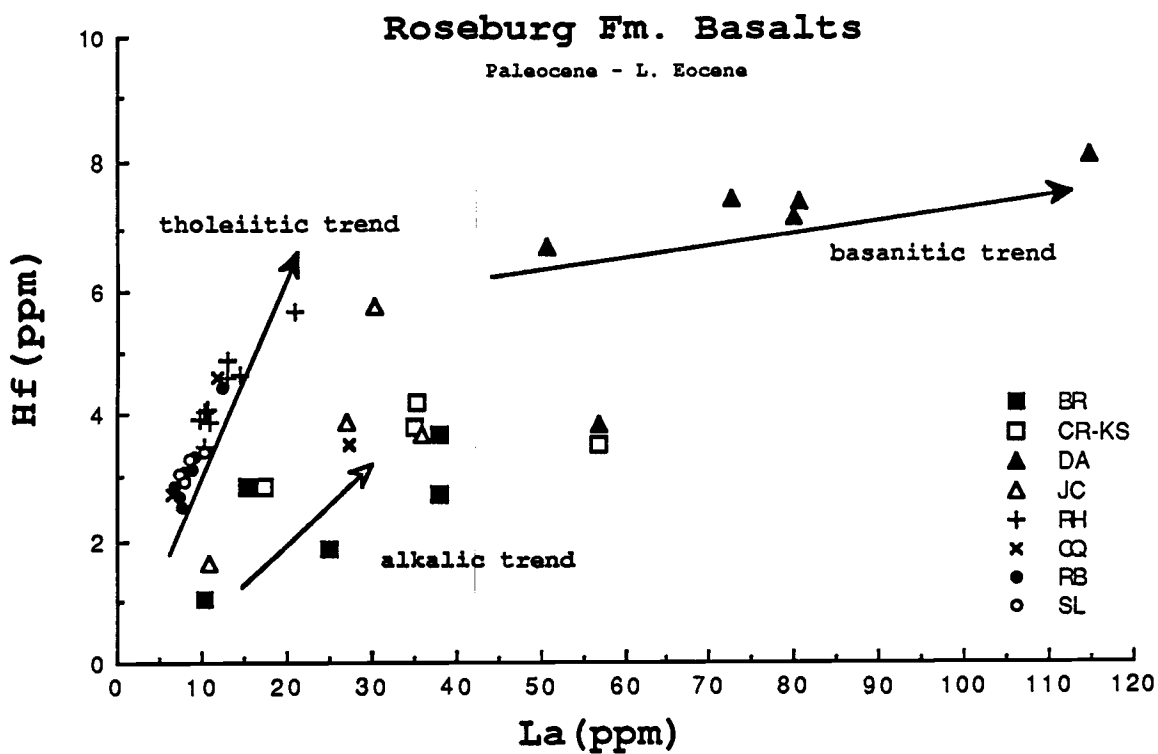


Figure 5.5 Hf/La scatter plot: a) Oregon Coast Range basalts. b) Washington Coast Range basalts.

Rare Earth Elements

The conclusion drawn from the incompatible element plots can be further tested by the variation in the relative abundances of the rare earth elements (REE). The REE display a continuum of geochemical properties from the light rare earth elements (LREE) to the heavy rare earth elements (HREE) which can be used to quantify petrogenetic processes occurring during magma generation and differentiation. Certain elements in this chemical group are specifically partitioned into major mineral phases which are present either in the mantle source (e.g. garnet) or become stable during the later stages of differentiation (e.g. plagioclase). Appearance or disappearance of these phases control the concentration of the REE in the final basaltic composition. The LREE are highly incompatible whereas the HREE are less incompatible and, in some instances the HREE are partitioned into high pressure mineral phases (e.g. Yb is strongly partitioned into garnet). Relative fractionations of the LREE/HREE are analogous to the "less" incompatible/"more" incompatible element ratios discussed above and their relative abundances are generally controlled by partial melting processes. The advantage of the REE over the incompatible element ratios lies in their mineral specific geochemical properties. A complete discussion on the petrogenetic modeling of the REE can be found in Hanson (1980) and, more recently, Haskin (1984). A brief qualitative assessment of the REE properties in major mineral phases (relevant to this study) and their effect on the REE concentration on the magma is given below (from Hanson, 1980):

Feldspar - Plagioclase strongly partitions Eu+2 but has minor effect on the overall REE pattern except for producing an Eu anomaly. The partitioning of Eu into plagioclase decreases with increasing oxygen fugacity of the melt system.

Garnet - Garnet increasingly partitions HREE according to their decreasing ionic radii. The presence of garnet in the source rock leads to a depletion of the HREE.

Orthopyroxene - Hypersthene and pigeonite do not strongly partition any of the REE. OPX fractional crystallization may lead to a slight enrichment of the LREE over the HREE.

Clinopyroxene - CPX partitioning of the REE is dependent on its composition but generally it has a greater affinity for the HREE than the LREEs.

Olivine - Olivine does not partition any of the REE and its presence in the source rock essentially enriches all the REE equally.

In general, the LREE are not significantly partitioned into any major mineral phase and their concentration increases in the magma as differentiation proceeds or as degree of partial melting decreases. The HREE are strongly partitioned into the high pressure mineral phases such as garnet and to a lesser degree clinopyroxene. The HREE concentrations in the liquid will be buffered by the presence of these minerals in the mantle until partial melting is sufficiently high to consume the garnet and/or clinopyroxene fraction of the residual mantle mineralogy. Once these minerals are consumed, the HREE concentration of the magma will increase or decrease in concert with the LREE (i.e. no fractionation will occur between the LREE and HREE). This characterization of the REE is extremely simplistic and does not take into account several magma generating processes which have been proposed to explain the diverse REE patterns found in OIB and MORB. A more quantitative modelling approach to this subject is beyond the scope of this project.

The chondrite normalized REE patterns for the Roseburg basalts are presented in Figures 5.6 - 5.10. The Siletz River Basalt REE data from Hill (1975) are plotted for

comparison in Figure 5.11. New REE data from the Washington Coast Range (Grays River, Black Hills) are plotted in Figures 5.12 and 5.13 along with Hill's data from the same areas. The REE abundance results for the Roseburg basalts are plotted on chondrite normalized REE diagrams and grouped according to their geographic location. The normalization values are taken from Ma et al. (1981). The coherence of REE patterns within outcrop areas in southern Oregon Coast Range shows that each location generally represents a stage in the differentiation of the Roseburg basaltic pile. Differentiation of the basaltic sequence evolves from flat or slightly fractionated REE patterns in the south to highly fractionated REE patterns to the north. The degree REE fractionation is consistent from one side of the basin to the other.

The Sugarloaf and Roseburg tholeiitic basalt exposures have REE patterns which are slightly enriched in LREE abundances 20-40x chondrite and HREE abundances 10-15x chondrite (Figure 5.6a and b). None of the samples analysed from the lower Roseburg tholeiitic unit show the characteristic LREE depleted patterns commonly associated with "normal" MORB ridge segments. These patterns are similar to transitional or enriched MORB compositions (Saunders, 1980; BVSP, 1981). The REE patterns of the Roseburg tholeiitic basalts are indistinguishable from those of the Siletz River lower tholeiitic unit (Figure 5.11b). In contrast, comparison of the tholeiites of the Oregon Coast Range with basalts from the Washington Coast Range reveal regional differences in their stages of differentiation. The Crescent and Metchosin basalts (Figures 5.12a, 5.13a and b) have flat to slightly enriched REE patterns similar to the Roseburg and Siletz River basalts but some samples are slightly LREE depleted. This would indicate a greater MORB affinity to these basalts than found in the south. The REE patterns of the Grays River and Black Hills (Figure 5.12b and c) resemble patterns found in the more evolved basalts of the Red Hill anticline area.

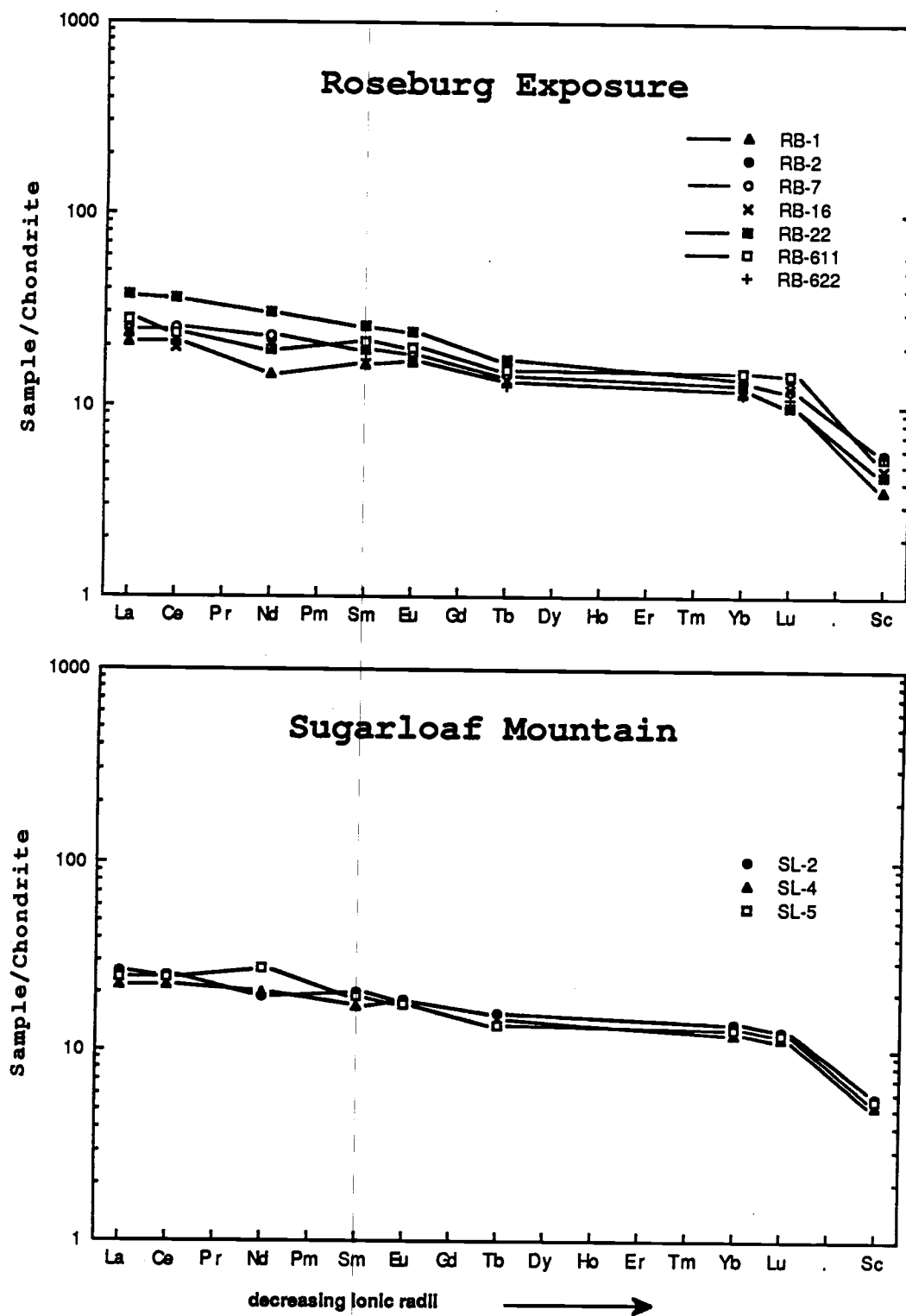


Figure 5.6 REE diagrams: a) Roseburg exposure b) Sugarloaf Mtn.

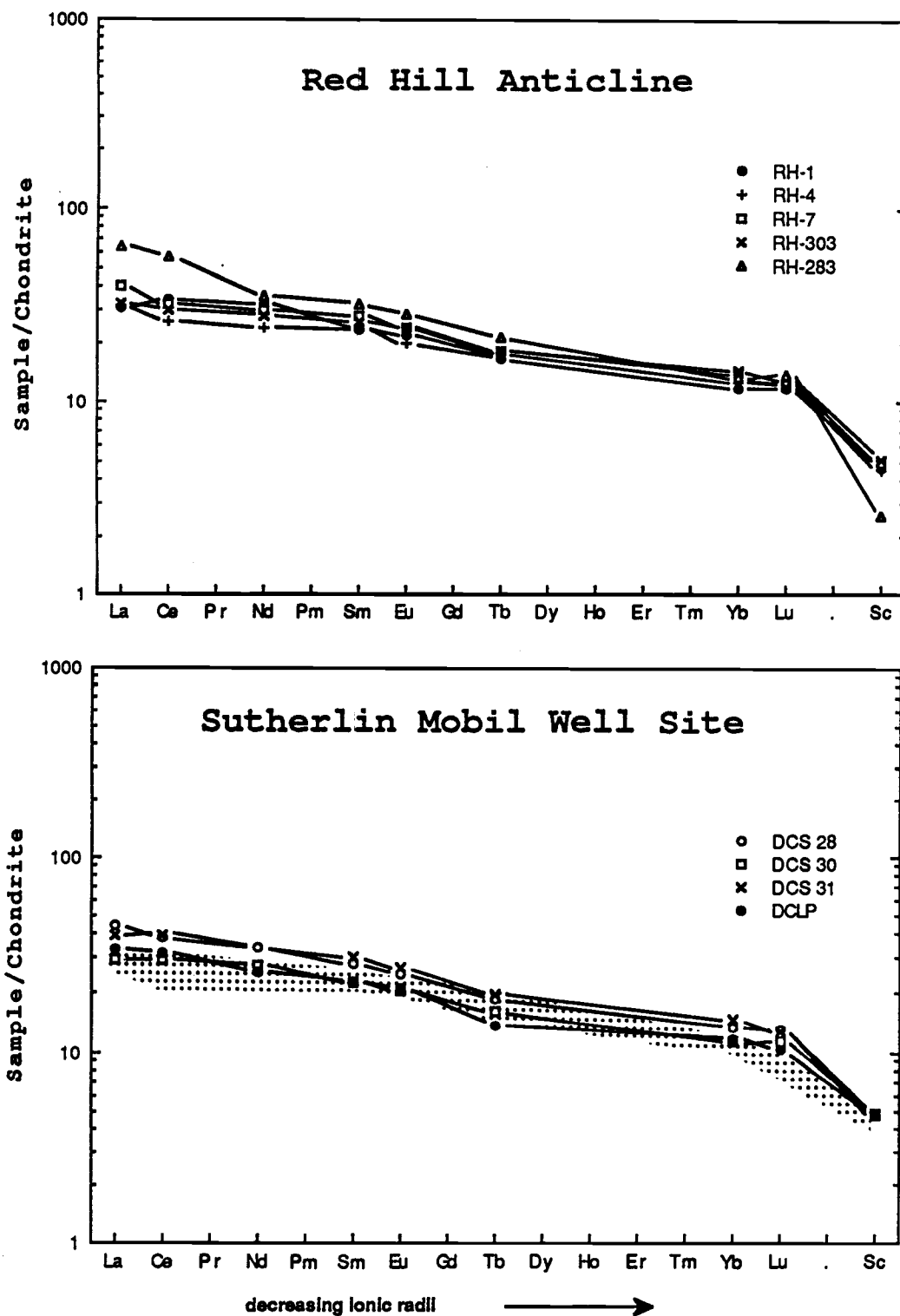


Figure 5.7 REE diagrams: a) Red Hill anticline b) Sutherlin test well site, dotted field represents range of the drill chip samples.

Some of the Coquille-Myrtle Point samples display REE patterns that are similar to the Sugarloaf and Roseburg tholeiites with comparable total REE contents but other samples exhibit lower abundances of the HREE and enriched LREE abundances (i.e. increased fractionation; Figure 5.8b). The range of LREE enrichment is 20-80x chondrite and the HREE are 9-14x chondrite. CQ-5 and CQ-11 were thought to be possible parental magmas based on their major element compositions. The parental nature of these samples is further supported by their low total REE abundance levels. Low total REE abundances together with high MgO and Ni abundances indicate the magma has not been substantially modified by crystal fractionation processes. The major element compositions of the Coquille-Myrtle Point basalts are more primitive (higher Mg* and Ni abundances) than the roughly equivalent Red Hill basalts on the eastern edge of the southern Oregon Coast Range. Basalts of the Red Hill anticline have slightly more fractionated REE patterns which suggests they may be more evolved than the Coquille-Myrtle Point basaltic rocks. LREE in the Red Hill area range from 30-40x chondrite and have HREE concentrations near 10-15x chondrite. As indicated by the field relationships and the major element trends, the trace element character of the Coquill-Myrtle Point and Red Hill basalt represent a transition from tholeiitic to more alkalic compositions.

Fractionation of the REE patterns continues to increase in the alkali basalt suite. The high Mg picrites and ankaramites from the the Blue Ridge Mountain exposure have LREE enrichments of 30-100x chondrite with HREE concentrations that vary from 6-13x chondrite. The increase in LREE abundances in these samples is accompanied by a similar increase in their HREE abundances resulting in REE patterns which "stack" on the REE diagram. Generally, stacking of REE patterns indicates an increase in total REE content without any fractionation of the light from the heavy REE. This is attributed to fractional crystallization of mineral phases which do not partition REE (e.g. olivine and/or plagioclase). The Jack Creek anticline samples also show a stacking REE pattern which

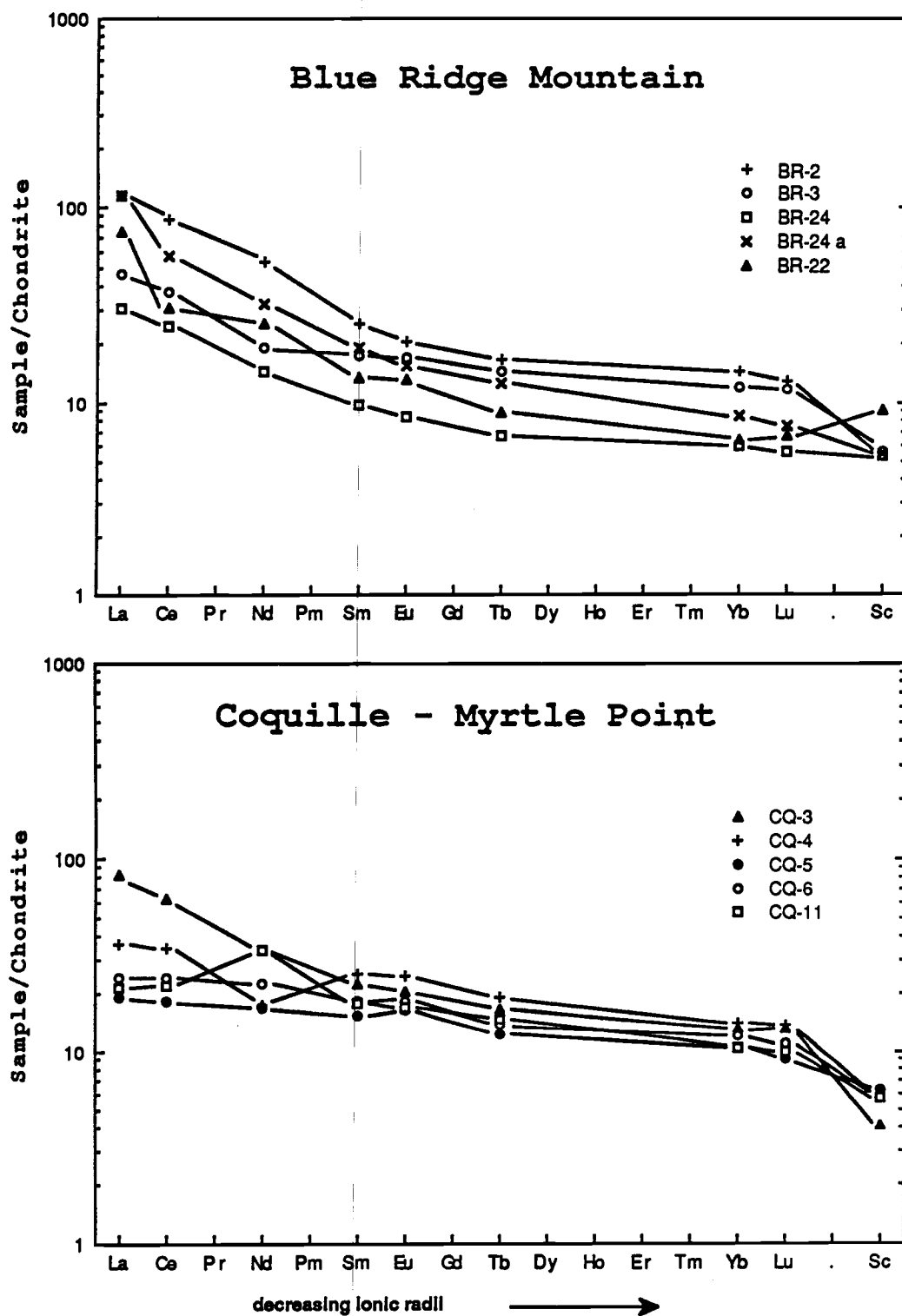


Figure 5.8 REE diagrams: a) Blue Ridge Mtn. b) Coquille-Myrtle Point exposure.

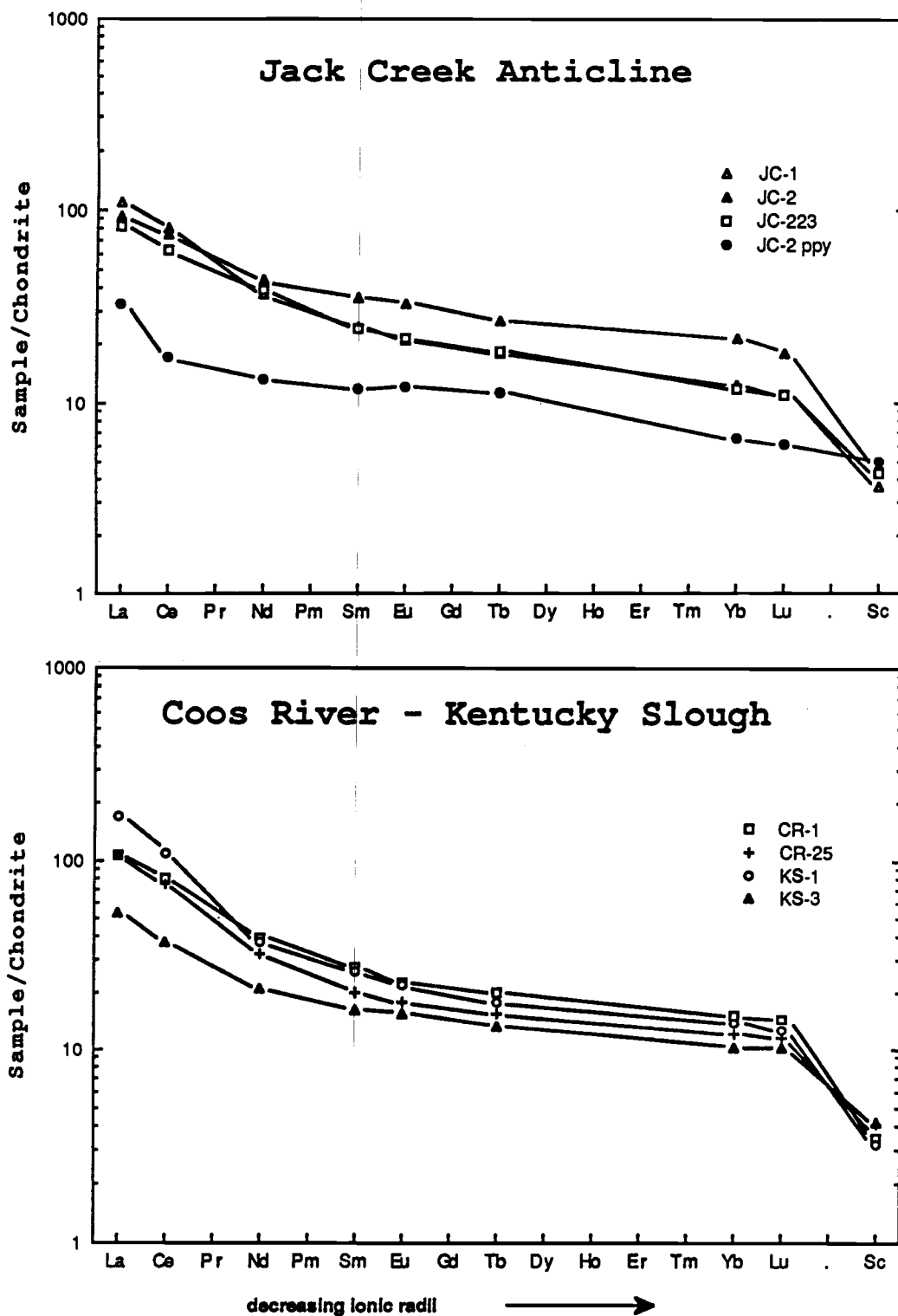


Figure 5.9 REE diagrams: a) Jack Creek Anticline b) Coos River-Kentucky Slough exposures

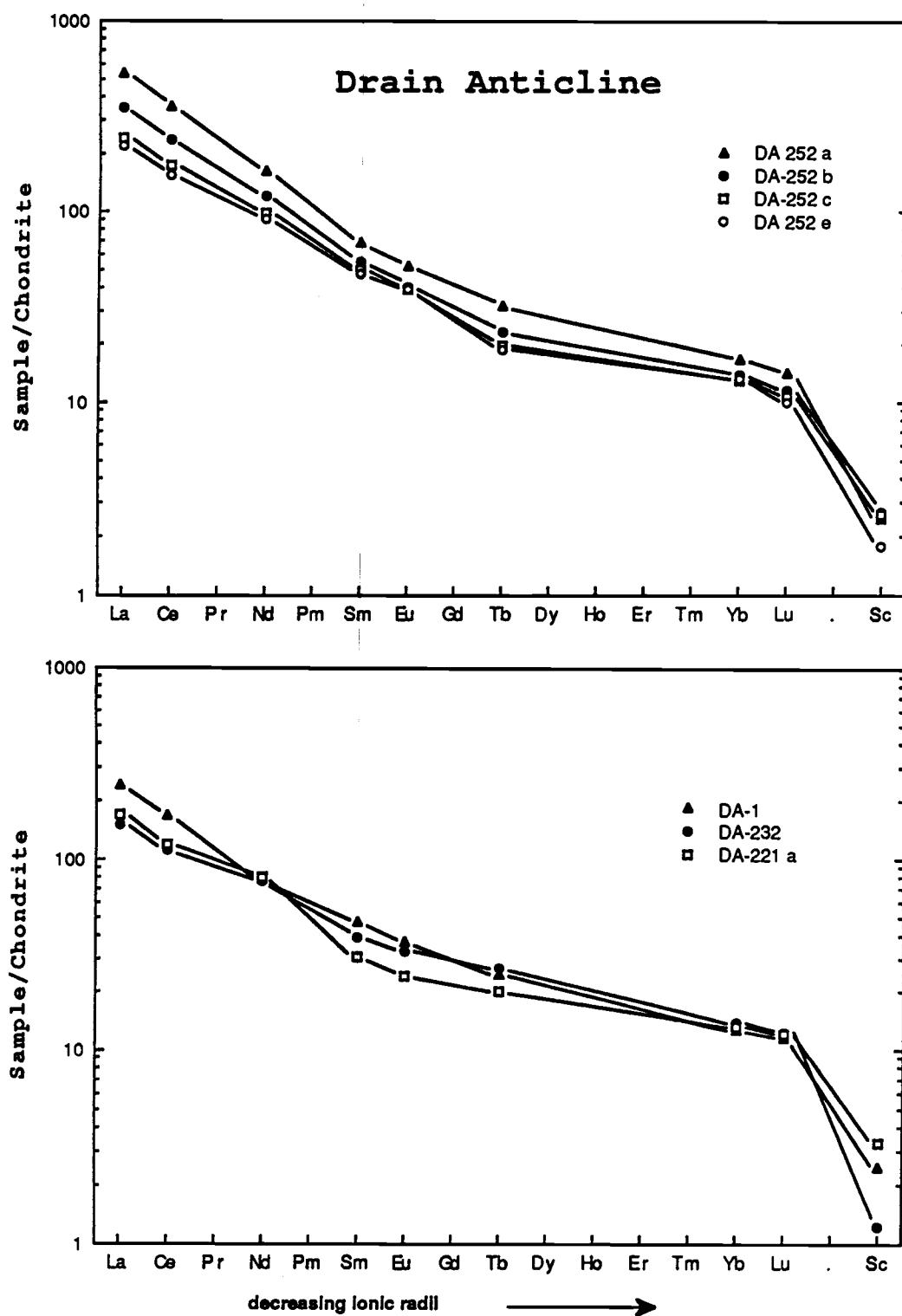


Figure 5.10 REE diagrams: Drain anticline exposure.

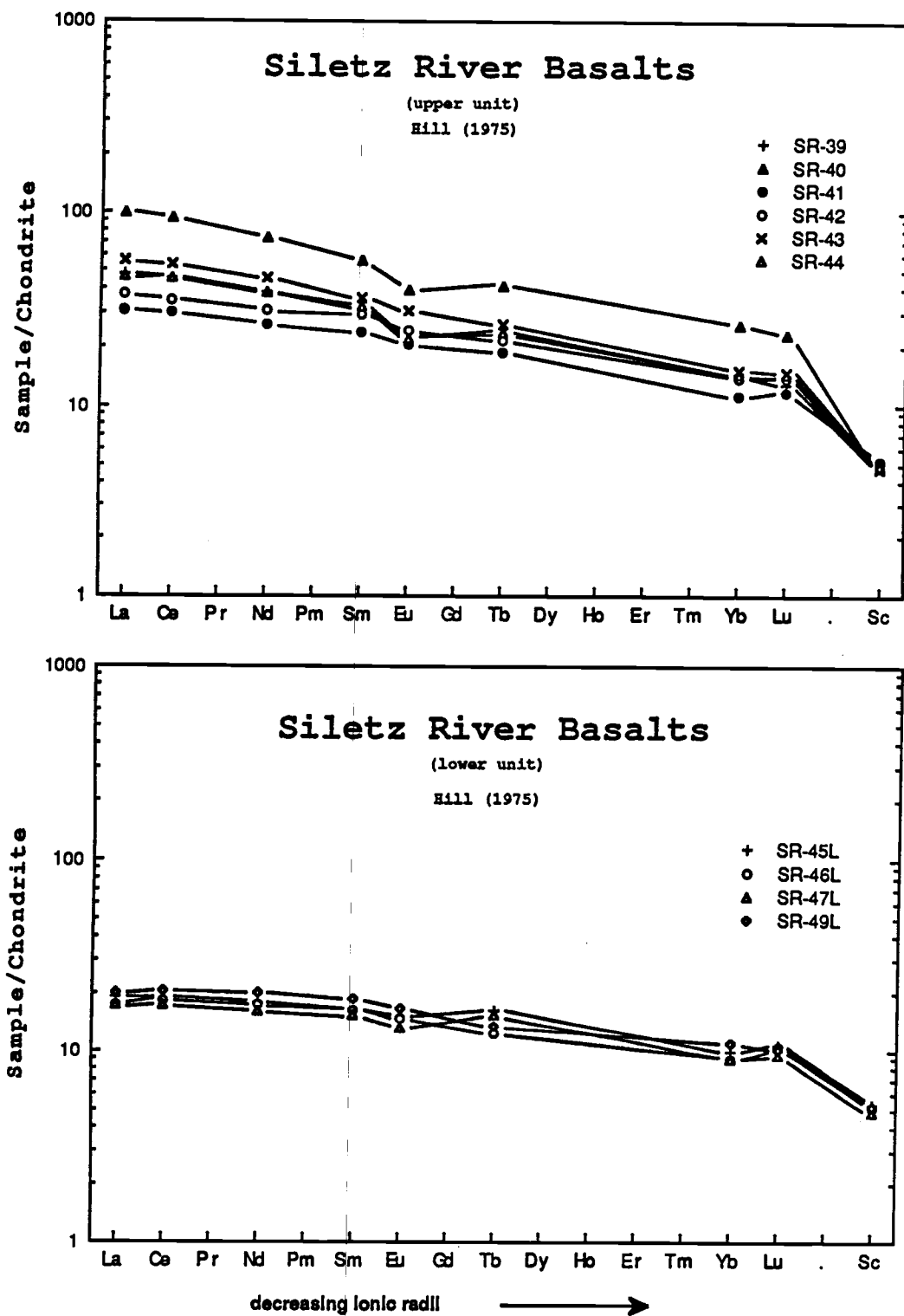


Figure 5.11 REE diagrams: a) upper Siletz River alkalic basalts b) lower Siletz River tholeiitic basalts

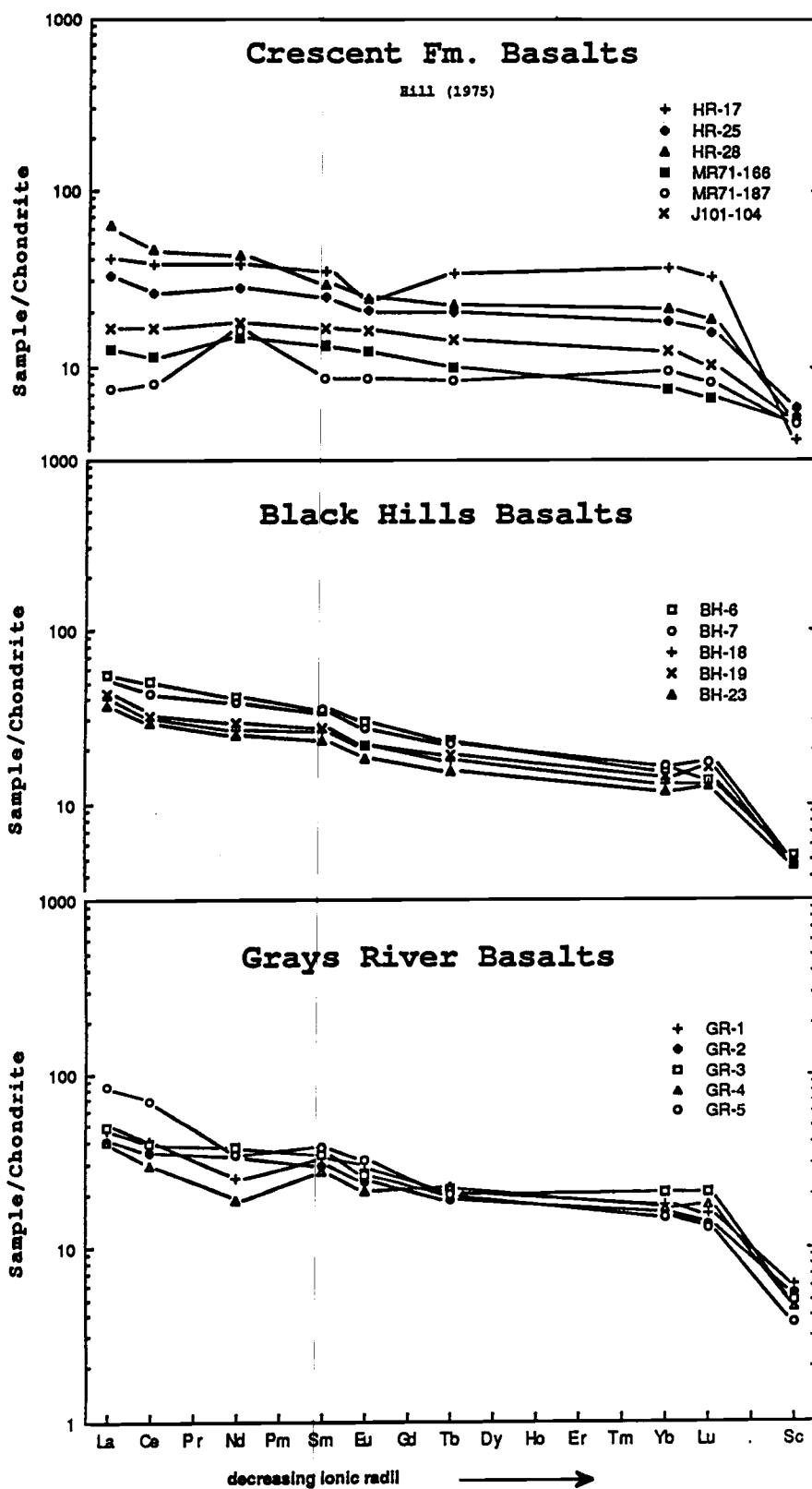


Figure 5.12 REE diagrams: Washington Coast Range a) Crescent Fm. b) Black Hills basalts c) Grays River basalts

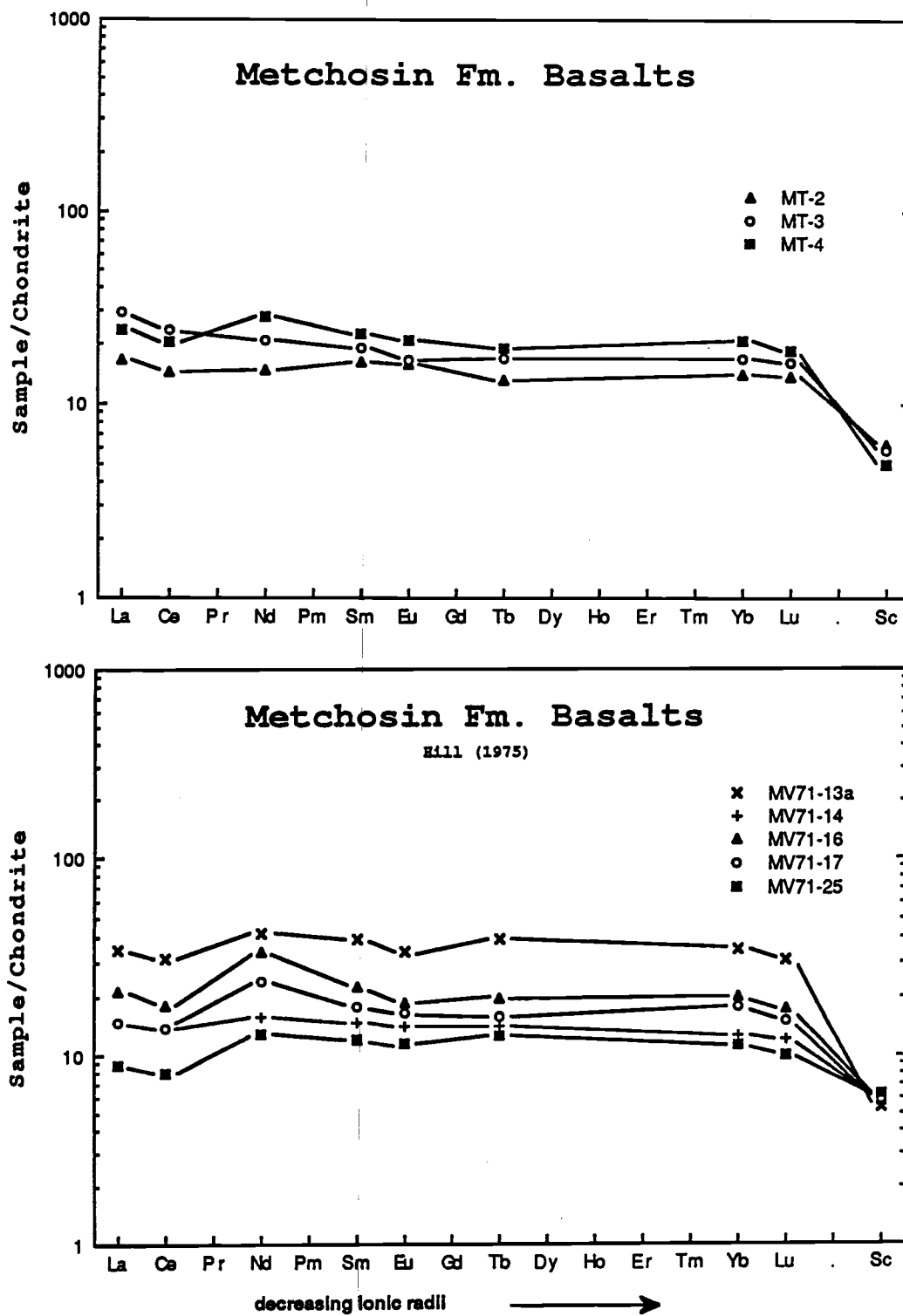


Figure 5.13 REE diagrams: British Columbia Metchosin Fm.

suggests crystal fraction has played a role in the differentiation of the alkali rocks in this area. Textural evidence of crystal fractionation in both areas is found in the increased occurrence of highly porphyritic basalt flows.

In contrast to the stacking REE patterns displayed by samples from the Blue Ridge and Jack Creek exposures, the undersaturated basanitic and alkalic rocks in the Drain, Coos River, Kentucky Slough areas have REE patterns which vary considerably in LREE concentrations yet the HREE abundance range is restricted. The buffering effect of the HREE is probably caused by a residual mineral phase such as garnet in the mantle source for the basanitic magmas which strongly partitions the HREE relative to the LREE. The basanitic sequence is extremely enriched in LREE with La 150-500x chondrite ((La/Sm)_n 3.9-7.6) and Yb 10-14x chondrite. These compositions can be explained by very small degrees of partial melting in the deep mantle where garnet is a stable residual phase (Sun and Hanson, 1975; Frey et al., 1978).

The amount of partial melting for the Roseburg basaltic suites can be qualitatively assessed on a log-log plot of (Ce/Yb)_n versus (Ce)_n (Figure 5.15a after Saunders, 1980). The Roseburg tholeiites and alkali basalts closely follow along trend D which is an equilibrium batch partial melting curve. Tick marks along the trend (see Figure 5.14) represent percentages of partial melting of a garnet lherzolite source (55% ol, 25% opx, 15% cpx, and 5% gt). According to this diagram, most of the alkali basalts could be derived from this type of source by ~5-8% partial melting and the tholeiites between ~10-15% partial melting. Bare in mind that this is not a well constrained model but serves to emphasize the dominate control of partial melting on the evolution of the Roseburg basalts. The relative differences in amounts partial melting neccessary to generate the alkalic and tholeiitic suites substantiates inferences made earlier from the incompatible element scatter plots. If fractional cystalization was a major differentiation mechanism for these basalts, the (Ce/Yb)_n ratio would remain nearly constant as the concentration of Ce

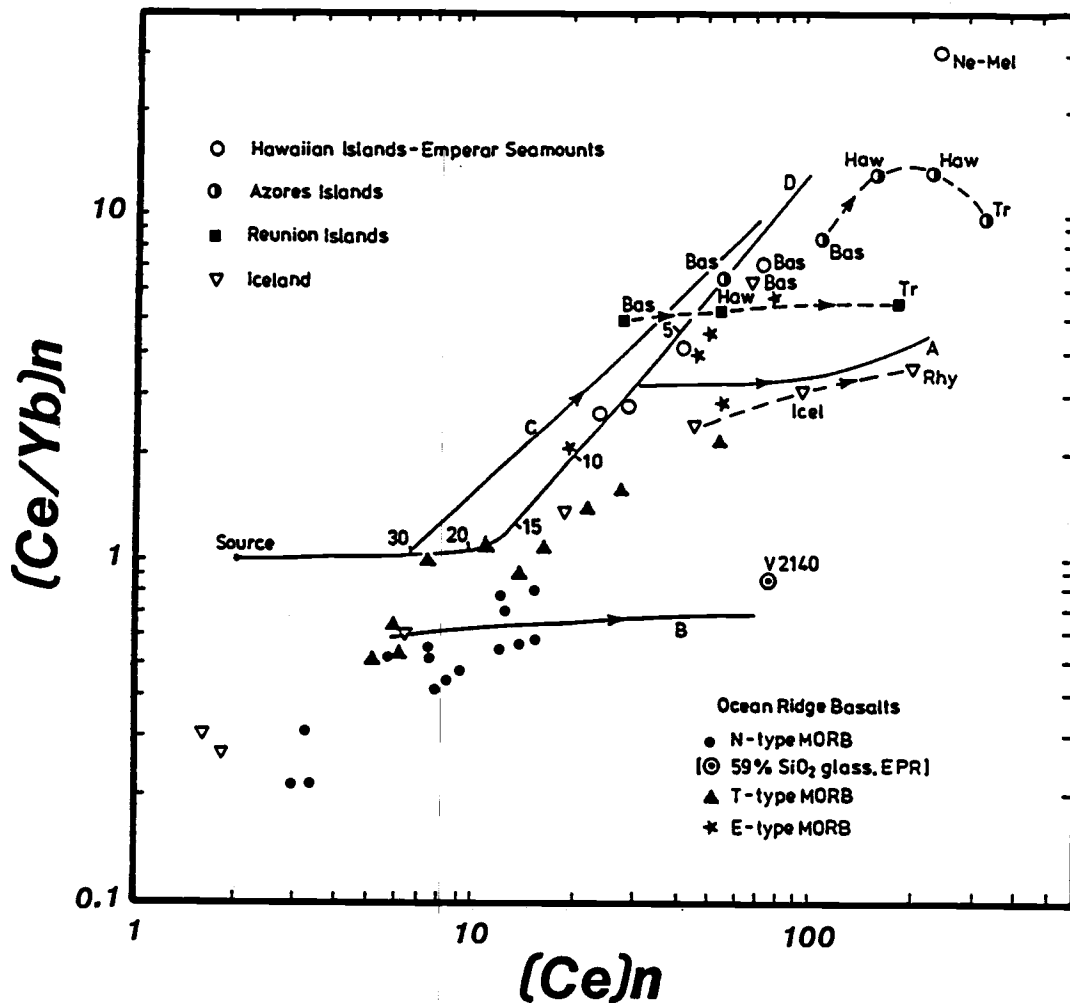


Figure 5.14 Representative oceanic igneous rocks plotted on a log-log plot of $(\text{Ce}/\text{Yb})_n$ ratio versus Ce_n . Fractionation trends indicated by trend lines: A - closed system fractional crystallization (low pressure); B - open system fractional crystallization (low pressure); C - open system fractional crystallization (high pressure eclogite fractionation); D - equilibrium batch partial melting (garnet lherzolite source, 55% ol, 25% opx, 15% cpx, 5% garnet, melting mode 10:20:40:30, respectively, and 2x chondritic REE abundances). Numbers and tick marks on batch melting curve indicate percentage melt. Broken lines indicate rock types from common volcanic centers. All points represent tholeiitic basalts except where indicated: Bas - alkali or alkali ol basalt; Ice - icelandite; Haw - hawaiite; Rhy - rhyolite; Tr - trachyte; Ne-Mel - nepheline-melilite basalt. (diagram reproduced from Saunders, 1984; see reference for details)

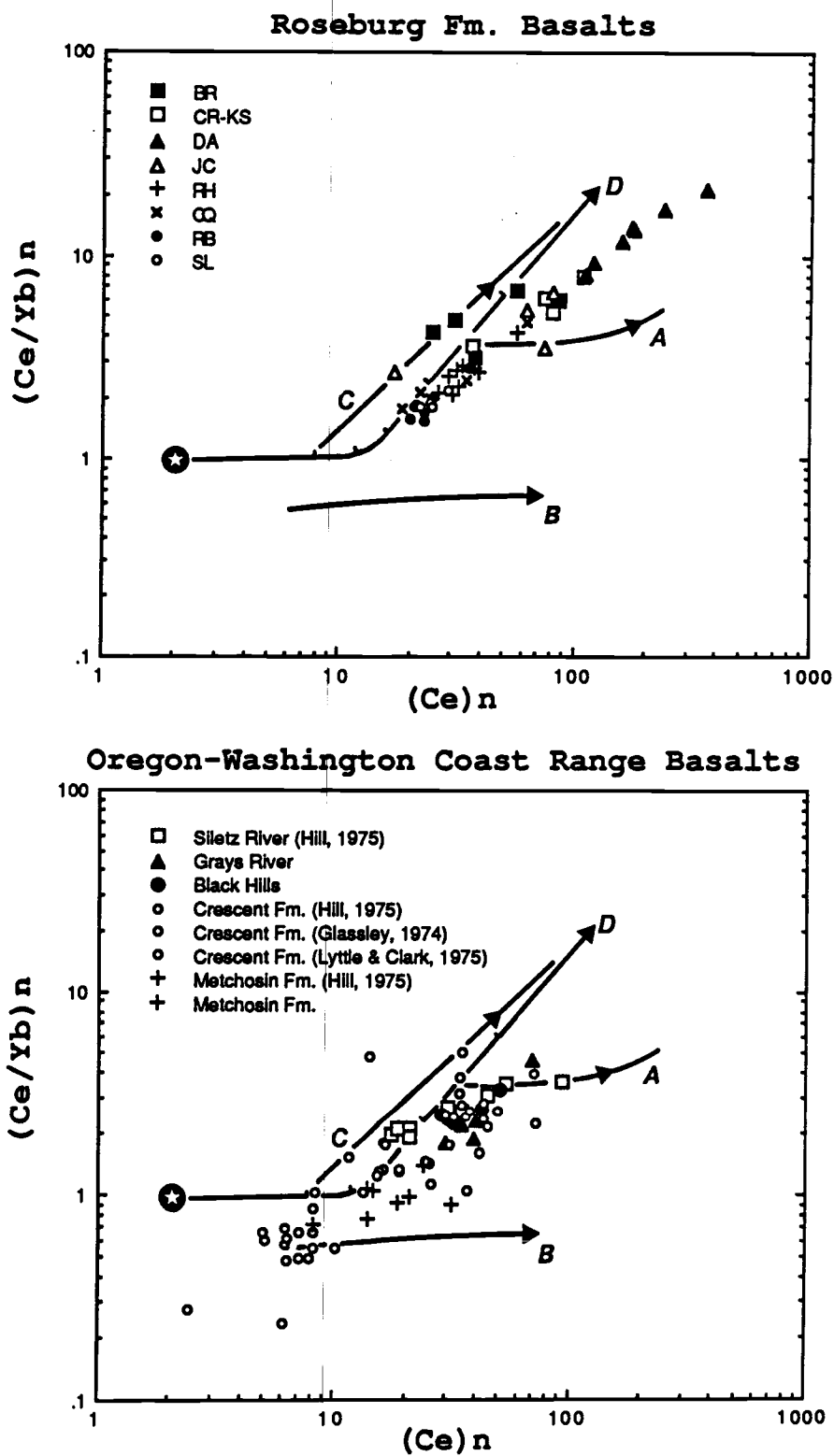


Figure 5.15 Oregon-Washington Coast Range plotted on a log-log plot of $(\text{Ce}/\text{Yb})_n$ ratio versus $\text{Ce}(n)$ (after Saunders, 1984). See Figure 5.14 for details.

increased. This fractional crystallization effect would result in data trends with a more horizontal dispersion on this diagram (trends A and B Figure 5.14).

Basalts from the other early Tertiary volcanic centers in the Oregon-Washington Coast Range are plotted on a $(Ce/Yb)_n$ - $(Ce)_n$ diagram in Figure 5.15b. The differences in the differentiation trends between the Roseburg basalts and the other coast range basalts are immediately evident. The Crescent and Metchisin basalts have lower concentrations of Ce and $(Ce/Yb)_n$ values ≤ 1 . Their differentiation trends indicate a substantial control by fractional crystallization. Both open and/or closed system fractional crystallization could apply to the evolution of these basaltic suites (trend lines B and A respectively). The Black Hill, Grays River, and the Siletz River basalts have compositions similar to the Roseburg tholeiites but the available data suggests closed system fractional crystallization may be a more important factor in the evolution of these rocks. The differentiation of the upper alkalic suite of the Siletz River basalts follows the closed system fractional crystallization trend (line A) very closely and illustrates the difference in the evolution of these rocks compared to the alkalic sequence of the Roseburg basalts.

Spider diagrams

The geochemical data of the early Tertiary Oregon-Washington Coast Range basalts have been normalized to the primordial mantle composition of Wood (1979) and plotted on an extended REE-type diagram referred to as a "spider diagram" (Figures 5.16-5.26). Several spider diagrams of average basalt types from Hawaii and the north Atlantic have been included for comparison. Spider diagrams are a useful visual presentation of large amounts of geochemical data that can be compared quickly and easily. Several variations of the spider diagram have been used in the literature and many different

normalizing compositions are found (e.g. MORB, ordinary chondrite, primitive earth, primordial mantle, etc). The spider diagram format below is after Wood et al. (1980) with slight modifications to include all of the REE analyzed in this study. The trace elements on this diagram are arranged in the order of their incompatibility with an assumed residual mantle mineralogy of olivine, orthopyroxene, and clinopyroxene with or without garnet and spinel. Generally, the incompatibility of the elements decrease from the highly incompatible L.I.L. elements on the left (Rb, Ba, Th, U, K) to the less incompatible HREE on the right. Several of the elements on this diagram can be partitioned into specific mineral phases during magmatic processes (i.e. Sr and Eu to plagioclase; K to biotite and phlogopite; Ta and Ti to Fe-Ti oxide minerals; P to apatite; Yb and Lu (HREE) to garnet). The utility of these plots is similar to the REE diagram but they provide a greater amount of petrogenetic information since the addition or removal of more major mineral phases can be detected. Alteration of the basalt samples can also be evaluated with this plot since many of the L.I.L elements are sensitive to seawater alteration (e.g. Sr, Rb, Ba, U).

The spider diagrams of Roseburg tholeiitic basalts are shown in Figure 5.17 and 5.18. Plots of average MORB (Pearce, 1983; Sun and Nesbitt, 1977) and E-type MORB from the north Atlantic are shown in Figure 5.16. The coast range basalts display a greater similarity to the E-type MORB (410-2 and 413-1) and the N-type MORB (409-2) from the north Atlantic than to the "average" MORB composition in Figure 5.16b. The Siletz River, Black Hills, Grays River, Crescent, and Metchosin basaltic rocks are given in Figures 5.24a, 5.25a, 5.25b, 5.26b, and 5.26a, respectively. These plots also demonstrate a similarity to E-type MORB but the enriched character of the basalts decreases towards a more N-type MORB composition in samples from the Metchosin Formation.

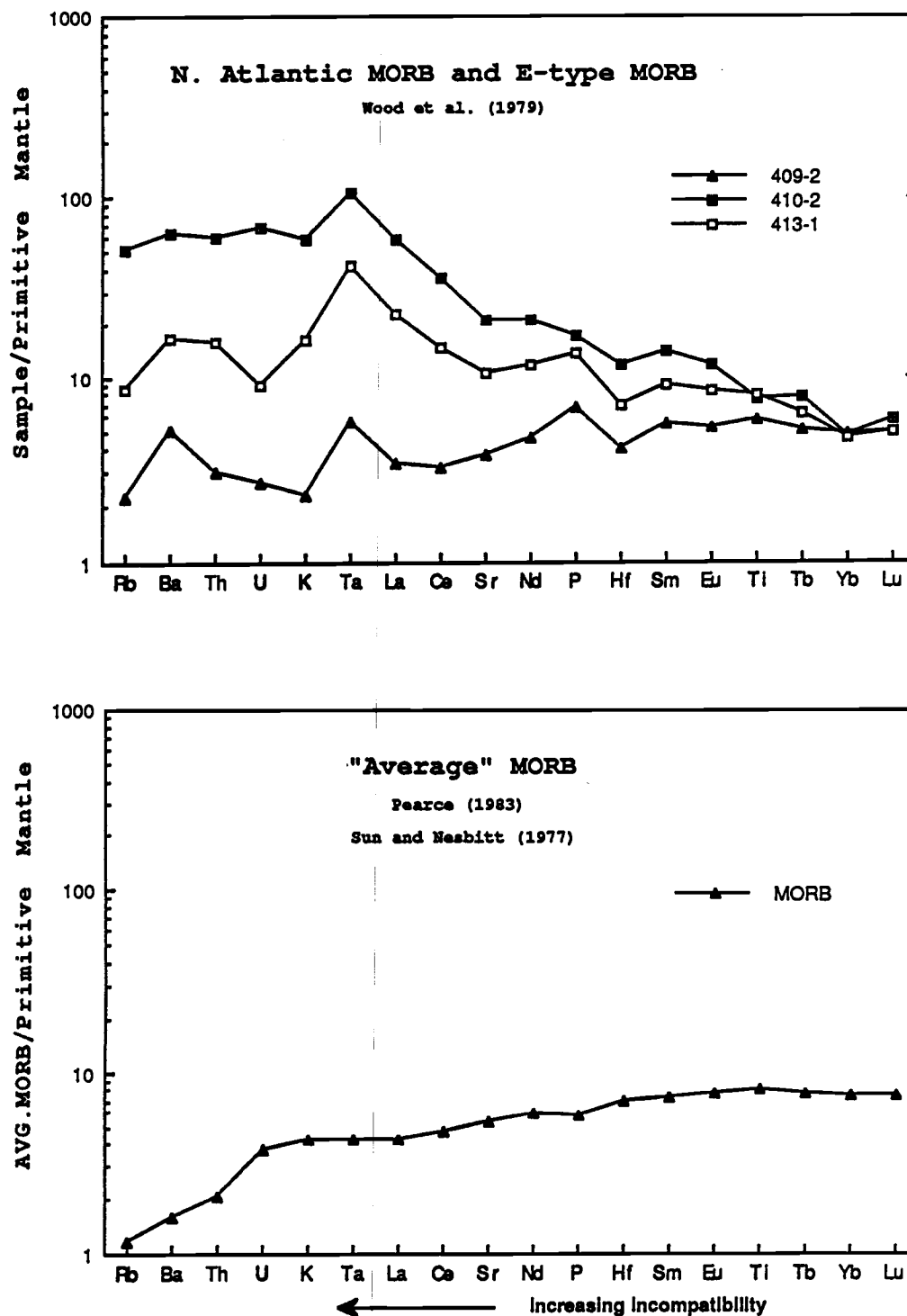


Figure 5.16 Spider diagram plots of north Atlantic MORB varieties and average MORB for comparison with the Oregon-Washington Coast Range basalts. Normalization values from Wood (1979).

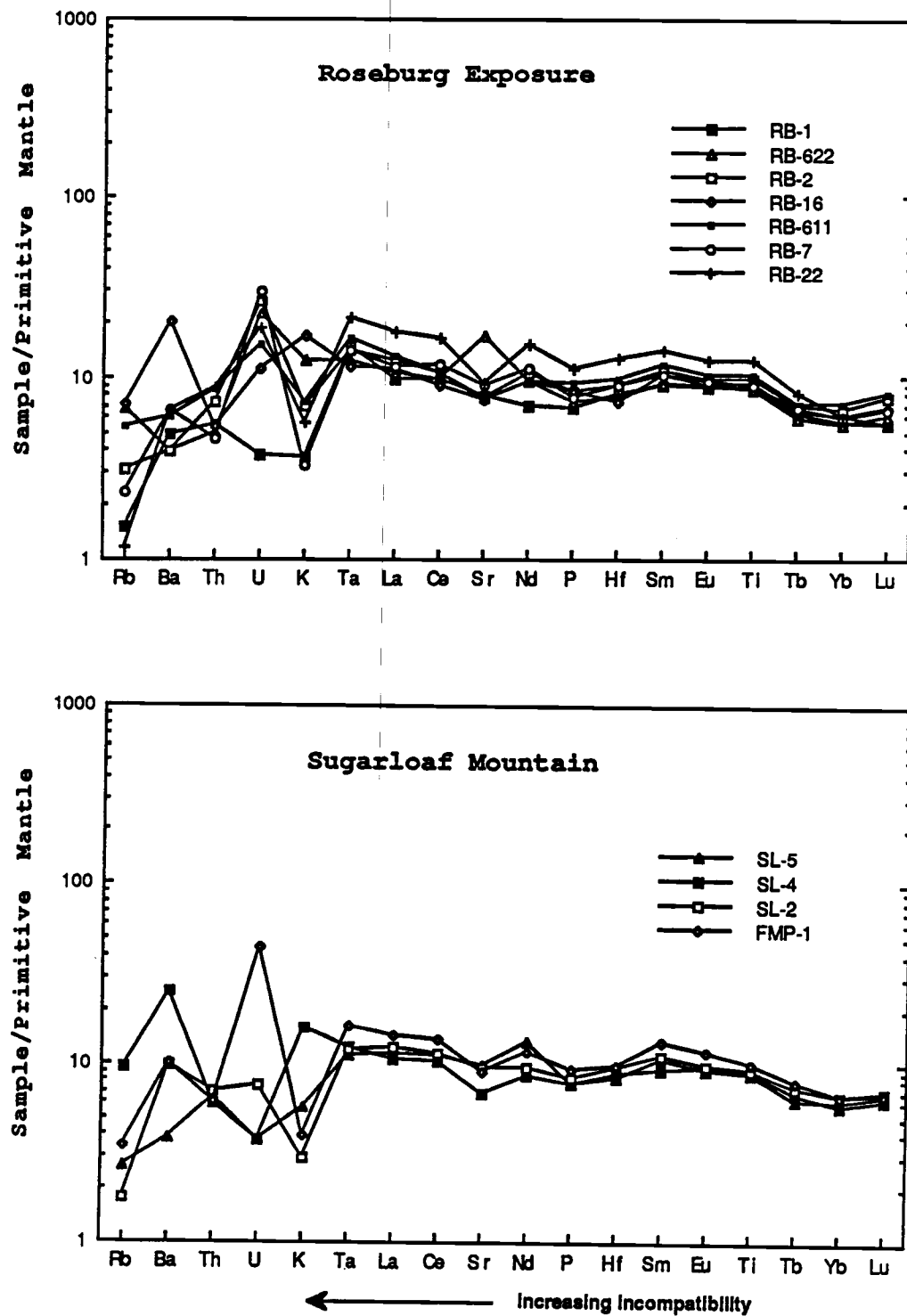


Figure 5.17 Spider diagram plots: a) Roseburg exposure b) Sugarloaf Mtn.

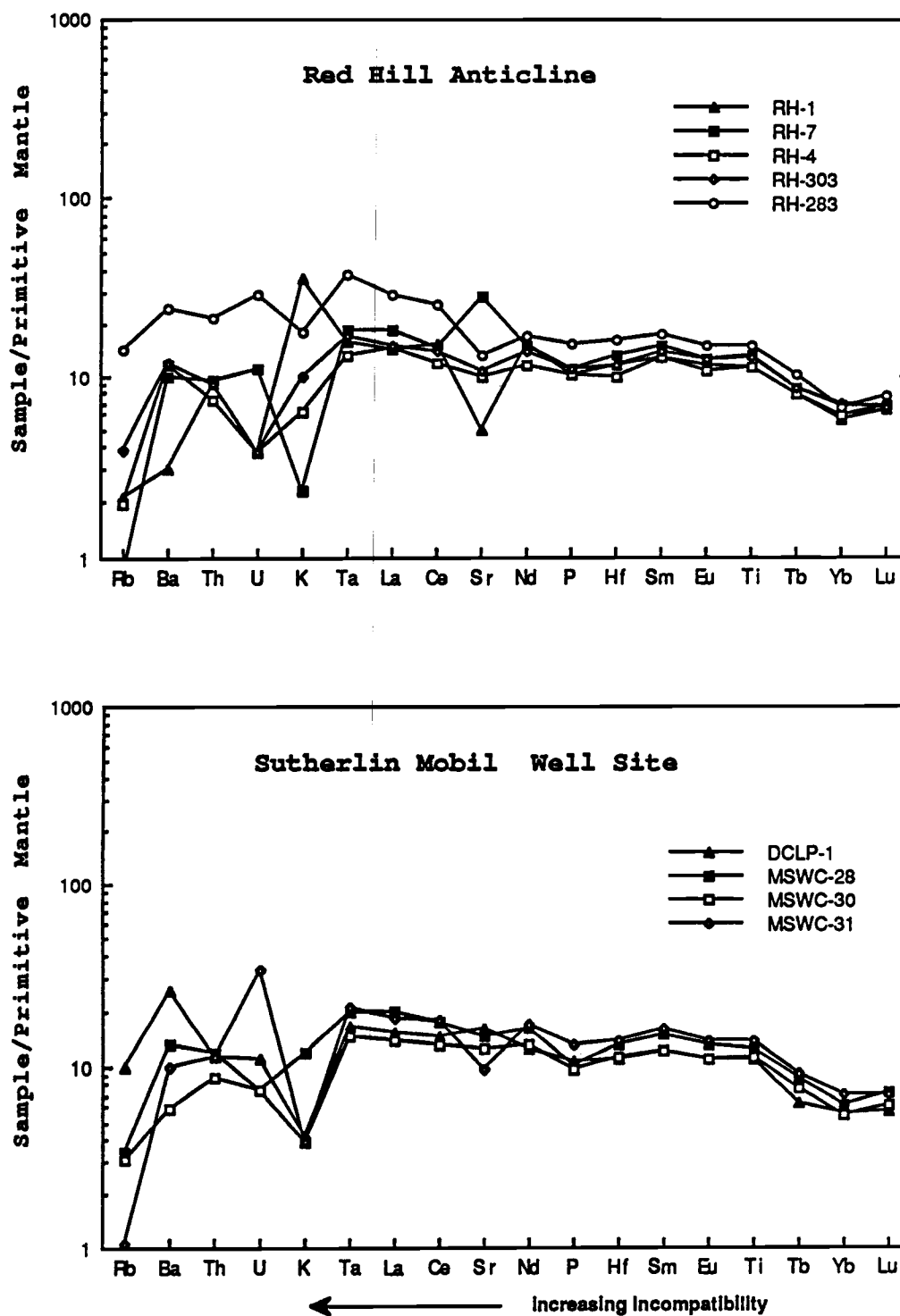


Figure 5.18 Spider diagram plots: a) Red Hill anticline b) Sutherlin Mobil well site.

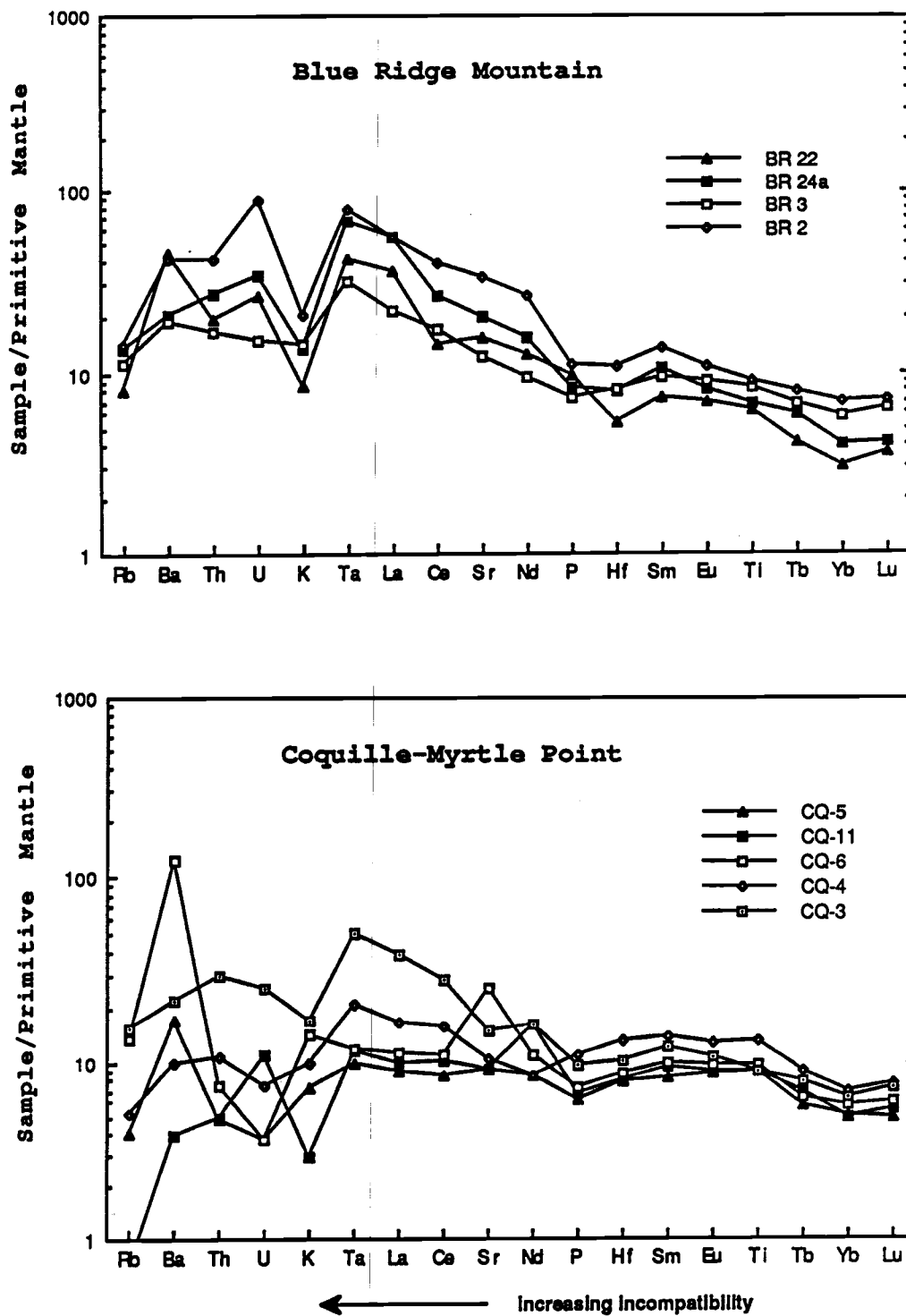


Figure 5.19 Spider diagram plots: a) Blue Ridge Mtn. b) Coquille-Myrtle Point exposure.

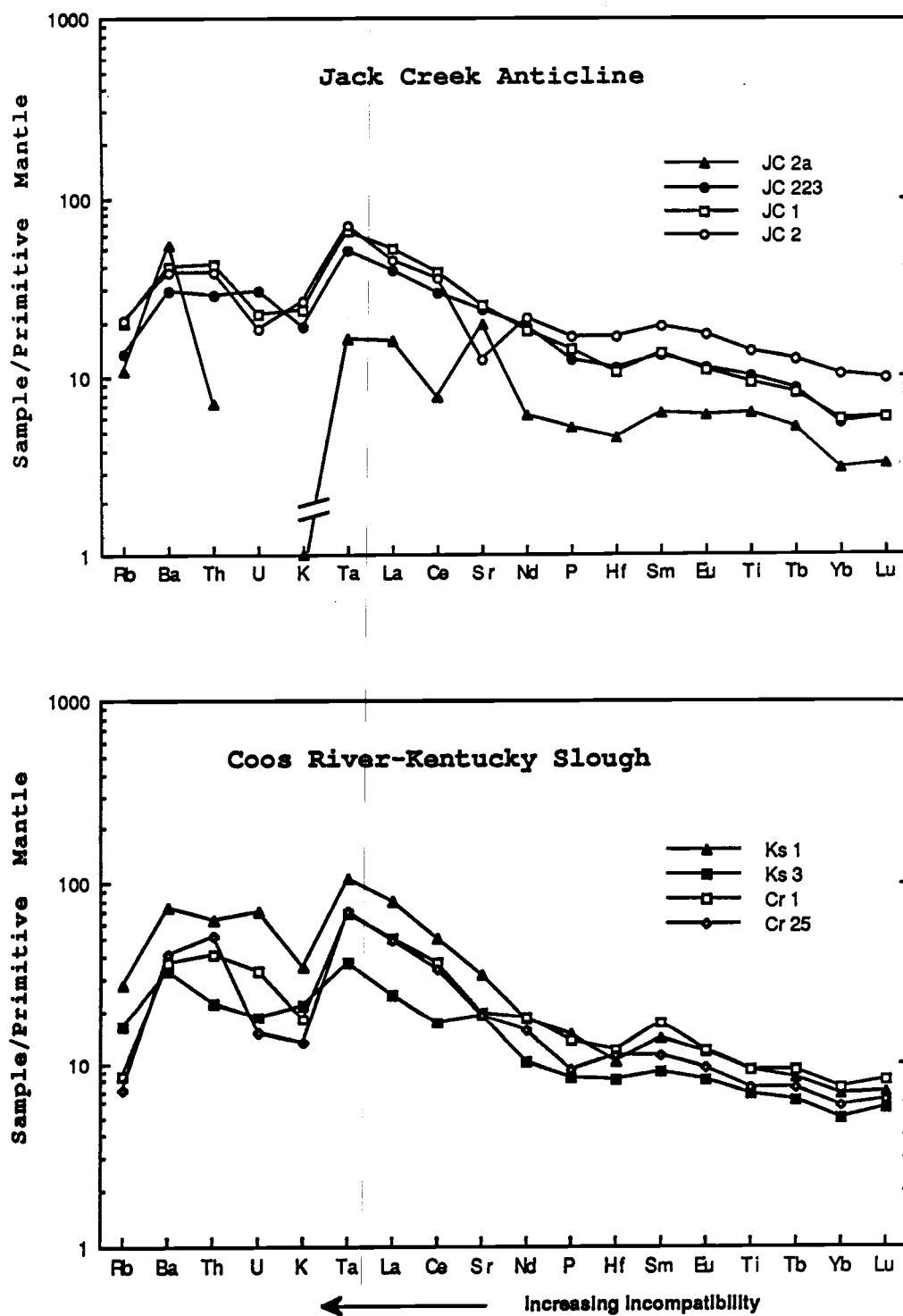


Figure 5.20 Spider diagram plots: a) Jack Creek anticline b) Coos River - Kentucky Slough exposures.

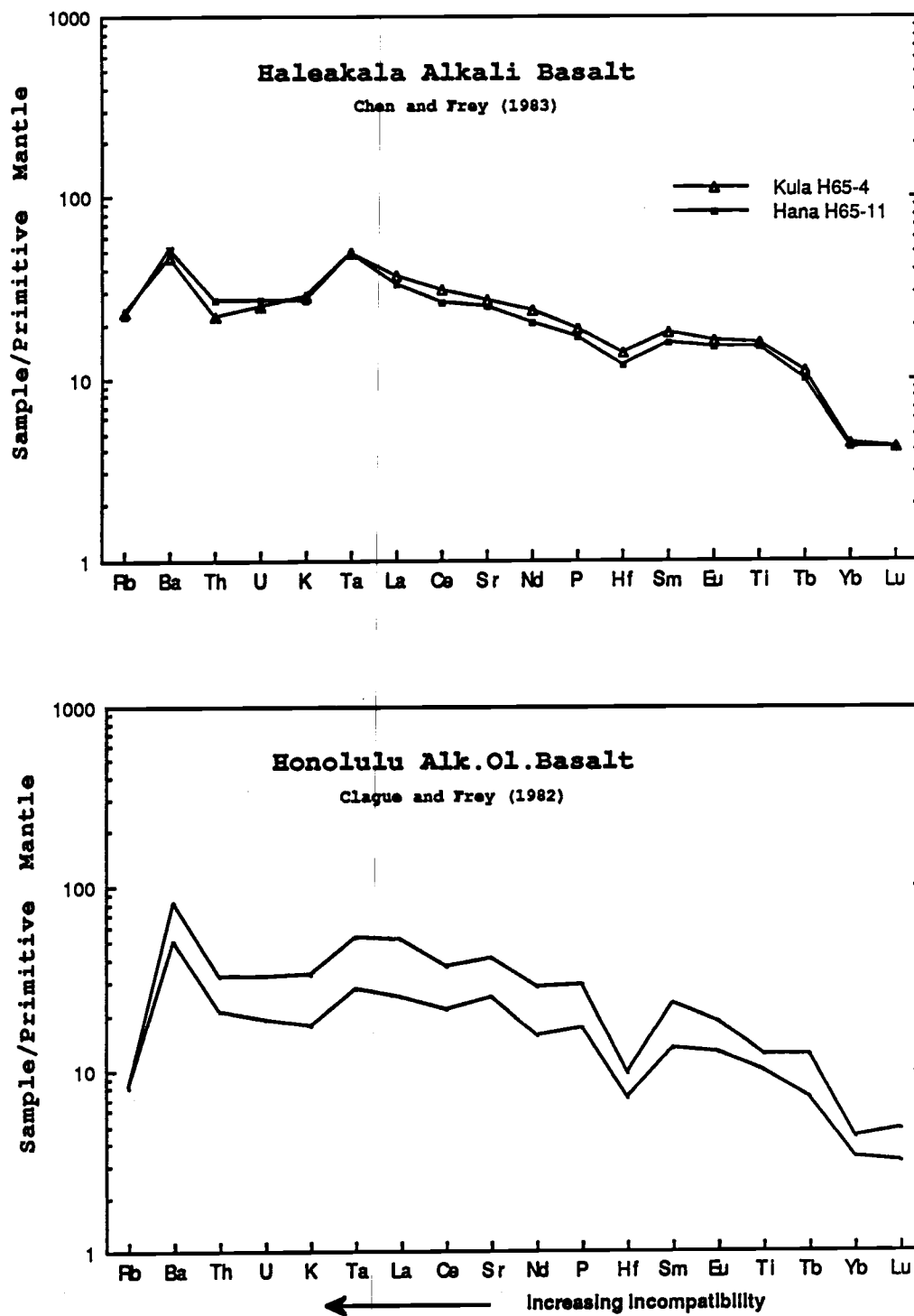


Figure 5.21 Spider diagram plots: Hawaiian alkali basalts for comparison with the Oregon-Washington Coast Range basalts.

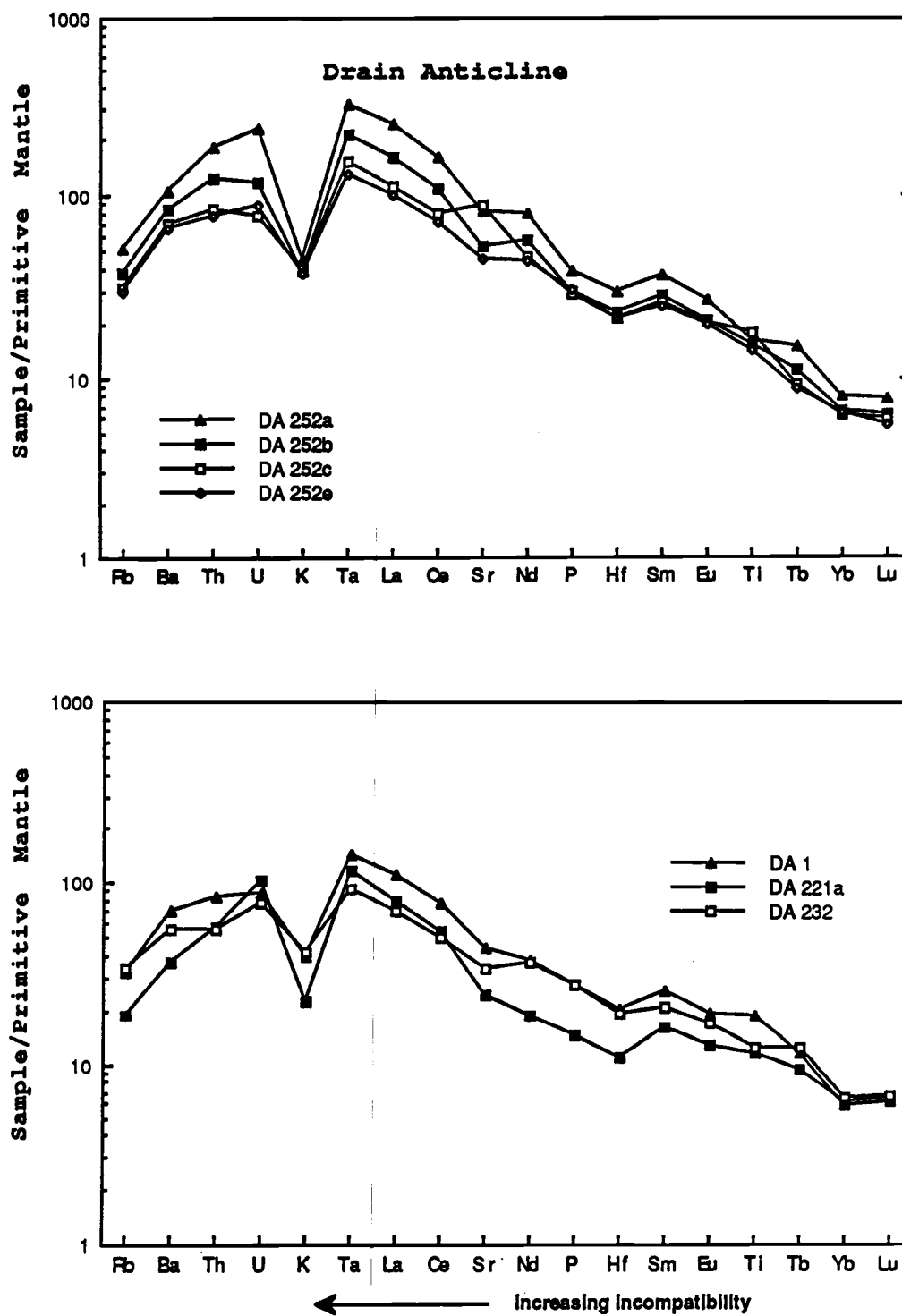


Figure 5.22 Spider diagram plots: Drain anticline exposure.

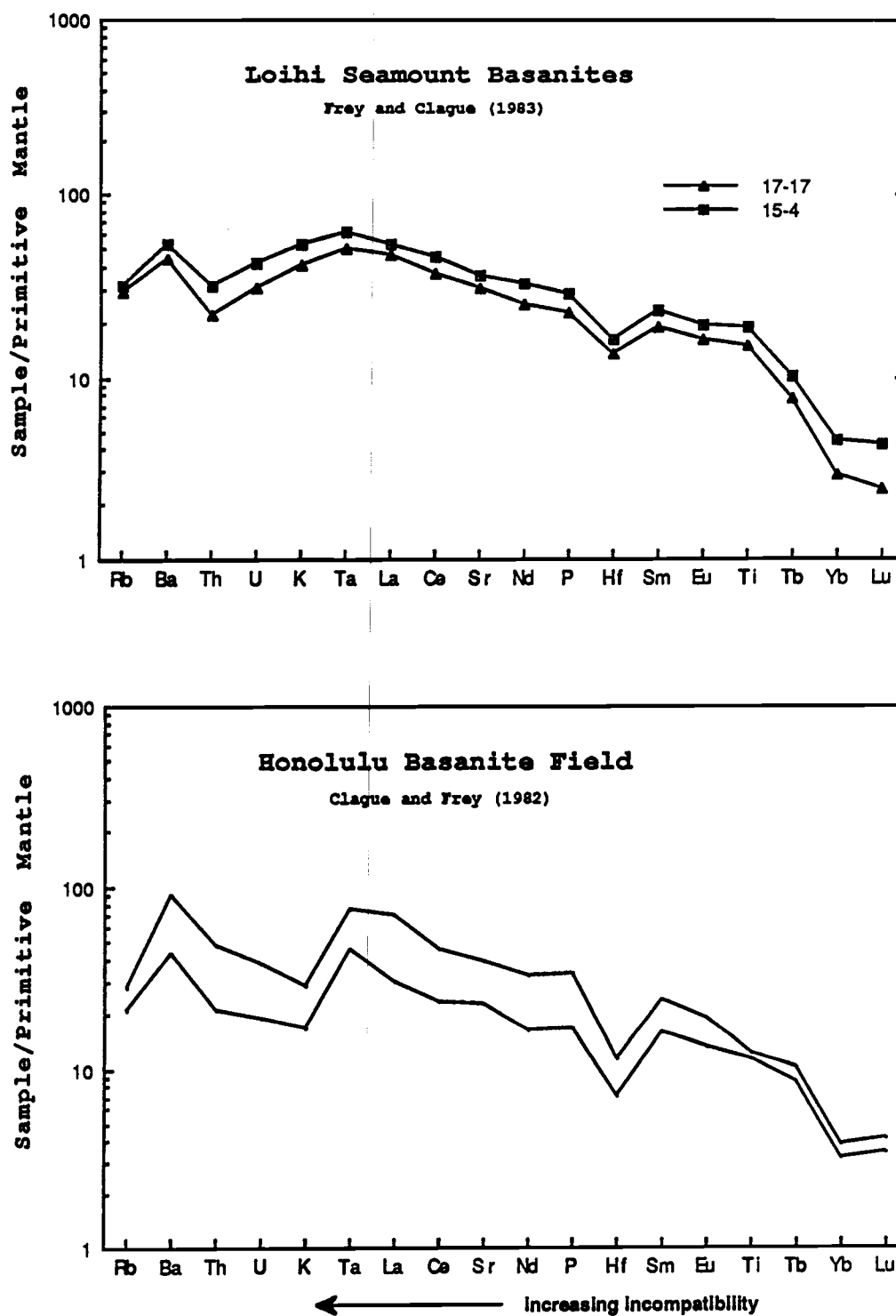


Figure 5.23 Spider diagram plots: Loihi seamount and Honolulu basanites for comparison with the Roseburg basanitic basalts from the Drain anticline area.

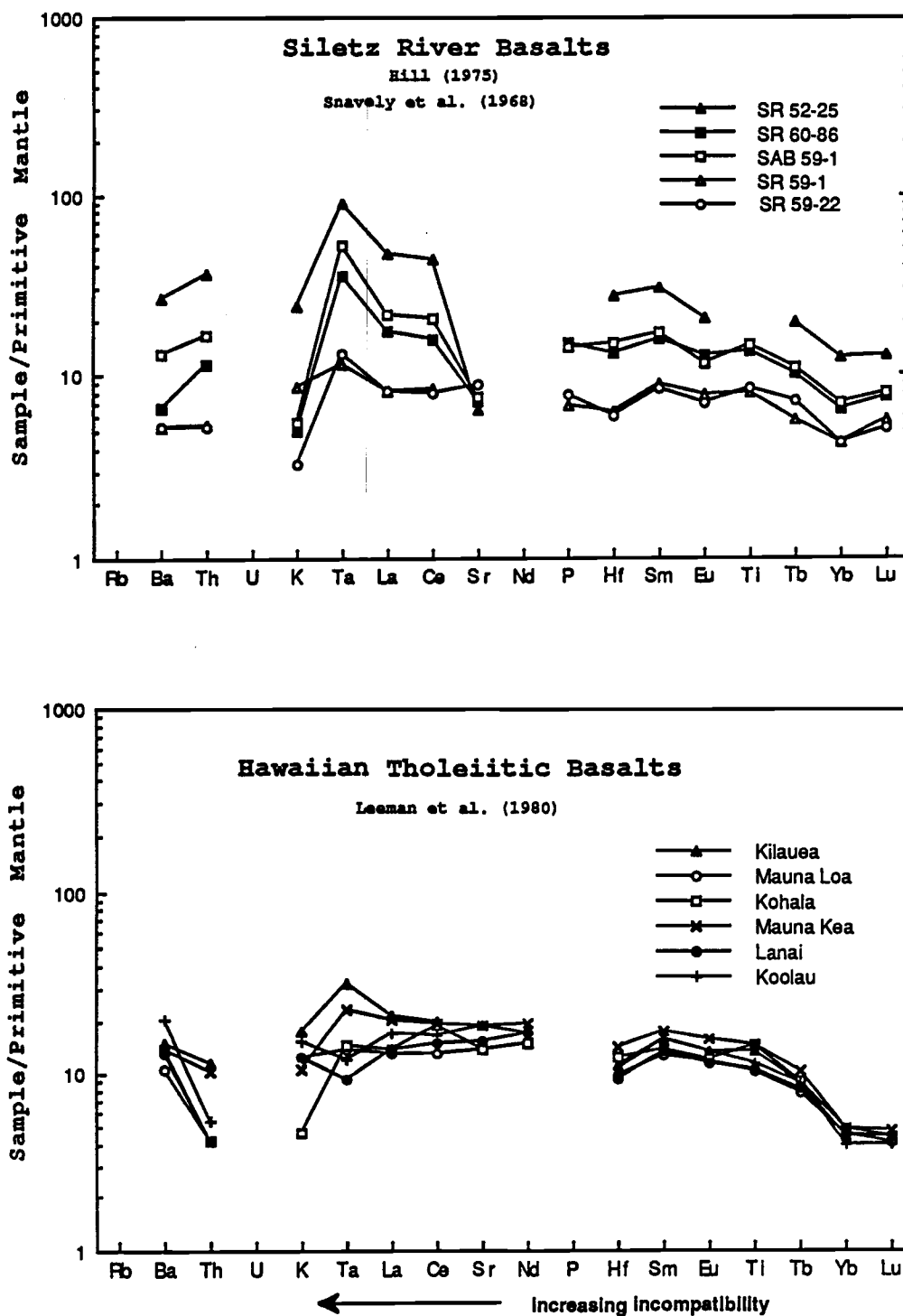


Figure 5.24 Spider diagram plots: a) Siletz River basalts b) average Hawaiian tholeiitic basalts for comparison with the Oregon-Washington Coast Range basalts.

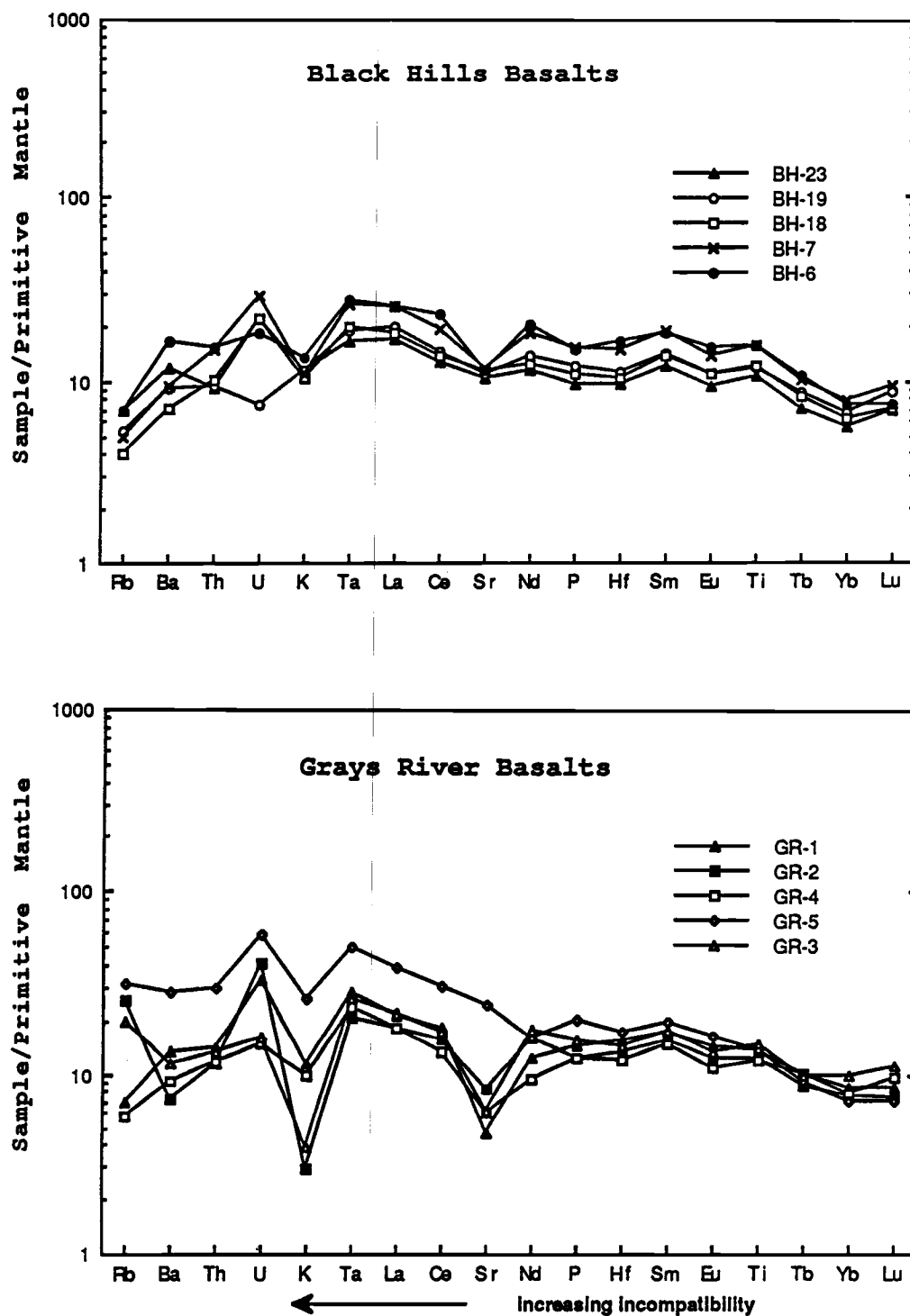


Figure 5.25 Spider diagram plots: Washington Coast Range a) Black Hill Basalts b) Grays River Basalts

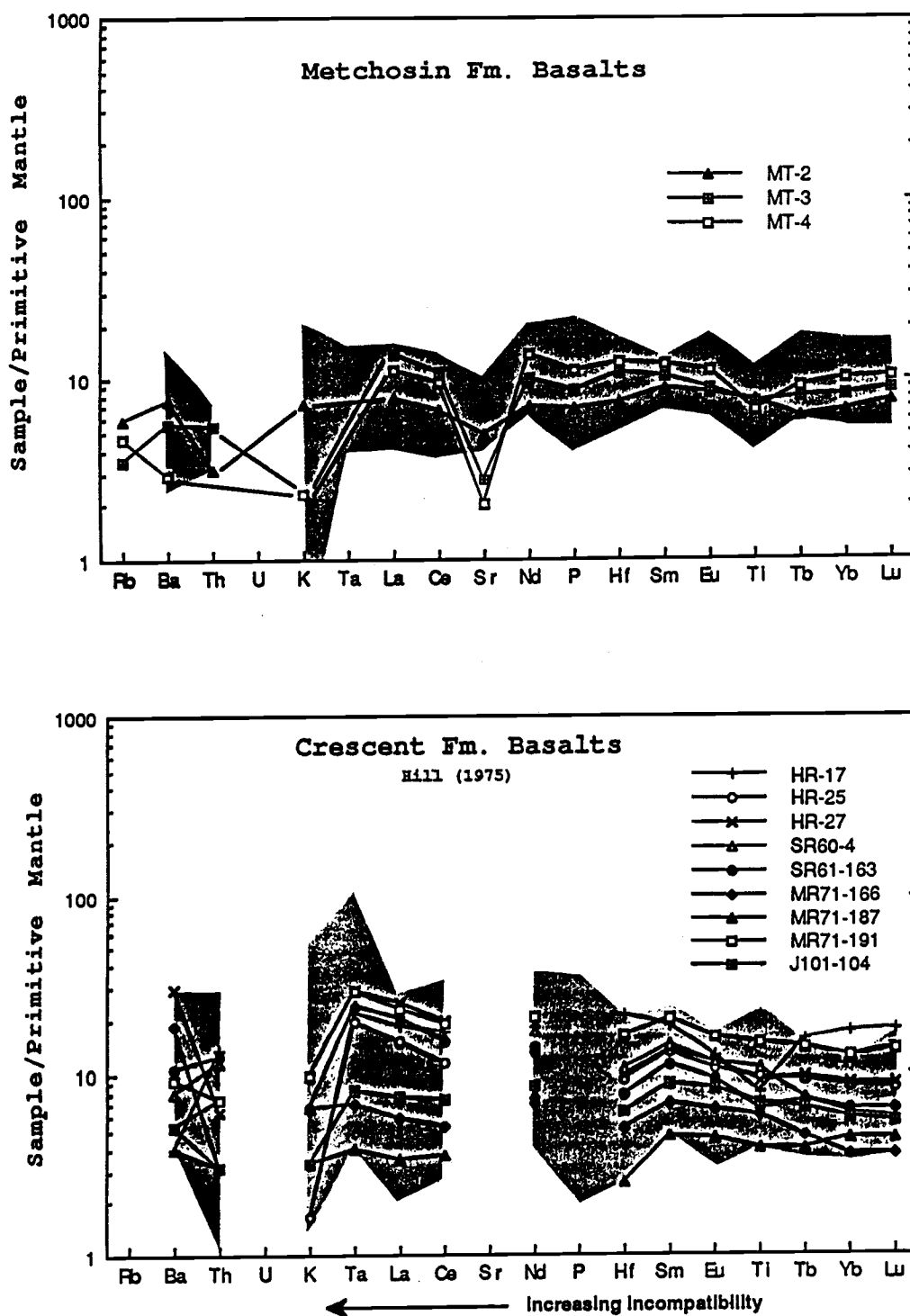


Figure 5.26 Spider diagram plots: Washington and British Columbia Coast Range a) Metchosin Fm. basalts, shaded field is a compilation of data from Hill (1975) and Muller (1980) b) Crescent Fm. basalts (Hill, 1975), shaded field is a compilation of data from Glassley (1974), Lytle and Clarke (1975, 1976).

The L.I.L. element variations are erratic on most of the diagrams because of the secondary alteration that has affected most of the samples. There is a noticeable inflection in all of the spider diagrams at Ta. The enrichments in element abundances relative to the primitive mantle composition drop off both to the right and to the left on the diagram. This pattern is characteristic of E-type MORB compositions (see Figure 5.16; Wood et al., 1979; Saunders, 1984). The relative decrease in the abundance pattern between Ta and Rb and the relative increase in the abundance pattern between Ta and Lu has been attributed to a two stage mantle process which has depleted the source in L.I.L. constituents by previous a melting episode(s) in the source of E-type MORB (Tarney et al., 1980). The depletion event has been overprinted with an enrichment event that has introduced Ta, La, Ce, etc. to the previously depleted mantle source. The cause for the selective increase in these L.I.L. constituents over Rb, Ba, Th, U, and K is not clear. This selective enrichment may reflect a greater geochemical tendency for Ta and the REE to be recycled back into the mantle and the preferential extraction of Rb, Ba, Th, U, and K during subduction zone magmatic processes. A better discussion of "veining" or "metasomatization" of the mantle and its role in the creation of enriched mantle sources for E-type MORB can be found in Wood (1979).

As stated earlier, the Roseburg basalts show a greater range in trace element abundances than any of the other early Eocene basaltic rocks in the Oregon-Washington Coast Range. The spider diagrams patterns of the other lower Eocene volcanic centers are relatively uniform and display the same "stacking" that was observed in the discussion of the REE variations. The best explanation for these geochemical characteristics is again the dominate role of fractional crystallization. More evidence for this differentiation process is exhibited by the notable Sr depletion in some of the samples. The Sr depletion is present in samples from all the basaltic sequences examined in this study but the available data suggests that at some volcanic centers, the magmatic process extracting Sr is

predominate. Sr can be strongly partitioned into plagioclase and this pattern seems to indicate that these basaltic suites have undergone a greater amount of plagioclase crystallization than the Roseburg basaltic sequence. The relative depletion in Sr varies within and between the different Oregon-Washington Coast Range volcanic centers. This observation may also be biased by the limited sample population from the other coast range basalt sequences compared to the extensive sampling of the Roseburg sequence. A more conclusive comparison must await further trace element results from these other areas.

CHAPTER 6: DISCUSSION

I. Summary of results

This investigation of the Roseburg basalts was undertaken to determine the geochemical evolution of the oldest volcanic rocks in the Oregon-Washington Coast Range. Two of the four main objectives outlined in the introduction have been addressed. The first objective concerned defining the petrogenetic and geochemical evolution of the basalts in relation to their geographic distribution around the rim the of the southern Oregon Coast Range Eocene basain. One of the fundamental contributions of this study is the identification of a progressive development of the volcanic system from the southern exposures of the basalt to the northern outcrops, and the coherency in the stages of differentiation displayed by basalts on either side of the basin. A similar trend has been observed in the Siletz River basalts in which the lower tholeiitic section crops out on the eastern side of the Coast Range basin and is separated from the upper alkalic section which crops out on the western side of the basin. Whether the distribution of rock types in these two areas is the result of structural rearrangements during the emplacement of the proposed seamount terrane or whether it represents the original distribution of the volcanic activity has yet to be determined. The structural styles in the two area are not directly comparable. The structural history of the Roseburg region suggests deeper levels of the Eocene stratigraphic section are exposed in the melange wedge on the western side of the Coast Range (Perttu and Benson, 1980; Ryberg, 1984). Picrites in the Blue Ridge Mountain area with chemical compositions indicative of olivine accumulation and alkalic rocks with intrusive rather than extrusive petrographic textures support this suggestion. Ryberg (1984) and Snavely and Wagner (1963) have shown that deposition of the

overlying deep water turbidites in the Roseburg and Siletz areas were deflected around structural highs which were interpreted as developing seamounts or oceanic islands. The subaerial eruption of alkalic basalts in both areas and the eruption of highly undersaturated basanitic magmas in the Roseburg basaltic sequence attest to the seamount / oceanic island barrier. The depositional relationships between the eruptive styles of the Roseburg basalts and sedimentation record an interrelated history of contemporaneous volcanism and sedimentation.

The second objective concerned evaluating the mantle source(s) involved in the production of the Roseburg basalt sequence. The L.I.L scatter plots of the Roseburg tholeiitic and alkalic basalts indicate they are both derived from a similar mantle composition, but the degree of partial melting of this mantle source is necessarily different to produce the two different magmatic suites. The data also suggest that the depth of melting is different between the two basalt suites. The presence of garnet as a residual mantle phase in the production the basanitic magmas is clearly evident from the very restricted range of HREE variation. The Roseburg basalts have LREE/HREE patterns that are slightly to extremely enriched. None of the samples collected in the southern Oregon Coast Range have depleted trace element characteristics typical of N-type MORB. The basaltic melts seem to have been extracted from a mantle with undepleted or enriched abundances of incompatible elements. Mantle sources of this nature are usually attributed to the direct influence of a hotspot-type chemical signature or to the mixing of a hotspot source with a depleted MORB source (i.e. the presence of T and E-type MORB compositions). The eruption of highly undersaturated basanitic magmas in the late stages of evolution of the Roseburg sequence suggests the development of this volcanic island was more directly influenced by hotspot volcanism than by MORB volcanism .

The last two objectives dealt with the geochemical relationships between the Roseburg basalts and the other five volcanic centers discussed in the text, and the chemical

similarities of the early Tertiary Coast Range rocks to the chemistry of basaltic magmas erupted in known plate tectonic environments. The relationships between the Roseburg basalts and the other lower Eocene basaltic sequences have been briefly discussed in each section. The chemical variations exhibited within and between the volcanic centers is proposed to be a consequence of the relative positions of hotspot volcanism, mid-ocean ridge spreading, and subduction to the sites of basaltic magma generation at each eruptive center. Rapid oblique convergence of the Farallon plate during this time is also an important factor in determining the relative positions of contemporaneous volcanic activity. Understanding the variations in the magmatic evolution of the basalts should lead to a better understanding of the possible plate orientations influencing the magnitude of magmatic chemical variations, the time dependence (if any) of those variations, and the distribution of the geochemical variations. Comparison of the chemical variations found in the Oregon-Washington Coast Range with chemical variations of basalts reported from known tectonic environments should help unravel the tectonic configuration of the northeast Pacific ocean basin during Paleocene to early Eocene time.

II. Plate Tectonic Models for Petrogenesis

The plate tectonic models for the origin of basaltic rocks in the Oregon-Washington Coast Range reviewed in Chapter 2 could be divided into two models. In model 1, basaltic magmas are generated in a marginal basin environment caused by oblique subduction of the Farallon plate beneath the North American plate. In model 2, basaltic melts are generated from an oceanic ridge environment that is influenced by the proximity of the Yellowstone hotspot. The two model are mutually exclusive because of the completely different plate orientations necessary for each model. The subducting plate

neccessary in model 1 would affectively impede upwelling of hotspot-type magmas from erupting on the ocean floor. Therefore, one of the models must be eliminated.

Model 1: Marginal basin/Continental Rifting

The plate tectonic development of back-arc or marginal basins has been discussed by serveral investigators (Karig, 1971; Taylor and Karner, 1983; Hynes and Mott, 1985; Fein and Jurdy, 1986). A short summary is presented below with attention focused on the possible plate tectonic configuration of the Pacific Northwest during the early Tertiary. The three main models of back-arc basin formation that have been proposed include mantle diapirism, induced asthenospheric convection, and global plate kinematics. The mechanism for rifting or spreading in the first two cases is directly linked to local subduction below the developing basin. The third case requires that marginal basins should form whenever the relative plate motions in the area cause local extensional regimes along a generally compressive subduction boundary. Taylor and Karner(1983) described this type of non back-arc, marginal basin as a "boundary basin". Boundary basins can form in a transform dominated spreading system which opens along short rift segments within a megashear between two plates. A modern analog for this plate tectonic configuration is found in the Andaman Sea. In this region the Burma plate is trapped between the continental China plate to the east and the oceanic Indian plate to the west. The highly oblique subduction of the Indian plate beneath the Burma and China plates has caused rifting of the Burma plate and development of a small boundary basin spreading center (Curaray et al., 1979). This is the type of plate tectonic configuration that has been envisioned in model 1 for the early Tertiary continental marginal basin of Washington and Oregon.

The geochemistry and petrogenesis of volcanic rocks from marginal basins have been discussed by Tarney et al. (1977, 1981), Saunders and Tarney (1979), and Wood et al. (1980,1982) and is summarized here. Marginal basin basalts are derived from mantle sources that can have enriched or depleted incompatible trace element abundances. Back-arc basin basalts display as much diversity in composition as normal mid-ocean ridge basalts but there is a tendency for back-arc basin magmas to be geochemically less depleted than N-type MORB in incompatible elements. Tarney et al. (1981) reviewed data on the western Pacific and the Scotia Sea back-arc systems and noted that the early stages of magma generation in back-arc settings produce basalts high in volatiles and enriched in incompatible elements (K, Rb, Ba, Sr, Th, U, and LREE) but depleted in high field strength (H.F.S.) elements (Nb, Ta, Ti, Zr). This enrichment in the large ion lithophile (L.I.L.) elements relative the H.F.S. elements is a characteristic of island arc magmas (Saunders et al., 1980). Depletion in the H.F.S. elements is possibly caused by the stabilization of titanium mineral phases such as rutile, ilmenite, and sphene which strongly partition Ta, Nb, and Ti (Wood et al., 1979). Hellman and Green (1979) have shown that the stabilities of rutile and sphene are enhanced under hydrous conditions and can be refractory phases even at relatively high degrees of mantle melting. The volatile enrichment and stabilization of the titanium-rich phases is a consequence of dewatering of the subducted slab beneath the incipient spreading center. The continued development of the spreading center causes the magma generating processes to evolve toward N-type or, more commonly, T-type MORB compositions. This is due to the removal of the back-arc ridge system away from the influence of the subducting slab by the continued spreading of the basin.

The marginal basin/back-arc basin model above is inherently associated with subduction. The plate motions in the northeast Pacific basin during the early Tertiary were similar to the plate tectonic configuration now present in the Andaman Sea and make this

model an appealing alternative to the ridge centered hotspot hypothesis based on proposed relative plate motions. However, the geochemical consequences of this model preclude its application to the Oregon-Washington Coast Range. If the Coast Range basalts were generated by oblique subduction of the Farallon plate beneath a marginal basin spreading system, then a hotspot chemical signature would be effectively eliminated by the presence of the intervening subducting slab. Presumably magma generation would also follow a time dependent differentiation path from early eruptions of arc related basalts with high volatile contents, enriched L.I.L. compositions and depleted H.F.S. element compositions and evolve toward T-type or N-type MORB compositions. The earliest magmatic activity in the Oregon-Washington Coast Range is represented by the Roseburg basalts. The spider diagrams of the Roseburg basalts have no indication of any H.F.S element depletions that could be attributed to the early development of a marginal basin above a subducting slab (Figures 5.17-5.22). In fact, the Roseburg basalts have the most enriched H.F.S element compositions of the province. None of the other Coast Range basalts display depletions in the H.F.S. elements which would indicate an arc related magmatic component in these rocks. The conclusion that must be drawn is that the geochemical evidence makes the marginal basin model highly unlikely.

Model 2: Oceanic Ridge / Hotspot

The relative influence of different tectonic environment on the generation of basalts in coast range province can be qualitatively evaluated on a ternary Th-Hf/3-Ta discrimination diagram (Figure 6.2). The distribution of basalt compositions from several oceanic settings is given in Figure 6.1 (Wood et al., 1980). Arc basalts plot between the Hf and Th apexes of the diagram away from the Ta apex because magma generation in this environment depletes the derivative magmas in Ta. MORB (field A), E-type MORB (field

B), and OIB magmas (field C) plot towards the middle of the diagram. None of the early Tertiary Coast Range basalts have any compositional affinities associated with island arc magmas. All of the basalt compositions plot in the MORB to OIB fields suggesting these two environments are the dominate sources for these basalts. This evidence supports conclusions from other studies in the Coast Range (Globerman, 1980; Hill, 1975; Muller, 1980; Duncan, 1982).

It is interesting to note that the Roseburg tholeiite compositional field overlaps that of the Metchosin and Crescent basalts (E-type MORB near the N-type MORB boundary). The other Coast Range tholeiitic and alkalic basalts plot in between the Metchosin-Crescent -Roseburg tholeiitic field and the highly enriched compositions of the Roseburg alkalic basalts and basanites. The L.I.L. element enrichments of the tholeiitic basalts is least pronounced in the northern section of the coast range province (Metchosin and Crescent Fm.), slightly more enriched in the southern section (as represented by the Roseburg tholeiites), and progressively more enriched in the central portions of the province. The alkalic basalt derivatives from the different volcanic centers tend to follow a different trend on this diagram. A progressive increase in enrichment is indicated towards the southern coast range from the north, although the Crescent alkali basalts overlap the central coast range distribution of data points. The Th-Hf-Ta diagram separates the Roseburg tholeiitic and alkalic basalts more distinctly than any of the other tholeiitic-alkalic basaltic series in the Oregon-Washington Coast Range. The reason for this may be related to the partial melting differentiation processes which generated the Roseburg basalts as opposed to the fractional crystallization processes which seem to affect the other magmatic systems.

A comparison of the Coast Range data (Figure 6.2) with data fields from known tectonic environments outlined in Figure 6.1 shows that the majority of the basalts in this province have chemical similarities to the Iceland tholeiitic basalts and the Reykjanes

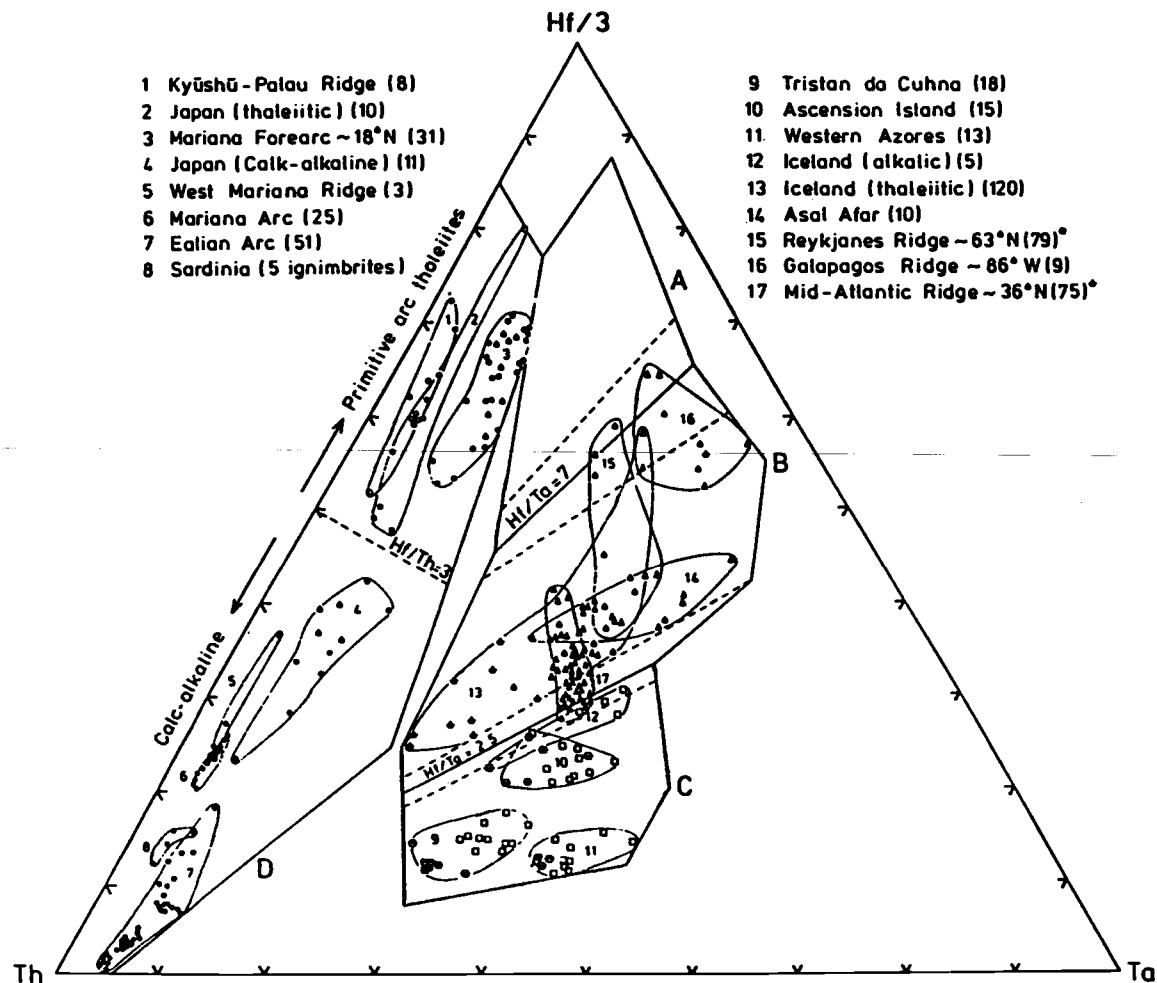


Figure 6.1 Representative oceanic igneous rocks plotted on a Th-Hf/3-Ta discrimination diagram after Wood (1980). A - N-type MORB field; B - E-type MORB field; C - Alkaline within-plate basalts and differentiates; D - Destructive plate-margin basalts and differentiates.

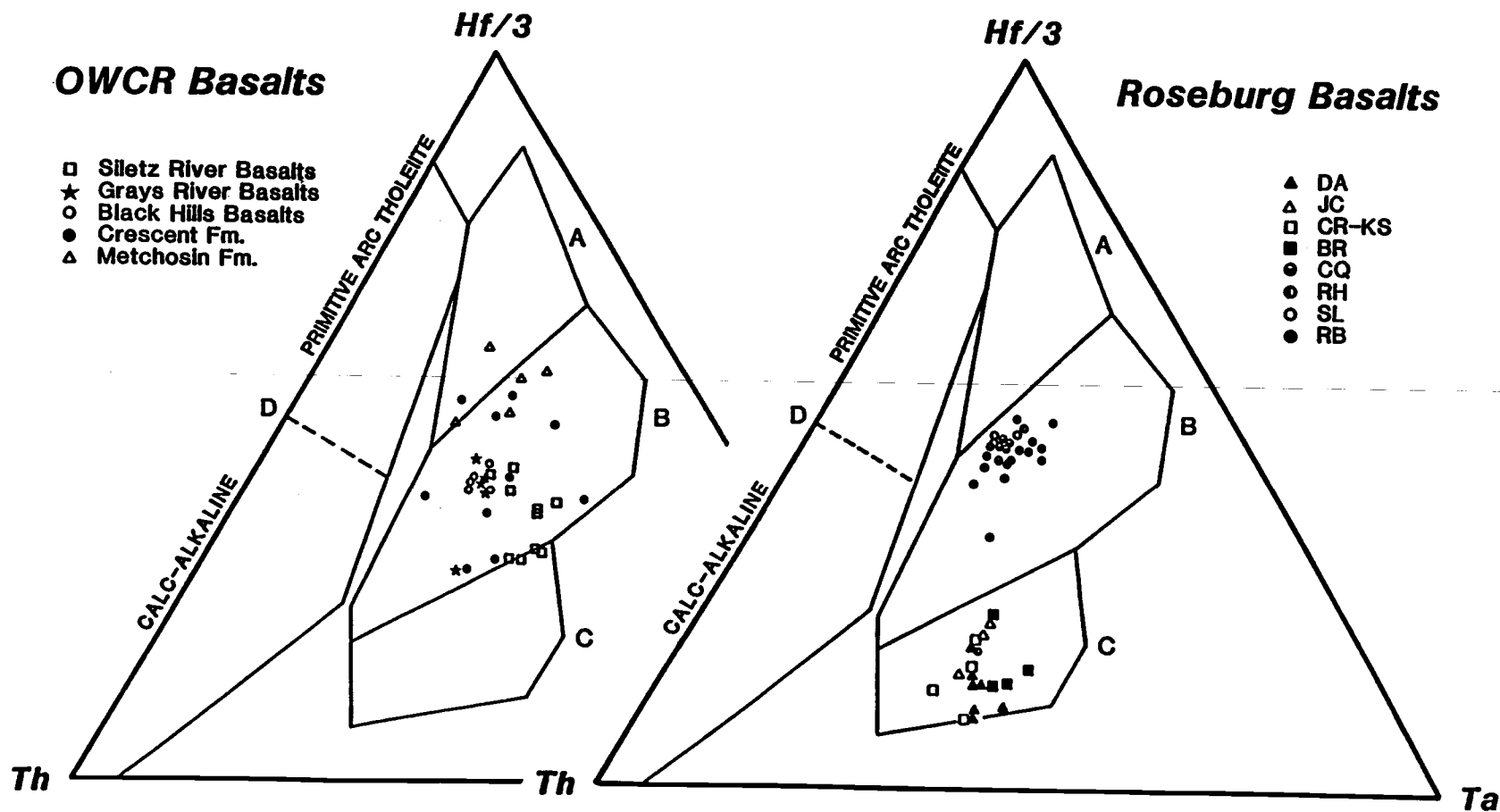


Figure 6.2 Oregon-Washington Coast Range (OWCR) basalts and Roseburg basalts plotted on a Th-Hf/3-Ta discrimination diagram of Wood (1980). Fields as in Figure 6.1. See text for discussion.

Ridge trend (i.e. a ridge centered hotspot scenario). The alkalic basalts and the basanites of the Roseburg basalts are the most distinctive compositions in the Coast Range. They plot exclusively in the OIB field and display relative chemical abundances similar to Ascension Island and the Western Azores. This is strong support for the dominate influence of hotspot volcanism in the generation of the Roseburg basaltic rocks.

The Th/Yb vs Ta/Yb variation diagram of Pearce (1983) shown in Figure 6.3 is added evidence that the geochemical trend in the coast range province follows compositional trends from slightly more enriched than N-type MORB towards marked within-plate enrichment (i.e. hotspot magmas). The evolution from primitive oceanic arc compositions towards N-type MORB is not evident as would be expected if the province erupted in a developing marginal basin. As in Figure 6.2, the distribution of points on the diagram shows the central coast range data points lying between the Metchosin-Crescent-Roseburg tholeiitic basalts and the Roseburg alkalic basalts. Normalization of Ta and Th to Yb values removes fractional crystallization effects on the concentration of these elements in the sample and provides information on the initial chemical composition of the mantle source region for the basalts (Pearce, 1983). From this diagram it may be inferred that the mantle source(s) for the Metchosin-Crescent-Roseburg tholeiites is the least enriched of the province or have undergone the greatest amount of partial melting of a homogeneous mantle source. The other basalts in the province are derived from a progressively more enriched mantle source(s) or from progressively smaller degrees of partial melting. Previous discussion of the other trace element variations suggests the latter explanation.

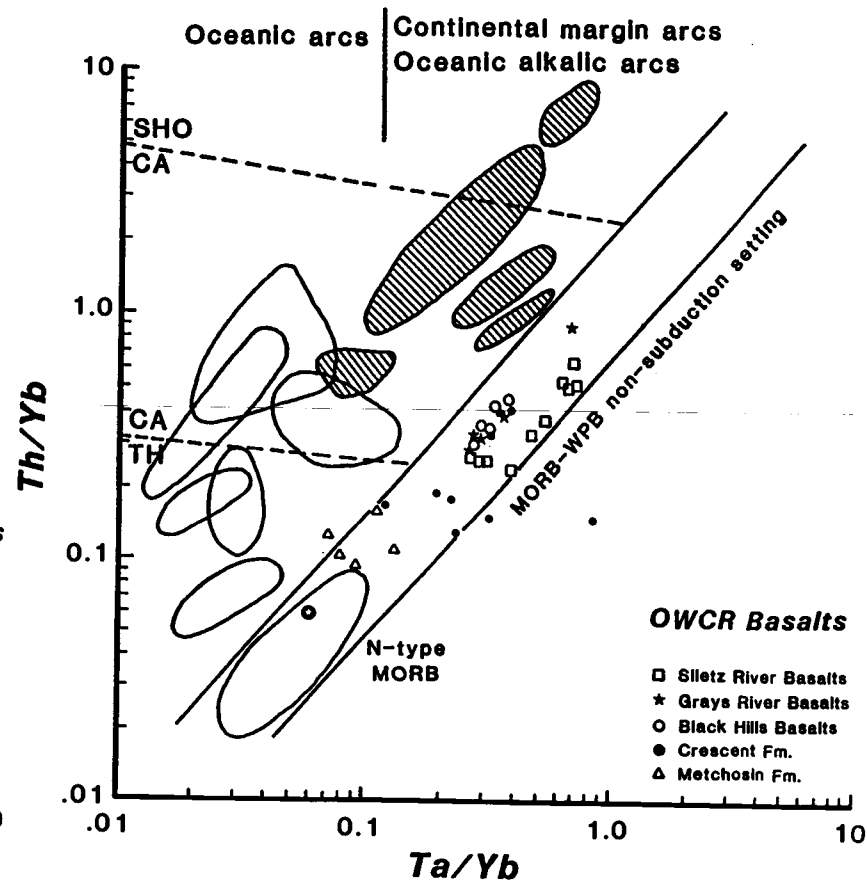
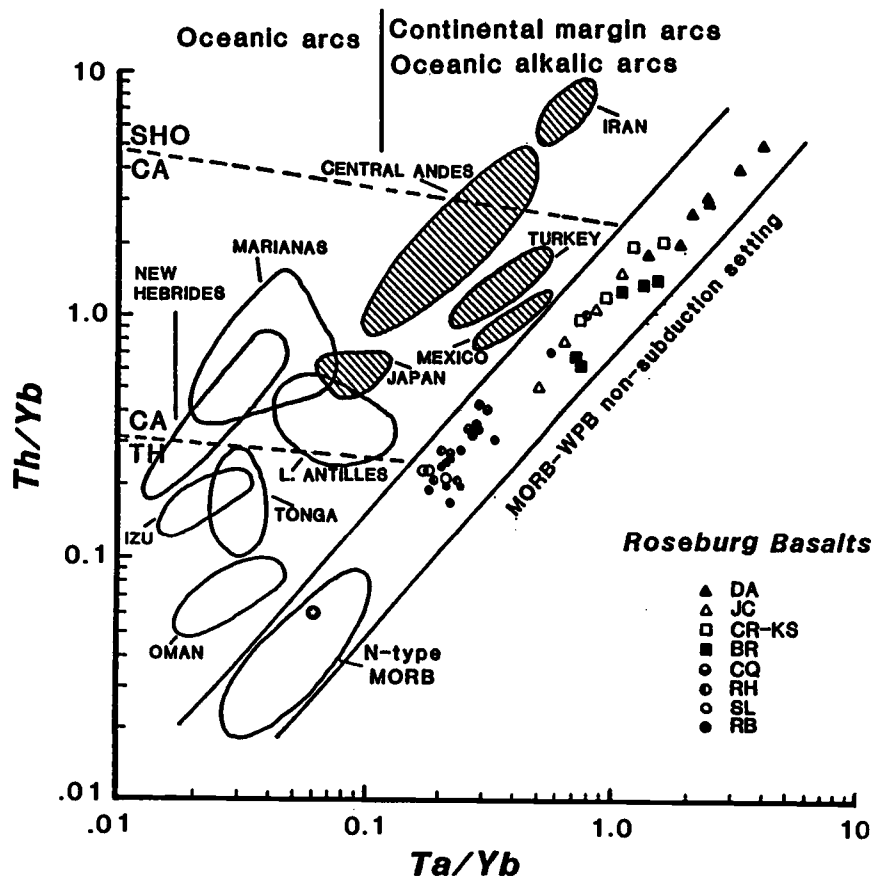


Figure 6.3 Oregon-Washington Coast Range (OWCR) basalts and Roseburg basalts plotted on a log-log plot of Th/Yb versus Ta/Yb. This diagram demonstrates the non-arc related geochemical characteristics of these basalts and also shows the relative enrichments between the early Tertiary volcanic centers in the coast range province (diagram after Pearce, 1983).

III. Conclusions

The major and trace element compositions of the Roseburg basaltic rocks have shown the greatest amount of geochemical diversity in the Oregon-Washington Coast Range. The variability in trace element compositions between the tholeiites and the alkali basalts has been explained by variable degrees of partial melting and depth of melting of a "homogeneous" mantle source. The mantle source for the tholeiitic and the alkalic suites is tentatively concluded to be the same based on the highly incompatible element ratio scatter plots. Isotopic data on these rocks would lead to a more conclusive characterization of their mantle source(s). Differentiation of the tholeiitic suite can be attributed to separation of one batch melt fraction from the mantle (10-15% melting) and subsequent fractional crystallization before eruption. The alkalic suite displays trace element characteristics that require three or more partial melting events with different melt percentages. Estimates of the degree of partial melting for the alkalic basalts range from less than 5% to 10% with the basanitic magmas being derived from the least amount of partial melting. The major element data indicate that olivine and clinopyroxene were major phases controlling the differentiation of the alkali basalts with plagioclase having a greater involvement in the tholeiitic basalts. The lack of significant HREE variation while LREE enrichment increases from ~1x chondritic values to over 500x chondritic values requires that garnet must also be a residual phase in the source of the alkalic rocks.

The geochemistry of other early Tertiary basalts (lower Eocene) in the Oregon-Washington Coast Range has been shown to be generally geographically controlled rather than time dependent. The Metchosin basalts show the most depleted compositions in the province but are comparable in age to the Siletz River Basalts which show no such depletions. The Crescent basalts display similar depletions but they tend to show a wide range in compositional variation. The enriched character of the basalt increases toward the

southern Oregon Coast Range where the highly undersaturated basanitic magmas of the Drain anticline area were erupted. This geochemical trend suggests that hotspot activity (Yellowstone hotspot) during Paleocene-early Eocene time was more influential on the Roseburg magma generating system. The hotspot influence on the compositions of the other volcanic centers seems to progressively diminish toward the north. This is a tentative conclusion because of the dearth of trace element data from the other volcanic centers in the province. The differentiation trends in the province also tend to show some variation with geographic distribution. The Metcoshin, Crescent, Black Hills, Grays River, and Siletz River basalt chemical variations all tend to follow fractional crystallization trends, whereas the chemical variation of the Roseburg magmas have been shown to be controlled more by partial melting.

The conclusions presented in this study are based on an extensive geochemical investigation of the Roseburg basalts and a large amount of geochemical information from other lower Eocene volcanic centers by other workers. In any geochemical comparison of data from various sources, there is a risk of making errors in data interpretation especially when differences are subtle. Also, comparisons of geochemical data become difficult if the data sets do not include results for the same chemical constituents. The relationship between magmatic events and tectonic events in the early Tertiary history of the Pacific Northwest continental margin can be resolved only if all the available data is compiled and processed together. This study attempted to do this. Further investigations of the Oregon-Washington Coast Range is important in understanding the variability in ocean crust geochemistry. A large section of oceanic crust such as this one provides an excellent opportunity to determine geochemical changes both within a volcanic pile and between the centers of volcanism. A comprehensive analytical study of all the basaltic rocks of the coast range is necessary before the details of the plate tectonic history of the region can be determined.

Bibliography

- American Commission on Stratigraphic Nomenclature, 1961. Code of stratigraphic nomenclature. Am. Assoc. Petroleum Geologists Bull., v. 45, pg. 645-665.
- Ando, A., and Terashima, S., 1985. Chemical composition of GSJ rock reference materials 1985. Geochemical Society of Japan, Annual meeting 1985, Tsukuba.
- Atwater, T., 1970. Implications of plate tectonics for the Cenozoic tectonic evolution of western North America. Geol. Soc. Am. Bull., v. 81, pg. 3513-3526.
- Baldwin, E.M., 1964. Thrust faulting in the Roseburg area, Oregon. Ore Bin, v. 26, no. 10, pg. 176-184.
- Baldwin, E.M., 1965. Geology of the south end of the Oregon Coast Range Tertiary Basin. Northwest Sci., v. 39, no. 3, pg. 93-103.
- Baldwin, E.M., 1974. Eocene stratigraphy of southwestern Oregon, Oregon Dept. of Geology and Mineral Indust., Bull. 83, 40p.
- Baldwin, E.M., and Perttu, R., 1980. Paleogene stratigraphy and structure along the Klamath borderland, Oregon. in Geologic field trips in western Oregon and southwestern Washington, Oles, K.F., Johnson, J.G., Niem, A.R., and Niem, W.A., eds. Oregon Department of Geology and Mineral Indust., Bull. 101, pg.9-37.
- Baldwin, E.M., Beaulieu, J.D., Ramp, L., Gray, J.J., Newton, V.C., Jr., and Mason, R.S., 1973. Geology and mineral resources of Coos County, Oregon. Oregon Department of Geology and Mineral Indust., Bull. 80, 82p.
- Beaulieu, J.D., 1971. Geologic formations of western Oregon west of longitude 120° 30'. Oregon Dept. Geol. and Min. Ind. Bull., v. 70, pp.72.
- Basaltic Volcanism Study Project, 1981. Basaltic volcanism on the terrestrial planets. Pergamon press, Inc., New York, 1286p.

- Bates, R.G., Beck, M.E., Jr., Burmester, R.F., 1981. Tectonic rotations in the Cascade Range fo southern Washington. *Geology*, v.9, pg. 184-189.
- Batiza, R., 1977. Age, volume, compositional and spatial relations of small isolated oceanic central volcanoes. *Marine Geol.*, v. 24, pg. 169-183.
- Batiza, R., 1982. Abundances, distribution and sizes of volcanoes in the Pacific Ocean and implications for the origin of non-hotspot volcanoes. *Earth and Planet. Sci. Lett.*, v. 60, pg. 195-206.
- Beck, M.E., Jr., 1980. Plaeomagnetic record of plate-margin tectonic processes along the western edge of North America. *Jour. Geophys. Res.*, v. 85, pg. 7115-7131.
- Beck, M.E., Jr., 1984. Has the Washington-Oregon Coast Range moved northward? *Geology*, v.12, pg. 737-740.
- Beck, M.E., Jr., and Engebretson, D.C., 1982. Paleomagnetism of small basalt exposures in the west Puget Sound area, Washington, and speculations on the accretionary origin of the Olympic Mountains. *Jour. Geophys. Res.*, v. 87, pg. 3755-3760.
- Beck, M.E., Jr., and Plumley, P.W., 1980. Paleomagnetism of intrusive rocks in the coast range of Oregon: Microplate rotations in middle Tertiary time. *Geolgy*, v. 8, pg. 573-577.
- Berg, J.W., Jr., Trembly, L., Emilia, D.A., Hutt, J.R., King, J.M., Long, L.T., McKnight, W.R., Sarmah, S.K., Souders, R., Thiruvathukal, J.V., and Vossler, D.A., 1966. Crustal refraction profile, Oregon Coast Range. *Bull. Seismol. Soc. Am.*, v.56, no.6, pg.1357-1362.
- Bougault, H., Joron, J.L., and Treuil, M., 1979. Alteration, fractional crystallization, partial melting, mantle properties from trace elements in basalts recovered on the

North Atlantic. Deep drilling results in the Atlantic Ocean: Oceanic Crust. Maurice Ewing, Ser. 2, pg. 352-368.

Bougault, H., Joron, J.L., and Treuil, M., 1980. The primordial chondritic nature and large-scale heterogeneities in the mantle: evidence from high and low partition coefficient in oceanic basalts. *Phil. Trans. R. Soc. Lond.*, v. 297, pg. 203-213.

Bougault, H., Treuil, M., 1980. Mid-Atlantic Ridge: zero-age geochemical variations between Azores and 22° N. *Nature*, v. 286, pg. 209-212.

Bromery, R.W., and Snively, P.D., Jr., 1964. Geologic interpretation of reconnaissance gravity and aeromagnetic surveys in northwestern Oregon. U.S. Geol. Surv. Bull. 1181-N, 13p.

Cady, W.M., 1975. Tectonic setting of the Tertiary volcanic rocks of the Olympic Peninsula, Washington. U.S. Geol. Surv., Jour. Res., vol. 3, pg. 573-582.

Chen, C.-Y., and Frey, F.A., 1983. Origin of Hawaiian tholeiite and alkalic basalt. *Nature*, v. 302, pg. 785-789.

Christie, D.M., Carmichael, I.S.E., and Langmuir, C.H., 1986. Oxidation states of mid-ocean ridge basalt glasses. *Earth Planet. Sci. Lett.*, v. 79, pg. 397-411.

Clague, D.A., and Frey, F.A., 1982. Petrology and trace element geochemistry of the Honolulu Volcanics, Oahu: implications for the oceanic mantle below Hawaii. *Jour. Petr.* v. 23, pg. 447-504.

Couch, R.W., and Braman, D.E., 1980. Geology of the continental margin near Florence, Oregon. in *Prospects for oil and gas in the Coos Basin, western Coos, Douglas, and Lane counties, Oregon*. V.C. Newton ed., Oregon Dept. Geol. and Mineral Indust. Oil and Gas investigation 6, pg. 16-22.

Couch, R.W., and Pitts, G.S., 1980. The structure of the continental margin near Coos Bay, Oregon. in *Prospects for oil and gas in the Coos Basin, western Coos,*

- Douglas, and Lane counties, Oregon. V.C. Newton ed., Oregon Dept. Geol. and Mineral Indust. Oil and Gas investigation 6, pg. 23-26.
- Curry, J.R., Moore, D.G., Lawver, L.A., Emmel, F.J., Raitt, R.W., Henry, M., and Kieckhefer, R., 1979. Tectonics of the Andaman Sea and Burma. Mem. Am. Assoc. Pet. Geol., v.29, pg.189-198.
- Duncan, R.A., 1982. A captured island chain in the coast range of Oregon and Washington. Jour. Geophys. Res., v.87, pg. 10,827-10,837.
- Dickinson, W.R., 1979. Cenozoic plate tectonics of the Cordilleran region in the United States, in Armentrout, J.M., M.R. Cole, and H. TerBest, Jr., eds., Cenozoic paleogeography of the western United States, Sacramento, Ca., Pacific Section, Soc. Econ. Paleontol. Mineral., pg.1-13.
- Dickinson, W.R., 1976. Sedimentary basins developed during evolution of Mesozoic-Cenozoic arc-trench system in western North America. Can. J. Earth Sci., v. 13, pg. 1268-1287.
- Diller, J.S., 1898. Roseburg folio, Oregon. U.S. Geol. Survey, Geol. atlas of U.S., folio no.49.
- Engelbreton, D.C., 1982. Relative motions between oceanic and continental plates in the Pacific basin. unpublished Ph.D. thesis, Stanford University, pp.211.
- Ewing, T.E., 1980. Paleogene tectonic evolution of the Pacific Northwest. J. Geol., v. 88, pg. 619-638.
- Fein, J.B., and Jurdy, D. M., 1986. Plate motion controls on back-arc spreading. Geophys. Res. Lett., v. 13, pg. 456-459.
- Frey, F.A., Green, D.A., and Roy, S.D., 1978. Integrated models of basalt petrogenesis: A study of quartz tholeiites to olivine melilitites from southeastern Australia utilizing geochemical and experimental petrological data. Jour. Petr., v. 19, pg.463-513.

- Frey, F.A., and Clague, D.A., 1983. Geochemistry of diverse basalt types from Loihi Seamount, Hawaii: petrogenetic implications. *Earth and Planet. Sci. Lett.*, v. 66, pg.337-355.
- Gast, Paul W., 1968. Trace element fractionation and the origin of tholeiitic and alkaline magma types. *Geochim. Cosmochim. Acta*, v. 32, pg.1057-1086.
- Gladney, E.S., Burns, C.E., and Roelandts, I., 1983. 1982 Compilation of elemental concentrations in eleven United States Geological Survey rock standards. *Geostandards Newsletter*, v. 7, no. 1, pg. 3-
- Gladney, E.S., and Goode, W.E., 1981. Elemental concentrations in eight new United States Geological Survey rock standards: A review. *Geostandards Newsletter*, v. 5, no. 1, pg. 31-64.
- Glassley, W., 1974. Geochemistry and tectonics of the Crescent Volcanic rocks, Olympic Peninsula, Washington. *Geol. Soc. Am. Bull.*, v.85, pg. 785-794.
- Glassley, W., 1976. New analyses of Eocene basalts from the Olympic Peninsula, Washington: Discussion. *Geol. Soc. Am. Bull.*, v.87, pg. 1200-1201.
- Globerman, B.R., 1980. Geology, Petrology, and Paleomagnetism of Eocene basalts from the Black Hills, Washington Coast Range. unpublished M.S. thesis, Western Washington University, Bellingham, Wa., pp. 373.
- Globerman, B.R., Beck, M.E., Jr., Duncan, R.A., 1982. Paleomagnetism and tectonic significance of Eocene basalts from the Black Hills, Washington Coast Range. *Geol. Soc. Am. Bull.*, v.93, pg. 1151-1159.
- Hanson, Gilbert N., 1980. Rare earth elements in petrogenetic studies of igneous systems. *Ann. Rev. Earth Planet Sci.*, v. 8, pg. 371-406.
- Hart, R.A., 1970. Chemical exchange between sea water and deep ocean basalts. *Earth and Planet. Sci. Lett.*, v. 9, pg. 269-279.

- Haskin, L.A., 1984. Petrogenetic modelling - use of rare earth elements: in Rare earth element geochemistry, (Henderson, P., ed.), Elsevier publishing, pg.115-152.
- Henderson, L.J., Gordon, R.G., and Engebretson, D.C., 1984. Mesozoic aseismic ridges on the Farallon Plate and southward migration of shallow subduction during the Laramide Orogeny. *Tectonics*, v. 3, pg. 121-132.
- Heller, P.L., and Ryber, P.T., 1983. Sedimentary record of subduction to forearc transition in the rotated Eocene basin of western Oregon. *Geology*, v.11, pg. 380-383.
- Hellman, P.L. and Green, T.H., 1979. The role of sphene as an accessory phase in the high-pressure partial melting of hydrous mafic compositions. *Earth Planet. Sci. Lett.*, v. 42, pg. 191-201.
- Hill, D.W., 1975. Chemical composition studies of Oregon and Washington coastal basalts. (M.S. Thesis), Oregon State University, Corvallis, Oregon.
- Hoover, L., 1963. Geology of the Anlauf and Drain quadrangles Douglas and Lane Counties, Oregon. *Geol. Surv. Bull.*, v. 1122-D, pg. D- 1-59.
- Hynes, A. and Mott, J., 1985. On the causes of back-arc spreading. *Geology*, v. 13, pg. 387-389.
- Irvine, T.N., and Baragar, W.R.A., 1971. A guide to the chemical classification of the common volcanic rocks. *Can. J. Earth Sci.*, v. 8, pg. 523-548.
- Jochum, K.P., Seufert, H.M., Spettel, B., and Palme, H., 1986. The solar-system abundances of Nb, Ta, and Y, and the relative abundances of refractory lithophile elements in differentiated planetary bodies. *Geochim. Cosmochim. Acta*, v. 50, pg. 1173-1183.
- Karig, D.E., 1971. Origin and development of marginal basins in the western Pacific. *J. Geophys. Res.*, v. 76, pg. 2542-2561.

- Kay, R.W. and Gast, P. W., 1973. The rare earth content and origin of alkali-rich basalts. *J. Geol.*, v. 81, pg. 653.
- Kay, R.W. and Hubbard, N.J., 1978. Trace elements in ocean ridge basalts. *Earth Planet. Sci. Lett.*, v. 38, pg. 95-116.
- Kennedy, W. Q., 1933. Trends of differentiation on basaltic magmas. *Amer. J. Sci.*, v. 25, pg. 239-256.
- Kokelaar, P., 1986. Magma-water interactions in subaqueous and emergent basaltic volcanism. *Bull. Volcanology*, v. 48, pg.275-289.
- Kushiro, I. and Kuno, H., 1963. Origin of primary basalt magmas and classification of basaltic rocks. *Jour. of Petrology*, v. 4, pg. 75-89.
- Langmuir, C.H., Bender, J.F., Bence, A.E., Hanson, G.N., 1977. Petrogenesis of basalts from the FAMOUS area: Mid-Atlantic Ridge. *Earth Planet. Sci. Letts.* v. 36, pg.133-156.
- Langmuir, Charles H., Vocke, Robert D. Jr., Hanson, Gilbert N., and Hart, Stanley R., 1978. A general mixing equation with applications to Icelandic basalts. *Earth Planet. Sci. Letts.* ,v. 37, pg. 380-392.
- Laul, J.C., 1979. Neutron activation analysis of geological materials. *Atomic Energy Review*, v. 17, no. 3, pg. 603-695.
- Leeman, W.P., Budahn, J.R., Gerlach, D.C., Smith, D.R., and Powell, B.N., 1980. Origin of Hawaiian tholeiites: trace element constraints. *Am. J. Sci.*, V. 280A, pg. 794-819.
- Loeschke, J., 1979. Basalts of Oregon (U.S.A) and their geotectonic environment. I. Petrochemistry of Tertiary basalts of the Oregon Coast Range. *N. Jb. Miner. Abh.*, v.134, pg.225-247.

- Lyttle, N. A., and Clark, D.B., 1975. New analyses of Eocene basalt from the Olympic Peninsula, Washington. *Geol. Soc. Am. Bull.*, v. 86, pg.421-427.
- Lyttle, N. A., and Clark, D.B., 1976. New analyses of Eocene basalt from the Olympic Peninsula: Reply. *Geol. Soc. Am. Bull.*, v.87, pg. 1201-1204.
- Ma, M-S., Laul, J.C., and Schmitt, R.A., 1981. Complementary rare earth element patterns in unique achondrites, such as ALHA 77005 and shergottites, and in the earth. *Proc. Lunar Planet. Sci. Conf.*, V. 12B, pg. 1349-1358.
- Macdonald, G.A. and Katsura, T. 1964. Chemical composition of Hawaiian lavas. *J. Petrol.*,v. 5, pg. 82-133.
- Magill, J., and Cox, A., 1980. Tectonic rotation of the Oregon western Cascades. Oregon Dept. Geol. and Min. Industries, special paper 10, p.67.
- Magill, J., and Cox, A., 1981. Post-Oligocene tectonic rotation of the Oregon Western Cascade Range and the Klamath Mountains. *Geology*, v.9, pg.127-131.
- Magill, J., R., Wells, R.E., Simpson, R.W., and Cox, A.C., 1982. Post 12 m.y. rotation of southwestern Washington. *Jour. Geophys. Res.*, v. 87, pg.3761-3776.
- Menard, H.W., 1969. Growth of drifting volcanoes. *J. Geophys. Res.*, v. 74, pg. 4827-4837.
- Miles, G.A., 1977. Planktonic foraminifera of the lower Tertiary Roseburg, Lookingglass, and Flournoy formations, Southwest Oregon. unpublished Ph.D. dissertation, Univ. Oregon, 374 p.
- Miles, G.A., 1981. Planktonic foraminifera of the lower Tertiary Roseburg, Lookingglass, and Flournoy formations (Umpqua Group), Southwest Oregon: in *Pacific Northwest Cenozoic Biostratigraphy* (Armentrout, J.M., editor), GSA Special Paper 184, p.85-103.

- Miyashiro, A., 1978. Nature of alkalic volcanic rock series. *Contrib. Mineral. Petrol.*, v. 66, pg. 91-104.
- Moore, J.G., Fleming, H.S., and Phillips, J.D., 1974. Preliminary model for extrusion and rifting at the axis of the Mid-Atlantic Ridge, 36° 48' north. *Geology*, V. 2, pg. 437-440.
- Moore, G.W., 1984. Tertiary dismemberment of western North America. *Tectonics, Third Circum-Pacific Energy and Mineral Resources Conference Transactions*. pg.607-611.
- Moore, J.C., Byrne, T., Plumley, P.W., Reid, M., Gibbons, H., and Coe, R.S., 1983. Paleogene evolution of the Kodiak Islands, Alaska: consequences of ridge-trench interaction in a more southerly latitude, *Tectonics*, v.2, pg.265-293.
- Morgan, W.J., 1972. Deep mantle convection plumes and plate motions. *Am. Assoc. Petrol. Geol. Bull.*, v. 56, no. 2, pg. 203-213.
- Muller, J.E., 1980. Chemistry and origin of the Eocene Metchosin Volcanics, British Columbia. *Can. J. Earth Sci.*, v. 17, pg. 199-209.
- Park, C.F., Jr., 1946. The spilite and manganese problems of the Olympic Peninsula, Washington. *Am. Jour. Sci.*, v. 244, no. 5, pg. 305-323.
- Pearce, J.A., 1983. Role of the sub-continental lithosphere in magma genesis at active continental margins: in *Continental basalts and mantle xenoliths*, (Hawkesworth, C.J., and Norry, M.J., eds.), Shiva publishing, pg. 230-249.
- Pearce, J.A. and Cann, J.R., 1973. Tectonic setting of basic volcanic rocks determined using trace element analyses. *Earth Planet. Sci Lett.*, v. 19, pg. 290.
- Peterson, D.W., and Moore, R.B., 1987. Geologic history and evolution of geologic concepts, Island of Hawaii: in *Volcanism in Hawaii V.I*, U.S. Geol. Surv. Prof. Paper 1350, pg. 149-190.

- Perttu, R.K., and Benson, G.T., 1980. Deposition and deformation of Eocene Umpqua Group, Sutherlin area, southwestern Oregon. *Oregon Geology*, v.42, pg.136-140.
- Ramp, L., 1972. Geology and mineral resources of Douglas county, Oregon. Oregon Dept. of Geol. and Min. Indus., Bull., v. 75, p.106.
- Robbins, J.M., Lyle, M., and Heath, G.R., 1984. A sequential extraction procedure for partitioning elements among co-existing phases in marine sediments. College of Oceanography, Oregon State University reference 84-3, pp. 45.
- Ryberg, P.T., 1984. Sedimentation, structure, and tectonics of the Umpqua Group (Paleocene to early Eocene), southwestern Oregon. unpublished Ph.D. dissertation, Univ. Arizona, 422p.
- Saunders, A.D., 1984. The rare earth element characteristics of igneous rocks from the ocean basins: in *Rare earth element geochemistry*, (Henderson, P., ed.), Elsevier publishing, pg. 205-236.
- Saunders, A.D. and Tarney, J., 1979. The geochemistry of basalts from a back-arc spreading centre in the East Scotia Sea. *Geochim. Cosmochim. Acta*, v. 43, pg. 555-572.
- Saunders, A.D., Tarney, J., and Weaver, S.D., 1980. Transverse geochemical variations across the Antarctic Peninsula: Implications for the genesis of calc-alkalic magmas. *Earth Planet. Sci. Letts.*, v. 46, pg. 344-360.
- Schilling, J.-G., 1971. Sea-floor evolution: rare-earth evidence. *Phil. Trans. Roy. Soc. Lond., Ser. A* 268, pg. 663-706.
- Simpson, R.W., and Cox, A., 1977. Paleomagnetic evidence for tectonic rotation of the Oregon Coast Range. *Geology*, v. 5, pg. 585-589.

- Smith, R.E. and Smith, S.E., 1976. Comments on the use of Ti, Zr, Y, Sr, K, P and Nb in classification of basaltic magmas. *Earth Planet. Sci. Lett.*, v. 32, pg. 114-120.
- Snively, P.D., Jr., 1984. Sixty million years of growth along the Oregon Continental Margin. in *United States Geological Survey Highlights in marine research*, U.S. Geol. Surv. Circular 938, pg. 9-18.
- Snively, P.D., Jr., and Wagner, H.C., 1963. Tertiary geologic history of Western Oregon and Washington, Wash. Div. Mines Geol. Rep. Invest., v.22, 24p.
- Snively, P.D., Jr., and Wagner, H.C., 1961. Differentiated gabbroic sills and associated alkalic rocks in the central part of the Oregon Coast Range, Oregon. *United States Geol. Surv. Res.* 1122-D, pg. D156-D161.
- Snively, P.D., Jr., Wagner, H.C., and Lander, D.L., 1980. Interpretation of the Cenozoic geologic history, central Oregon continental margin: Cross-section summary. *Geol. Soc. Am. Bull.*, v. 91, pt.1, pg. 143-146.
- Snively, P.D., Jr., Wagner, H.C., and MacLeod, N.S., 1965. Preliminary data on compositional variations of Tertiary volcanic rocks in the central part of the Oregon Coast Range. *Ore Bin*, v. 27, pg. 101-117.
- Snively, P.D., Jr., MacLeod, N.S., and Wagner, H.C., 1968. Tholeiitic and alkalic basalts of the Eocene Siletz River Volcanics, Oregon Coast Range, *Am.J. Sci.*, v.266, pg. 454-481.
- Snively, P.D., Jr., MacLeod, N.S., and Wagner, H.C., 1980. Geology of the west-central part of the Oregon Coast Range. in *Geologic field trips in western Oregon and southwestern Washington*, Oles, K.F., Johnson, J.G., Niem, A.R., and Niem, W.A., eds. Oregon Department of Geology and Mineral Indust., Bull. 101, pg. 39-76.
- Sun, S.S. and Hanson, G.N., 1975a. Evolution of the mantle: geochemical evidence from alkali basalt. *Geology*, v. 3, pg. 297-302.

- Sun, S.S. and Hanson, G.N., 1975b. Origin of Ross Island Basanitoids and limitations upon the heterogeneity of mantle sources for alkali basalts and nephelinites. *Contrib. Mineral. Petrol.*, v.52, pg. 77-106
- Sun, S.S., and Nesbitt, R.W. 1977. Chemical heterogeneity of the Archean mantle, composition of the Earth and mantle evolution. *Earth and Planet. Sci. Letts.*, v.35, pg. 429-448.
- Sun, S.S., Tatsumoto, M., and Schilling, J.G., 1975. Mantle plume mixing along the Reykjanes Ridge axis: lead isotopic evidence. *Science*, v. 190, pg. 143-149.
- Tarney, J., Saunders, A.D., and Weaver, S. D., 1977. Geochemistry of volcanic rocks from the island arcs and marginal basins of the Scotia Arc region. *Island Arcs, Deep Sea Trenches and Back-Arc Basins*, Maurice Ewing Ser., Eds, M. Talwani and W.C. Pitman III, v. 1, pg. 367-377.
- Tarney, J., Saunders, A.D., Matthey, D.P., Wood, D.A., and Marsh, N. G., 1981. Geochemical aspects of back-arc spreading in the Scotia Sea and western Pacific. *Phil. Trans. R. Soc. Lond.*, v. 300, pg. 263-285.
- Tarney, J., Wood, D.A., Saunders, A.D., Cann, J.R., and Varet, J., 1980. Nature of mantle heterogeneity in the North Atlantic: evidence from deep sea drilling. *Phil. Trans. R. Soc. Lond.*, v. 297, pg. 179-202.
- Tarney, J., Wood, D.A., Varet, J., Saunders, A.D., and Cann, J.R., 1979. Nature of mantle heterogeneity in the North Atlantic: Evidence from Leg 49 basalts. *Deep Drilling Results in the Atlantic Ocean: Oceanic Crust* . Maurice Ewing, Ser. 2, pg.352-368.
- Tilley, C.E., 1950. Some aspects of magmatic evolution. *Quar. Jour. Geol. Soc. London*, v. 106, pg. 37-61.
- Taylor, B. and Karner, G. D., 1983. On the evolution of marginal basins. *Rev. of Geophys. and Space Phys.*, v. 21, pg. 1727-1741.

- Wells, F.G., and Waters, A.C., 1935. Basaltic rocks in the Umpqua Formation. *Geol. Soc. Am. Bull.*, v. 46, pg. 961-972.
- Wells, F.G., and Waters, A.C., 1934. Quicksilver deposits of southwestern, Oregon. *United States Geol. Surv. Bull.*, v. 850, pg.
- Wells, R.E., Engebretson, D.C., Snavely, P.D., Jr., and Coe, R.S., 1984. Cenozoic plate motions and the volcano-tectonic evolution of western Oregon and Washington, *Tectonics*, v.3, no. 2, pg.2.
- White, W. M. and Schilling, J.G., 1978. The nature and origin of geochemical variation in Mid-Atlantic Ridge basalts from the central North Atlantic. *Geochim. Cosmochim. Acta*, V. 42, pg. 1501-1516.
- Wood, David A., 1979. A variably veined suboceanic upper mantle- Genetic significance for mid-ocean ridge basalts from geochemical evidence. *Geology*, v. 7, pg. 499-503.
- Wood, David A., 1980. The Application of a Th-Hf-Ta diagram to problems of tectomagmatic classification and to establishing the nature of crustal contamination of basaltic lavas of the British Tertiary Volcanic Province. *Earth Planet. Sci. Letts.*, v. 50, pg. 11-30.
- Wood, D.A., Joron, J.L., Marsh, N.G., Tarney, J., and Treuil, M. 1980. Major and trace element variations in basalts from the north Phillipine Sea drilled during Deep Sea Drilling Project Leg 58: A comparative study of back-arc-basin basalts with lava series from Japan and mid-ocean ridges. *Init. Repts. Deep Sea Drilling Project*, v. 58, pg. 873-894.
- Wood, David A., Joron, Jean-Louis, and Treuil, Michel, 1979. A re-appraisal of the use of trace elements to classify and discriminate between magma series erupted in different tectonic settings. *Earth Planet Sci. Letts.*, v. 45, pg. 326-336.

- Wood, D.A., Marsh, N.G., Tarney, J., Joron, J.L., Fryer, P., and Treuil, M., 1982. Geochemistry of igneous rocks recovered from a transect across the Mariana Trough, arc, fore-arc, and trench, sites 453 through 461, Deep Sea Drilling Project Leg 60. Init. Repts. Deep Sea Drilling Project, v. 60, pg. 611-645.
- Yoder, H. S., Jr., and Tilley, C.E., 1957. Basalt magmas. Ann. Rept. geophys. Lab., Carnegie Instn. Wash. Yearb., v. 56, pg. 156-161.
- Yoder, H.S., Jr., and Tilley, C.E., 1962. Origin of basalt magmas: An experimental study of natural and synthetic rock systems. J. Petrol., v. 3, pg. 342-532.

APPENDIX

APPENDIX A

SAMPLE COLLECTION LOCALITIES

<u>Sample</u>	<u>Quadrangle</u>	<u>Section</u>	<u>Township/Range</u>	
RB-1	Sutherlin	SE 1/4, 17	T26S	R4W
RB-2	Sutherlin	SW 1/4, 40	T26S	R5W
RB-22	Glide	SW 1/4, 2	T25S	R4W
RB-611	Roseburg	NW 1/4, 15	T27S	R5W
RB-622	Roseburg	NW 1/4, 15	T27S	R5W
RB-16	Glide	SW 1/4, 10	T26S	R4W
RB-7	Glide	NW 1/4, 29	T26S	R4W
SL-5	Bridge	SW 1/4, 23	T29S	R12W
SL-4	Bridge	NE 1/4, 14	T29S	R12W
SL-2	Bridge	SW 1/4, 20	T29S	R11W
FMP-1 (sill)	Bandon	NW 1/4, 19	T27S	R14W
CQ-5	Myrtle Pt.	SE 1/4, 30	T28S	R12W
CQ-11	Myrtle Pt.	NE 1/4, 29	T28S	R12W
CQ-6	Coquille	NW 1/4, 19	T28S	R12W
CQ-4	Myrtle Pt.	SE 1/4, 20	T28S	R12W
CQ-3	McKinley	NW 1/4, 10	T28S	R12W
RH-1	Anlauf	NW 1/4, 12	T23S	R5W
RH-7	Sutherlin	NE 1/4, 18	T24S	R5W
RH-4	Anlauf	SW 1/4, 9	T23S	R4W
RH-303	Anlauf	NW 1/4, 5	T23S	R4W
RH-283	Drain	SW 1/4, 15	T23S	R5W
DCLP-1 (dike)	Glide	NE 1/4, 1	T25S	R5W
MSWC-28 (4010.4 m)	Glide	NE 1/4, 1	T25S	R5W
MSWC-30 (4013.4 m)	Glide	NE 1/4, 1	T25S	R5W
MSWC-31 (4014.9 m)	Glide	NE 1/4, 1	T25S	R5W
BR-22	McKinley	NE 1/4, 10	T27S	R12W
BR-24	McKinley	SW 1/4, 11	T27S	R12W
BR-24a	McKinley	SW 1/4, 11	T27S	R12W
BR-3	Daniels Creek	SW 1/4, 24	T26S	R12W
BR-2	McKinley	SE 1/4, 10	T27S	R12W
CR-25	Allegany	NW 1/4, 27	T25S	R12W
CR-1	Allegany	SE 1/4, 27	T25S	R12W
KS-3	Allegany	SW 1/4, 3	T25S	R12W
KS-1	Allegany	SW 1/4, 26	T24S	R12W
JC-2a	Drain	NE 1/4, 17	T22S	R6W
JC-223	Drain	SE 1/4, 8	T22S	R6W
JC-1	Drain	NE 1/4, 16	T22S	R6W
JC-2	Drain	NE 1/4, 17	T22S	R6W

Appendix A (cont.)

<u>Sample</u>	<u>Quadrangle</u>	<u>Section</u>	<u>Township/Range</u>	
DA-1	Drain	SE 1/4, 17	T22S	R5W
DA-252a	Drain	SE 1/4, 24	T22S	R6W
DA-252b	Drain	SE 1/4, 24	T22S	R6W
DA-252c	Drain	SE 1/4, 24	T22S	R6W
DA-252e	Drain	SE 1/4, 24	T22S	R6W
DA-221a	Drain	SE 1/4, 40	T22S	R5W
DA-232	Drain	NW 1/4, 19	T22S	R5W

Washington-British Columbia Coast Range (splits of samples from Duncan, 1982)

MT-2	Happy Valley Rd., 3 km S of Langfor, B.C.			
MT-3	East Sooke Rd., at Speyside Rd., Metchosin, B.C.			
MT-4	0.5 km East of Sooke Gabbro, East Sooke Rd., B.C.			
BH-23	Rochester	SW 1/4, 7	T16N	R4W
BH-19	Rochester	SW 1/4, 18	T17N	R4W
BH-18	Rochester	NE 1/4, 15	T17N	R4W
BH-7	Shelton	NW 1/4, 18	T18N	R4W
BH-6	Shelton	NW 1/4, 14	T18N	R3W
GR-1 (W77-24R)	S. Bend	NE 1/4, 18	T12N	R9W
GR-2 (W77-27R)	N. Nemah	Center, 10	T12N	R9W
GR-3 (W77-31R)				
GR-4 (W77-36R)	Raymond	NE 1/4, 32	T13N	R8W
GR-5 (W77-58R)	S. Bend	SW 1/4, 35	T15N	R9W

APPENDIX B

NORMALIZATION VALUES

Chondritic Normalization
(Ma et al., 1981)

La	.329
Ce	.863
Nd	.620
Sm	.206
Eu	.077
Tb	.046
Yb	.211
Lu	.036
Sc	7.9

Primitive Mantle Normalization
(Wood, 1979)

Rb	.860
Ba	7.56
Th	.096
U	.027
K ₂ O (%)	.0303
Ta	.043
La	.710
Ce	1.90
Sr	23.0
Nd	1.29
P ₂ O ₅ (%)	.0207
Hf	.350
Sm	.385
Eu	.148
TiO ₂ (%)	.2002
Tb	.099
Yb	.442
Lu	.066